

ELUCIDATING THE FLAVIN REDUCTASE MECHANISM IN THE  
ALKANESULFONATE MONOOXYGENASE SYSTEM  
FROM ESCHERICHIA COLI

Except where reference is made to the work of others, the work described in this dissertation is my own or was done in collaboration with my advisory committee.  
This dissertation does not include proprietary or classified information.

---

Benlian Gao

Certificate of Approval:

---

Marie W. Wooten  
Professor  
Biological Science

---

Douglas C. Goodwin  
Associate Professor  
Chemistry and Biochemistry

---

Holly R. Ellis, Chair  
Assistant Professor  
Chemistry and Biochemistry

---

Evert C. Duin  
Assistant Professor  
Chemistry and Biochemistry

---

Joe F. Pittman  
Interim Dean  
Graduate School

ELUCIDATING THE FLAVIN REDUCTASE MECHANISM IN THE  
ALKANESULFONATE MONOOXYGENASE SYSTEM  
FROM ESCHERICHIA COLI

Benlian Gao

A Dissertation

Submitted to

the Graduate Faculty of

Auburn University

in Partial Fulfillment of the

Requirements for the

Degree of

Doctor of Philosophy

Auburn, Alabama  
December 15, 2006

ELUCIDATING THE FLAVIN REDUCTASE MECHANISM IN THE  
ALKANESULFONATE MONOOXYGENASE SYSTEM  
FROM ESCHERICHIA COLI

Benlian Gao

Permission is granted to Auburn University to make copies of this dissertation at its discretion, upon request of individuals or institutions and at their expense.  
The author reserves all publication rights.

---

Signature of Author

---

Date of Graduation

## VITA

Benlian Gao, daughter of Lubin Gao and Guixiang Shao, was born on March 20, 1964, in Yinan, Shandong Province, the People's Republic of China. She graduated with a Bachelor's degree in Forestry in 1986 from Shandong Agricultural University. She received her M.S. degree in Forestry in 1991 from Henan Agricultural University. From 1988 to 1998, she lectured as an assistant professor in Henan Agricultural University. She married Peisheng Cong in the year of 1991. They have one son, Zhengyang Cong. In spring 2002, she entered the Graduate School at Auburn University in the Department of Chemistry and Biochemistry and is currently pursuing the Ph.D degree.

DISSERTATION ABSTRACT

ELUCIDATING THE FLAVIN REDUCTASE MECHANISM IN THE

ALKANESULFONATE MONOOXYGENASE SYSTEM

FROM *ESCHERICHIA COLI*

Benlian Gao

Doctor of Philosophy, December 15, 2006  
(M.S., Henan Agricultural University, 1991)  
(B.S., Shandong Agricultural University, 1986)

167 Typed Pages

Directed by Holly R. Ellis

The two-component alkanesulfonate monooxygenase system from *Escherichia coli* is comprised of an FMN reductase (SsuE) and a monooxygenase enzyme (SsuD) that together catalyze the oxidation of alkanesulfonate to the corresponding aldehyde and sulfite products. To determine the effects of protein interactions on catalysis, the steady state kinetic parameters for SsuE were determined in single-enzyme assays and in the presence of the monooxygenase enzyme and alkanesulfonate substrate. In single-enzyme kinetic assays, SsuE followed an ordered sequential mechanism, with NADPH as the first substrate to bind and NADP<sup>+</sup> as the last product to dissociate. However, in the presence of SsuD and octanesulfonate the kinetic mechanism of SsuE is altered to a rapid equilibrium ordered mechanism, and the  $K_m$  value for FMN is increased 10-fold. These

results suggest that both the SsuD enzyme and alkanesulfonate substrate are required to ensure that the FMN reductases reaction proceeds to form the ternary complex with the subsequent generation of reduced flavin.

Rapid reaction kinetic analyses of SsuE were performed to define the microscopic steps involved in SsuE catalyzed flavin reduction. A weak charge-transfer complex between the flavin and pyridine nucleotide was identified in these studies. Results from single-wavelength analyses at 450 and 550 nm showed that reduction of FMN occurs in three distinct phases. Following the binding of FMN and NADPH to SsuE (MC-1, Michaelis complex), an initial fast phase ( $241 \text{ s}^{-1}$ ) corresponds to the interaction of NADPH with FMN (CT-1, charge-transfer complex). The second phase is a slow conversion ( $11 \text{ s}^{-1}$ ) to form a charge-transfer complex of reduced  $\text{FMNH}_2$  with  $\text{NADP}^+$  (CT-2). The conversion of CT-1 to CT-2 is the step representing electron transfer from the pyridine nucleotide to the flavin. The third step ( $19 \text{ s}^{-1}$ ) is the decay of the charge-transfer complex to the Michaelis complex of SsuE with bound products (MC-2). Results from isotope studies with the  $[4(\text{R})\text{-}^2\text{H}]\text{NADPH}$  substrate demonstrates the rate-limiting step in flavin reduction is electron transfer from NADPH to FMN. In addition, electron transfer is inhibited at high flavin concentrations, further implicating this step as rate-limiting. While the utilization of flavin as a substrate by the alkanesulfonate monooxygenase system is novel, the mechanism for flavin reduction follows an analogous reaction path as standard flavoproteins. Based on the steady-state and pre-steady-state kinetic analyses of SsuE, a reaction mechanism has been elucidated for the flavin reductase catalyzed reaction in the alkanesulfonate monooxygenase system.

## ACKNOWLEDGEMENTS

I would like to firstly express my deepest appreciation to my advisor, Dr. Holly R. Ellis, for her consistent support and invaluable academic guidance as a respectful professor. My dissertation would not be possible without her support and guidance. Secondly, I would like to thank my knowledgeable committee members, Dr. Marie Wooten, Dr. Douglas Goodwin, and Dr. Evert Duin for their constructive suggestions to my dissertation. I also want to thank my lab colleagues, Kholis Abdurachim, Xuanzhi Zhan, Honglei Sun, Russell Carpenter, and Erin Imsand Massey for their meaningful discussions and help. I also give my thanks to my many friends not only in Auburn but also across the U.S. for their kindly help to my family during my graduate study here. I definitely want to thank my husband and my son for their solid support and understanding. Last but not least, I want to thank the Department of Chemistry and Biochemistry, Auburn University, and National Science Foundation for their funding support in my research.

Style Manual Used: Biochemical and Biophysical Research Communications

Computer Software Used: Microsoft Word, ChemDraw, Microsoft Excel, KaleidaGraph, EnzFitter



## TABLE OF CONTENTS

ABSTRACT.....	v
ACKNOWLEDGEMENTS.....	vii
TABLE OF CONTENTS.....	ix
LIST OF TABLES AND FIGURES.....	xii
CHAPTER ONE: LITERATURE REVIEW.....	1
1.1 Sulfur assimilation in bacterial systems.....	1
1.2 The two-component alkanesulfonate monooxygenase system.....	11
1.3 Flavin chemistry.....	15
1.4 Characterization of flavin reductase SsuE.....	27
1.5 Steady-state reaction mechanisms.....	28
1.6 Pre-steady-state kinetic mechanisms of flavin reductases.....	38
1.7 The flavin transfer mechanism in two-component monooxygenase system.....	40
1.8 Summary.....	46
CHAPTER TWO: MATERIALS AND METHODS.....	47
2.1 Biochemical and chemical reagents.....	47
2.2 Construction of expression vectors.....	48
2.3 Expression and purification of the alkanesulfonate monooxygenase proteins.....	50
2.4 Determination of molecular weight and quaternary structure of SsuE and SsuD.....	53

2.5 Substrate specificity assay .....	54
2.6 Data analyses .....	55
2.7 Flavin binding experiments.....	55
2.8 Steady-state kinetic measurements of SsuE.....	56
2.9 Data analyses for the steady-state kinetic mechanism of SsuE .....	58
2.10 Synthesis of [4(R)- <sup>2</sup> H]NADPH .....	59
2.11 Stopped-flow kinetic experiments.....	61
2.12 Data analyses of pre-steady-state complexes.....	64
2.13 Mutagenesis of double displacement of leucine to methionine .....	65
2.14 Preparation of M9 media .....	67
2.15 Expression and purification of selenomethionyl SsuE .....	67
2.16 Circular dichroism of wild-type SsuE and SeMet SsuE .....	68
2.17 Activity assay of SeMet SsuE.....	68
2.18 Crystallization of wild-type SsuE and SeMet SsuE.....	69
CHAPTER THREE: RESULTS .....	70
3.1 Protein expression and purification .....	70
3.2 Biophysical characterization of SsuE and SsuD.....	72
3.3 Substrate specificity studies of SsuE .....	72
3.4 FMN affinity assays.....	75
3.5 Steady-state kinetic analysis of the SsuE enzyme .....	81
3.6 Steady-state kinetic parameters with varying ratios of SsuD:SsuE .....	84
3.7 Steady-state kinetic mechanism of the SsuE enzyme in the presence of the SsuD enzyme and alkanesulfonate substrate .....	89

3.8 Pre-steady-state kinetic analysis of SsuE enzyme .....	92
3.9 Site-directed mutagenesis of SsuE.....	109
3.10 Single crystal of native SsuE and SeMet SsuE.....	110
3.11 The X-ray pattern and pseudo-precession image of native SsuE.....	115
CHAPTER FOUR: DISCUSSION.....	118
4.1 Biophysical and Biochemical characterization of SsuE and SsuD proteins.....	119
4.2 Steady-state kinetic mechanism of SsuE .....	120
4.3 Steady-state kinetic mechanism with SsuD monooxygenase present.....	122
4.4 Pre-steady-state kinetic mechanism of SsuE .....	125
4.5 Crystallization of SsuE .....	133
4.6 Summary .....	134
REFERENCES .....	139

## LIST OF TABLES AND FIGURES

Table 1.1 Kinetic parameters of alkanesulfonate monooxygenase .....	14
Table 3.1 Kinetic parameters for SsuE .....	78
Table 3.2 Kinetic parameters for SsuE with SsuD.....	88
Table 3.3 Steady-state kinetic parameters for SsuE.....	91
Figure 1.1 Cysteine biosynthesis from sulfate and alkanesulfonate in <i>E. coli</i> .....	2
Figure 1.2 Organization of the <i>E. coli</i> gene <i>ssuEADCB</i> operon .....	5
Figure 1.3 Uptake and desulfonation of taurine and alkanesulfonate in <i>E. coli</i> .....	6
Figure 1.4 Genetic gene organization of related <i>ssu</i> and <i>msu</i> operons .....	8
Figure 1.5 Gene expression regulation in sulfur assimilation of <i>E. coli</i> .....	10
Figure 1.6 Proposed mechanism of alkanesulfonate monooxygenase from <i>E. coli</i> .....	13
Figure 1.7 Proposed catalytic mechanism for the alkanesulfonate monooxygenase system .....	16
Figure 1.8 Structure of lumiflavin, riboflavin, FMN, and FAD molecules .....	17
Figure 1.9 Oxidation states of flavin mononucleotide (FMN) .....	19
Figure 1.10 Flavin spectra at different oxidation states .....	21
Figure 1.11 Mechanism of activation of oxygen by reduced flavin .....	24
Figure 1.12 Activity of SsuE in the presence of various flavin substrates .....	29
Figure 1.13 Structure of NADPH (X=PO <sub>3</sub> <sup>2-</sup> ) and NADH (X=H).....	30

Figure 1.14 Scheme of Bi Bi sequential reaction mechanisms.....	32
Figure 1.15 Double-reciprocal plots of a sequential mechanism.....	33
Figure 1.16 Double-reciprocal plot of a competitive inhibition .....	34
Figure 1.17 Proposed reaction mechanism of the flavin reductase Fre .....	37
Figure 1.18 Charge-transfer complex formation of Fre.....	39
Figure 1.19 Model of transient flavin transfer .....	45
Figure 2.1 The pET21a vector expression system .....	49
Figure 2.2 Cloning of alkanesulfonate monooxygenase genes (SsuE and SsuD) .....	51
Figure 2.3 Location of deuterated hydrogen in NADPH.....	60
Figure 2.4 Illustration of stopped-flow single mixing mode .....	62
Figure 2.5 The SsuE sequence with mutation sites underlined .....	66
Figure 3.1 SDS-PAGE of samples from alkanesulfonate monooxygenase proteins .....	71
Figure 3.2 Mass spectrometric analyses of SsuE and SsuD .....	73
Figure 3.3 The $g^*$ (s) value distribution of SsuD protein .....	74
Figure 3.4 Initial velocities with flavin substrates .....	76
Figure 3.5 Initial velocities with pyridine nucleotide substrates .....	77
Figure 3.6 Fluorescence quenching of SsuE by the addition of FMN.....	79
Figure 3.7 Fluorimetric titration of the SsuE or SsuD with FMN .....	80
Figure 3.8 Initial velocity patterns of the SsuE catalyzed reduction of FMN .....	82
Figure 3.9 Initial velocity patterns of the SsuE catalyzed reduction of FMN .....	83
Figure 3.10 Inhibition of the SsuE enzyme with the product inhibitor NADP <sup>+</sup> .....	85
Figure 3.11 Reaction mechanism for SsuE catalyzed reduction of FMN.....	86
Figure 3.12 Kinetic analysis with varying ratios of SsuD:SsuE .....	87

Figure 3.13 Initial velocity patterns of the SsuE catalyzed reduction by FMN with SsuD and octanesulfonate .....	90
Figure 3.14 Rapid equilibrium ordered sequential mechanism .....	93
Figure 3.15 Diode array spectra monitoring the absorbance change.....	94
Figure 3.16 Charge-transfer complex formation during flavin reduction.....	95
Figure 3.17 Single wavelength absorbance traces at 450 and 550 nm .....	97
Figure 3.18 Charge-transfer complex formation with SsuE only or SsuE+SsuD.....	99
Figure 3.19 Flavin reduction dependence on NADPH concentrations.....	100
Figure 3.20 The dependence of the observed rates on NADPH concentration in SsuE catalyzed flavin reduction.....	102
Figure 3.21 The dependence of the observed rates on NADPH concentration in SsuE catalyzed flavin reduction ( $k_{1obs}$ , $k_{2obs}$ ) .....	103
Figure 3.22 FMN dependence on charge-transfer complex formation.....	104
Figure 3.23 The dependence of the observed rates on FMN concentration in SsuE catalyzed flavin reduction.....	106
Figure 3.24 Flavin inhibition on charge-transfer complex formation.....	107
Figure 3.25 Single wavelength absorbance traces at 550 nm with NADPH and [4(R)- <sup>2</sup> H]NADPH .....	108
Figure 3.26 SDS-PAGE of purified SeMet SsuE and wild-type SsuE.....	111
Figure 3.27 CD spectra of SeMet SsuE and wild type SsuE .....	112
Figure 3.28 The hexagonal rod crystal of SsuE protein.....	113
Figure 3.29 The SeMet SsuE crystal co-crystalized with FMN .....	114
Figure 3.30 X-ray diffraction pattern of the native SsuE protein .....	116

Figure 3.31 The pseudo-precession image of the native SsuE protein .....	117
Figure 4.1 Structure showing Phe225 stacks between FMN and NADH in phthalate dioxygenase reductase.....	129
Figure 4.2 Alignment of the RXXS motif of SsuE with flavin reductases.....	130
Figure 4.3 Proposed reaction scheme for SsuE catalyzed reaction .....	132
Figure 4.4 Hydrogen-bonding of the active site in FNR .....	137

## CHAPTER ONE

### LITERATURE REVIEW

#### *1.1 Sulfur assimilation in bacterial systems*

Sulfur is an essential element for all organisms. In bacteria, sulfur assimilation from inorganic sulfate primarily occurs through the cysteine biosynthetic pathway [1]. Sulfur directly contributes to the biosynthesis of sulfur-containing amino acids such as cysteine and methionine, and also sulfur-containing prosthetic groups and coenzymes. Bacterial organisms can obtain sulfur from a broad range of sulfur sources, including inorganic sulfate and organic sulfur compounds (Figure 1.1) [2]. Sulfate, the major sulfur source for bacteria, can be transferred from the environment to the cell through a series of transport proteins, reduced to sulfite and sulfide and then used to synthesize cysteine *via* the cysteine biosynthetic pathway (Figure 1.1) [2]. In the absence of sulfate and cysteine, a set of enzymes is induced that allow some bacterial organisms to utilize organic sulfur sources for the synthesis of essential sulfur-containing components. Although different sulfur compounds enter the sulfur metabolic pathway through distinct mechanisms, they are all converted to sulfide before incorporation into cysteine.

In aerobic environments, the sulfur content is primarily composed of sulfonates and sulfate esters. In contrast, inorganic sulfur is poorly represented and comprises less



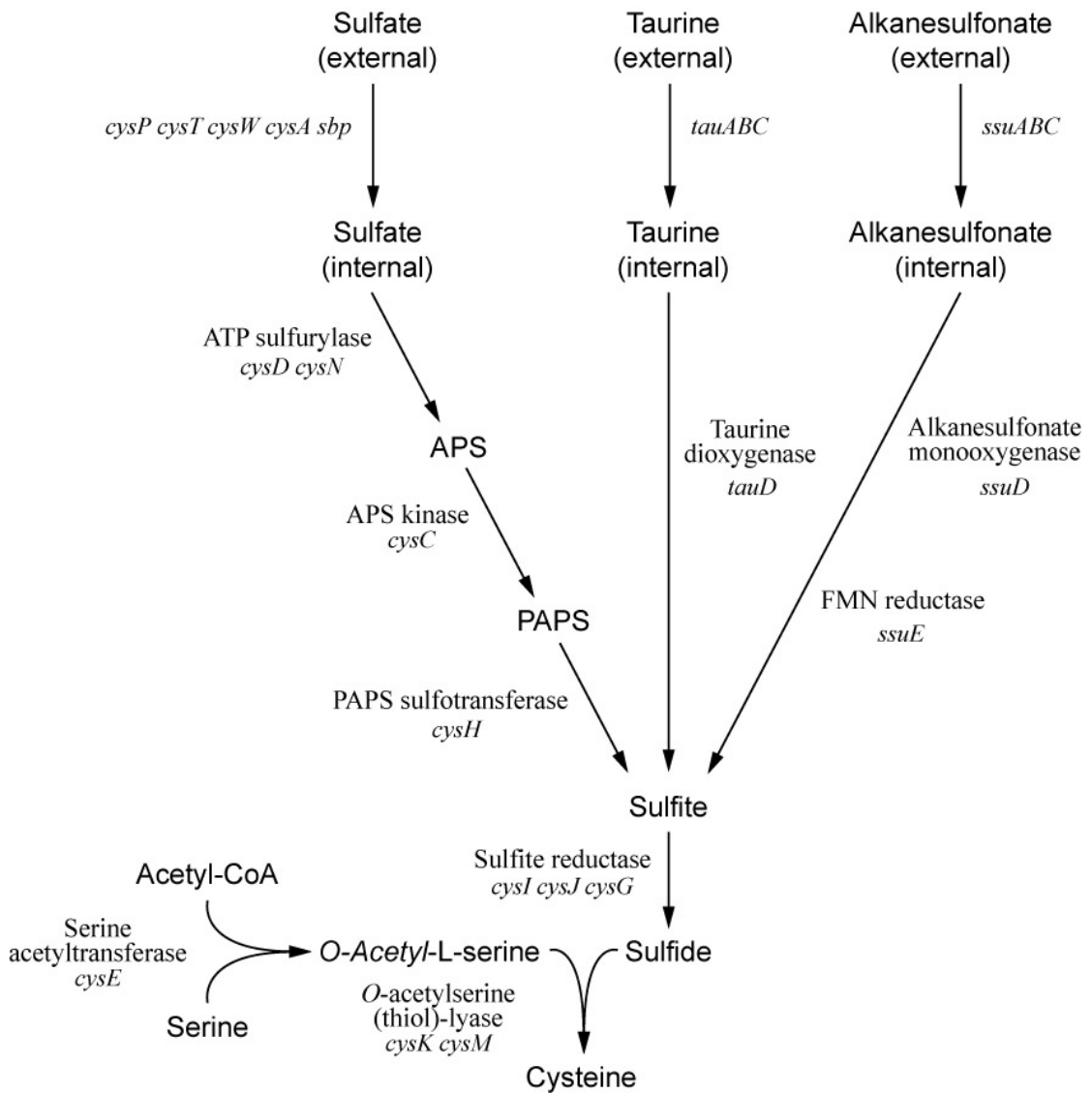


Figure 1.1. Cysteine biosynthesis from sulfate and alkanesulfonate in *E. coli* [2].

than 5% of the total sulfur content. Therefore, bacteria must have alternative sources for obtaining this element from organosulfur compounds to meet their sulfur requirements [3].

#### *1.1.1 Sulfate starvation induced gene expression*

Sulfate or cysteine starvation induces a set of proteins involved in the utilization of taurine and alkanesulfonate as sulfur sources under aerobic conditions [1, 4, 5,]. In *Escherichia coli*, minimal medium deprived of sulfate leads to the increased synthesis of sulfate starvation-induced (Ssi) proteins involved in obtaining sulfur from alternate sources [6]. The genes and proteins involved in sulfonate-sulfur utilization have been identified by two independent approaches: two-dimensional gel electrophoresis and transposon mutagenesis with  $\lambda placMu9$  [1, 4]. The identification of these proteins was based on the assumption that the expression of Ssi proteins would be repressed by sulfate and cysteine. By comparing cells grown with and without sulfate or cysteine, several Ssi proteins were identified which included the sulfate-binding protein (Sbp), cysteine-binding protein (FliY), *O*-acetyl serine lyase (CysK), alkyl-hydroperoxide reductase C22 (AhpC), and TauD. The *O*-acetyl serine lyase (CysK), also called cysteine synthase, catalyzes the formation of cysteine from free or bound sulfide and *O*-acetyl-L-serine [7]. As a result, this step represents the turning point of incorporation of reduced sulfur into organic compounds in microorganisms [7]. The alkylhydroperoxide reductase C22 (AhpC) catalyzes the cysteine-mediated reduction of peroxide substrates with the concomitant formation of a cysteinesulfenic acid (Cys-SOH) within the enzyme [8, 9], and the detoxification of organic hydroperoxides (ROOH) to their corresponding alcohols [10, 11]. TauD is an  $\alpha$ -ketoglutarate-dependent dioxygenase that utilizes taurine as a

sulfur source, and catalyzes the conversion of taurine to sulfite and aminoacetaldehyde.

Proteins that utilize alkanesulfonate designated Ssi4 and Ssi6 were mapped to the chromosome of *E. coli* by hybridization analysis [2, 6]. Five open reading frames were present and the operon was designated *ssuEADCB* (*ssu* for sulfonate-sulfur utilization) (Figure 1.2). The function of these genes and the encoding proteins were identified through mutagenesis studies. The genes *ssuA*, *B*, and *C* encode the ABC-type transport system for the uptake of aliphatic sulfonates, while *ssuD* and *E* encode the SsuD (Ssi6) and SsuE (Ssi4) proteins required for direct desulfonation of alkanesulfonates.

### *1.1.2 Sulfonate uptake system and desulfonation*

In *E. coli*, cell growth is dependent on sulfate as the principle sulfur source for the synthesis of sulfur-containing biomolecules. However, expression of two gene clusters, *tauABCD* and *ssuEADCB*, are required for the utilization of alkanesulfonate compounds from the environment when sulfate is limiting. Both systems are composed of an ABC-type transporter for the uptake of alkanesulfonates from the periplasm to the cytoplasm (Figure 1.3) [2]. TauA and SsuA are believed to function as periplasmic sulfonate binding proteins. TauB and SsuB act as ATP binding proteins, whereas TauC and SsuC, the integral membrane components, are putative aliphatic sulfonate transport permease proteins in the ABC transporter system [2].

In addition to ABC transport proteins, oxygenase enzymes TauD and SsuD are expressed from these operons. TauD is capable of taurine desulfonation coupled to the

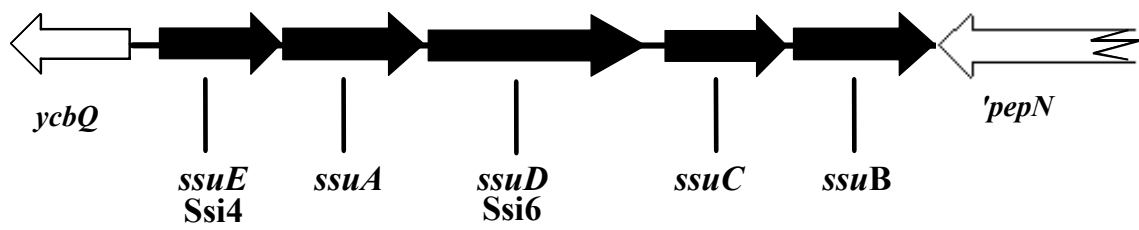


Figure 1.2. Organization of the *E. coli* gene *ssuEADCB* operon [6].

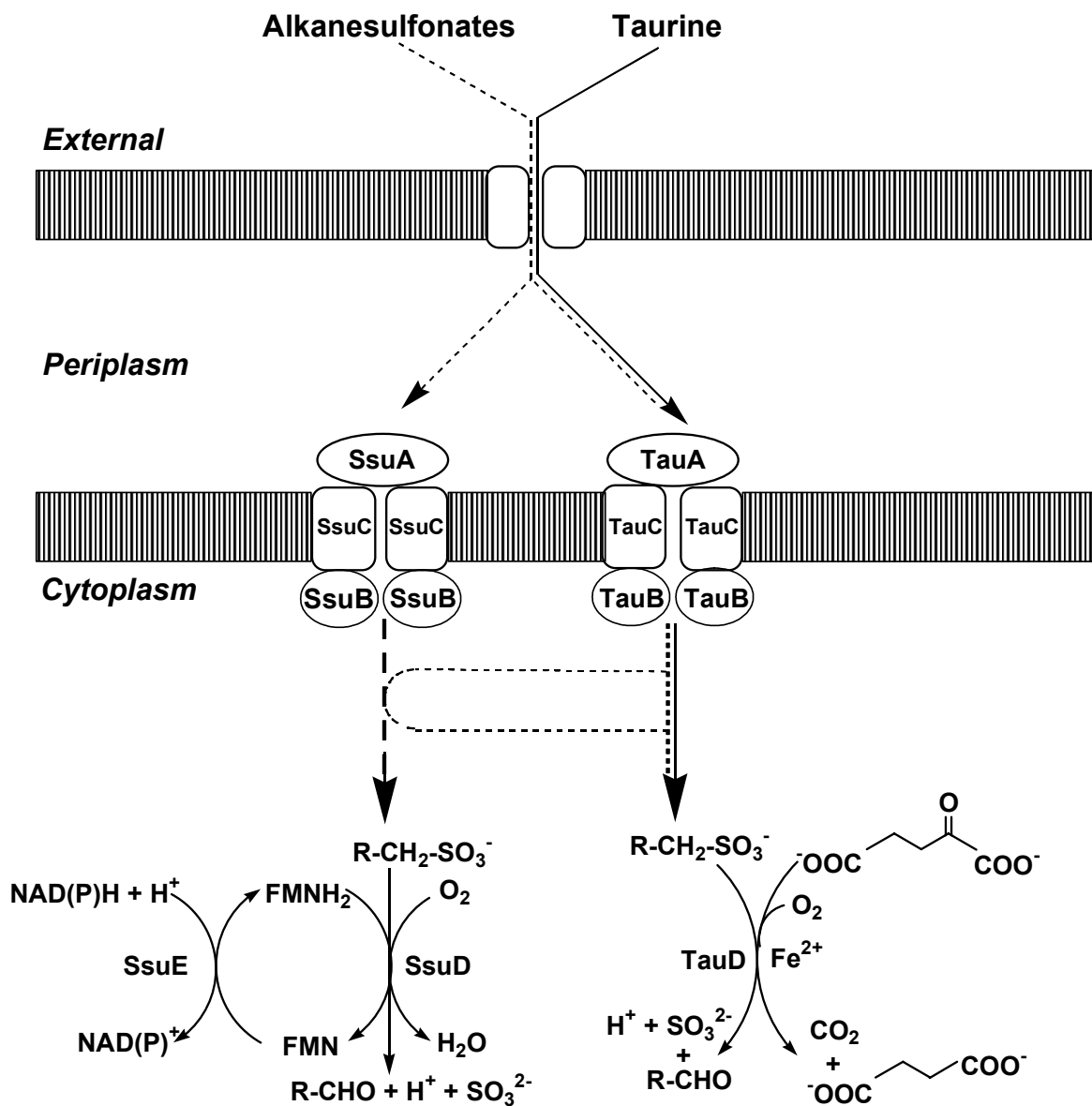


Figure 1. 3. Uptake and desulfonation of taurine and alkanesulfonates in *E. coli* [2].

decarboxylation of  $\alpha$ -ketoglutarate. SsuD is a reduced flavin mononucleotide-dependent alkanesulfonate monooxygenase that liberates sulfite from alkanesulfonates. The reduced flavin is supplied by the flavin reductase SsuE. Disruption of *tauB*, *tauC*, or *tauD* expression resulted in the inability of taurine to be utilized as a sulfur source, but did not affect the use of aliphatic sulfonates as sulfur sources [1]. Conversely, deletion of *ssuEADCB* prevented the transport and utilization of alkanesulfonates, but did not affect the use of taurine as a sulfur source [12]. This complementary effect upon substrate transportation and desulfonation is controlled by substrate availability in the environment.

### 1.1.3 Gene cluster arrangement

The SsuED proteins are expressed from the *ssuEADCB* operon under control of a single promoter and have only been identified in bacteria (Figure 1.4) [3]. The arrangement of genes within the operons may vary with species, but they all contain the monooxygenase gene *ssuD*, together with genes encoding the ABC-type transporter proteins. Another gene encoding an NAD(P)H-dependent flavin reductase SsuE is present in most bacteria except for *Bacillus subtilis*. The gene encoding the corresponding flavin reductase in *B. subtilis* is present at a different location on the chromosome [13]. In *Pseudomonas putida*, although the SsuD protein has 77% identity with the *E. coli* protein, the enzyme is able to utilize aromatic sulfonates in addition to alkanesulfonates. The additional enzyme component required for aromatic desulfonation, SsuF, is related to the clostridial molybdopterin-binding proteins [3]. Deletion analyses of various combinations of the *ssu* genes located on the *P. putida* operon has shown that

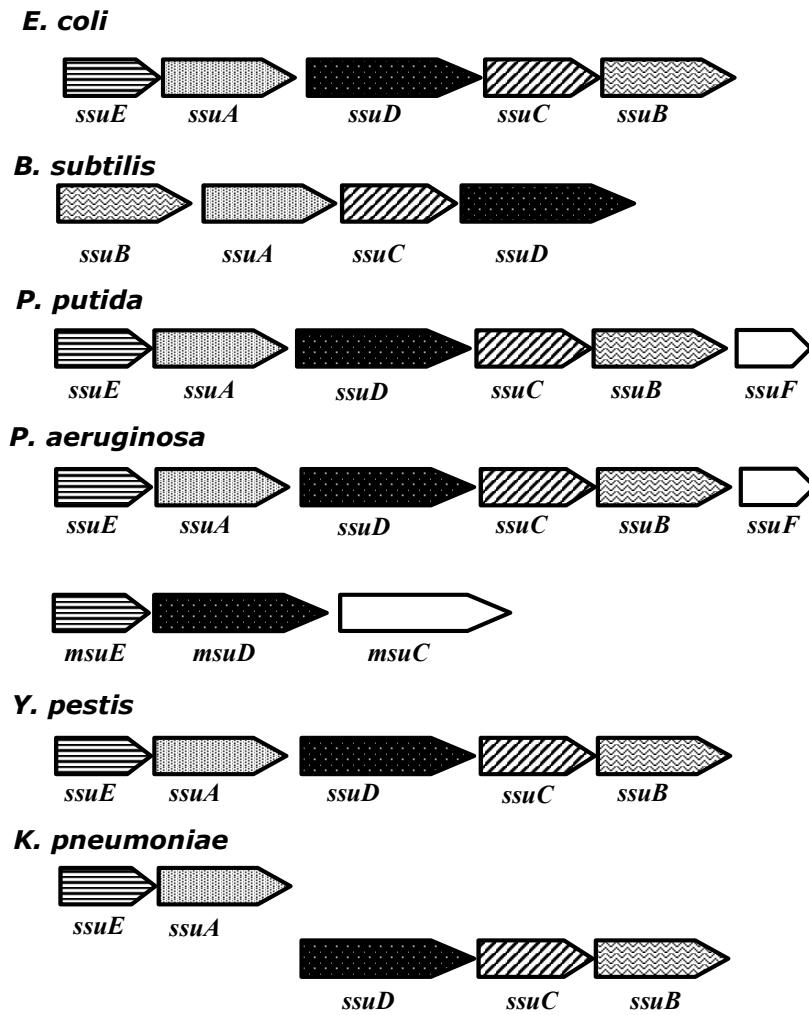


Figure 1. 4. Genetic gene organization of related *ssu* and *msu* operons [3].

SsuF is absolutely required for growth with aliphatic and aromatic sulfonates [3].

The expression of the *ssu* genes was shown to be under control of the LysR-type transcriptional regulator proteins CysB and Cbl (Figure 1.5) [2]. The CysB protein is regarded as the master regulator that positively regulates the expression of the genes encoding sulfur assimilation proteins. CysB is not directly involved in the expression of the *ssu* genes but serves as the activator for Cbl which is directly involved in the activation of *ssu* gene expression. The Cbl protein, which is 45% identical in sequence to CysB, binds upstream of the *ssu* promoter and acts as a transcriptional activator for *ssu* gene expression [6]. Therefore, CysB and Cbl must be coexpressed to trigger the expression of the *ssu* genes. When sulfate levels are sufficient, Cbl no longer binds to the promoter, and *ssu* proteins are not expressed. Sulfate or the sulfite desulfonation product may act as an anti-inducer for Cbl in the control of gene expression.

#### *1.1.4 Environmental application of organosulfur biodegradation*

Alkanesulfonates occur naturally in the soil and are readily biodegradable by aerobic processes. Problems are often encountered when they are produced industrially as surfactants, dyestuffs, and cement additives. Alkanesulfonate pollution is associated with toxicity in fish from polluted water, and these toxic effects include destruction of the gills, damage to chemoreceptors, and histological abnormalities [14]. Although the damage to aquatic organisms has been studied, the toxicity to humans is unknown. There is currently no effective method to eradicate the presence of these compounds in wastewater treatment plants.



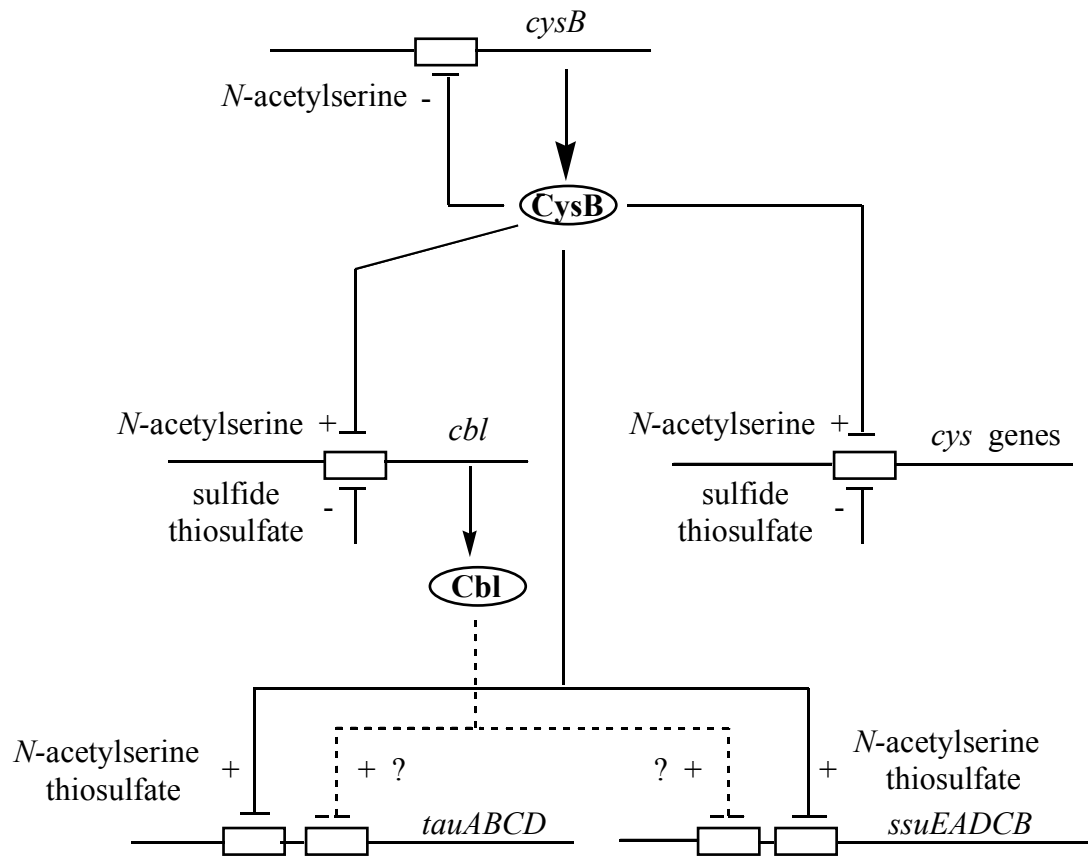


Figure 1.5. Gene expression regulation in sulfur assimilation of *E. coli* [2].

Fossil fuels are another major source of environmental pollution that have a profound impact on human daily life. The combustion of fossil fuels releases a large amount of sulfur dioxide into the air causing human health problems and damage to plants. The traditional method to remove organosulfur from crude oil-derived fuels is hydrodesulfurization, but it is not effective for fuels containing a significant amount of benzothiophenes and dibenzothiophenes [15]. Substantial efforts have been directed toward the development of biotechnology for desulfurization of fossil fuels [16]. One possible method to eliminate these toxic organic sulfur compounds is through bioremediation. An attractive candidate for this purpose is the alkanesulfonate monooxygenase system because the organosulfur compounds can be removed under mild conditions with low expense. Therefore, the mechanistic understanding of this two-component system may prove important in developing a bioremediation method for the desulfonation of these recalcitrant compounds.

### *1.2 The two-component alkanesulfonate monooxygenase system*

Many characterized bacterial enzymes catalyze a single distinct reaction, however, enzymes working as complex systems with multifunctions have increasingly been identified [17]. Enzyme systems coexpressed on the same operon under the control of a single promoter are usually involved in a similar function. The alkanesulfonate monooxygenase system is an example of a complex system involved in the desulfonation reaction of alkanesulfonates [2]. Interestingly, the overall reaction is tightly coupled between a flavin reductase (SsuE) and a flavin dependent monooxygenase (SsuD). SsuE is proposed to catalyze the reduction of FMN to form reduced FMNH<sub>2</sub>, while SsuD is an FMNH<sub>2</sub> dependent monooxygenase directly involved in the conversion of

alkanesulfonate to sulfite and the corresponding aldehyde [18]. Thus, FMNH<sub>2</sub> is the functional link between the two enzyme components. In the overall reaction scheme, SsuE catalyzes the reduction of FMN with reducing equivalents provided by NAD(P)H to form FMNH<sub>2</sub>, and then FMNH<sub>2</sub> is transferred to SsuD. The reduced flavin bound to SsuD activates molecular oxygen to form an active peroxyflavin species that is directly involved in the cleavage of the carbon-sulfur bond with the release of aldehyde and sulfite (Figure 1.6) [18]. The SsuD monooxygenase enzyme is able to desulfonate a broad range of substrates, ranging from C-2 to C-10 unsubstituted alkanesulfonates, substituted ethanesulfonic acids, and sulfonated buffers (Table 1.1) [18]. However, the preferred substrates for SsuD are decanesulfonic acid, octanesulfonic acid, and 1,3-dioxoisoindolineethanesulfonic acid.

Bacterial flavin-dependent monooxygenases that utilize reduced flavin as a substrate are continually emerging, and include proteins involved in the degradation of herbicides, the synthesis of antibiotics, desulfurization reactions, and bioluminescence. All of these two-component enzyme systems rely on a flavin reductase and a monooxygenase enzyme for catalytic activity. Two groups of flavin reductases are associated with the flavin-dependent monooxygenase family of enzymes. One group are the standard flavoproteins with a distinct flavin spectrum as purified, and the other group are the flavin reductases that do not contain any flavin prosthetic group and use flavin as a substrate. Several flavin reductases that belong to the standard flavoproteins provide reduced flavin to bacterial luciferase, nitrilotriacetate monooxygenase, EDTA monooxygenase, and pristinamycin IIA synthase [19-24]. Flavin reductase enzymes that do not contain flavin as a prosthetic group are associated with chlorophenol 4-monooxygenase, valanimycin

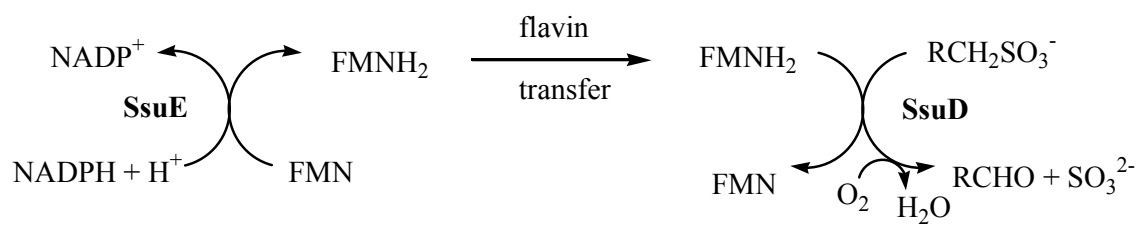


Figure 1. 6. Proposed mechanism of alkanesulfonate monooxygenase from *E. coli* [18].

Table 1. 1. Kinetic parameters of alkanesulfonate monooxygenase [18].

Sulfonated substrate	$K_m$	$V_{max}$	$k_{cat}/K_m$
	$\mu M$	units/mg	min <sup>-1</sup> $\mu M^{-1}$
Decanesulfonic acid (25–500 $\mu M$ )	35	1.4	6.7
Octanesulfonic acid (33–666 $\mu M$ )	44	1.6	6.1
1,3-Dioxo-2-isoindolineethanesulfonic acid (33–500 $\mu M$ )	114	4.1	6.0
2-(4-Pyridyl)ethanesulfonic acid (33–500 $\mu M$ )	139	3.8	4.6
Hexanesulfonic acid (50–500 $\mu M$ )	95	2.3	4.0
<i>N</i> -Phenyltaurine (50–500 $\mu M$ )	237	4.6	3.2
4-Phenyl-1-butanesulfonic acid (70–500 $\mu M$ )	110	1.8	2.7
Pentanesulfonic acid (70–500 $\mu M$ )	189	2.0	1.8
MOPS (70–1000 $\mu M$ )	617	4.1	1.1
Butanesulfonic acid (250–1000 $\mu M$ )	870	3.3	0.6
PIPES (333–3000 $\mu M$ )	1110	2.4	0.4

monooxygenase, 4-hydroxyphenylacetate 3-monooxygenase, and styrene monooxygenase [25-28].

The SsuD monooxygenase enzyme depends on reduced flavin provided by SsuE to activate molecular oxygen for the oxygenolytic desulfonation of alkanesulfonates. Based on studies of other flavin monooxygenases a catalytic mechanism can be proposed for the alkanesulfonate monooxygenase system (Figure 1.7). The reductive half-reaction in which the enzyme is reduced by the substrate occurs by SsuE while the oxidative half-reaction in which oxygen accepts an electron pair from the enzyme occurs following transfer of the reduced flavin to SsuD. Molecular oxygen is activated by the reduced flavin to form the peroxyflavin (Fl-OO-). Attack of the peroxyflavin on the C1 carbon of the alkanesulfonate leads to release of the sulfite product and the formation of a peroxyflavin-alkane adduct. This type of peroxyflavin-substrate intermediate has also been proposed for cyclohexanone monooxygenase and bacterial luciferase [29, 30]. Hydrogen abstraction from the alkane by an active-site base leads to the rearrangement of the alkane-flavin adduct to form the aldehyde product and the hydroxyflavin (Fl-OH). The hydroxyflavin would rapidly dehydrate to regenerate the oxidized flavin.

### *1.3 Flavin chemistry*

Flavin (7,8-dimethylisoalloxazine) is abundant in nature, either free or bound to proteins [31]. Conventionally, flavin is a general name for lumiflavin, riboflavin, flavin mononucleotide (FMN), and flavin adenine dinucleotide (FAD) (Figure 1.8). The diverse functions of flavins is dependent on the covalent linkage of functional groups to the isoalloxazine ring. Lumiflavin contains a methyl group at the N-10 position of the isoalloxazine ring. Riboflavin is composed of an isoalloxazine ring covalently bonded to

## SsuE

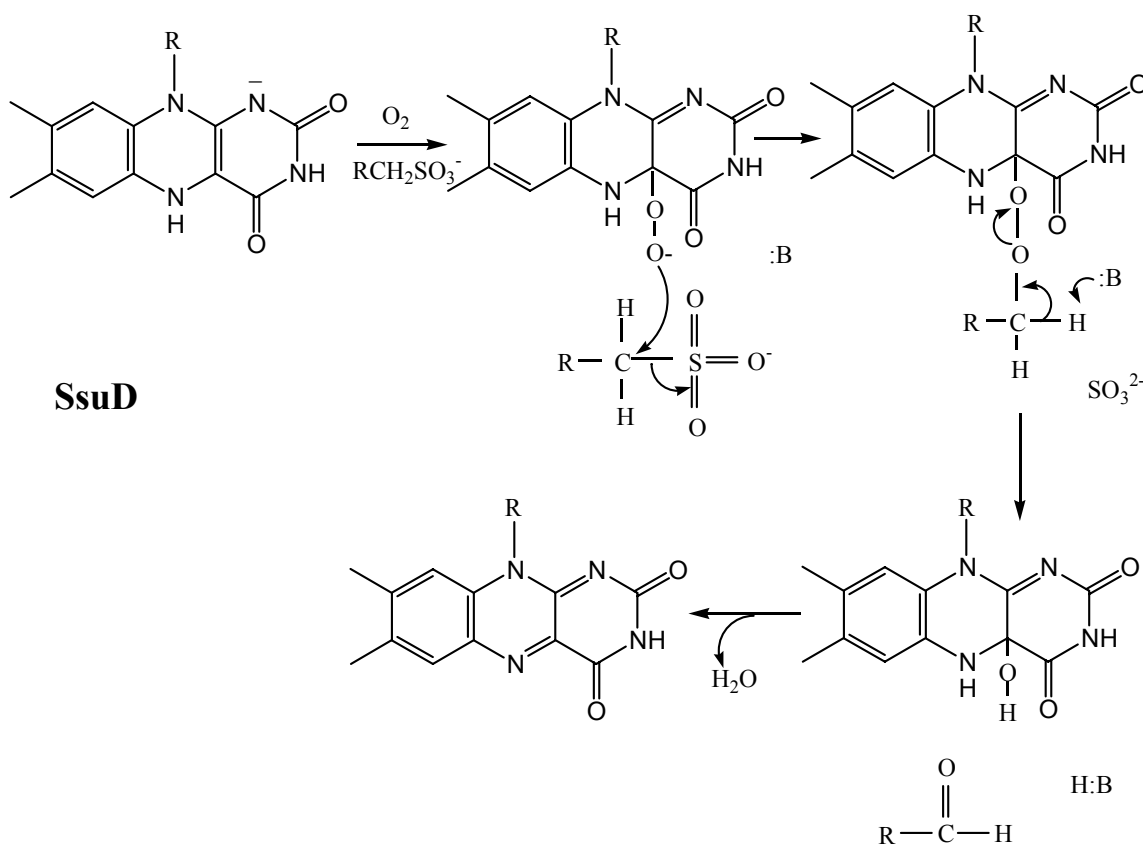
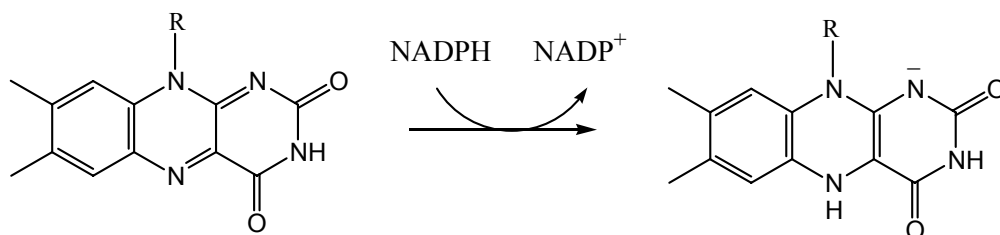


Figure 1.7. Proposed catalytic mechanism for the alkanesulfonate monooxygenase system.

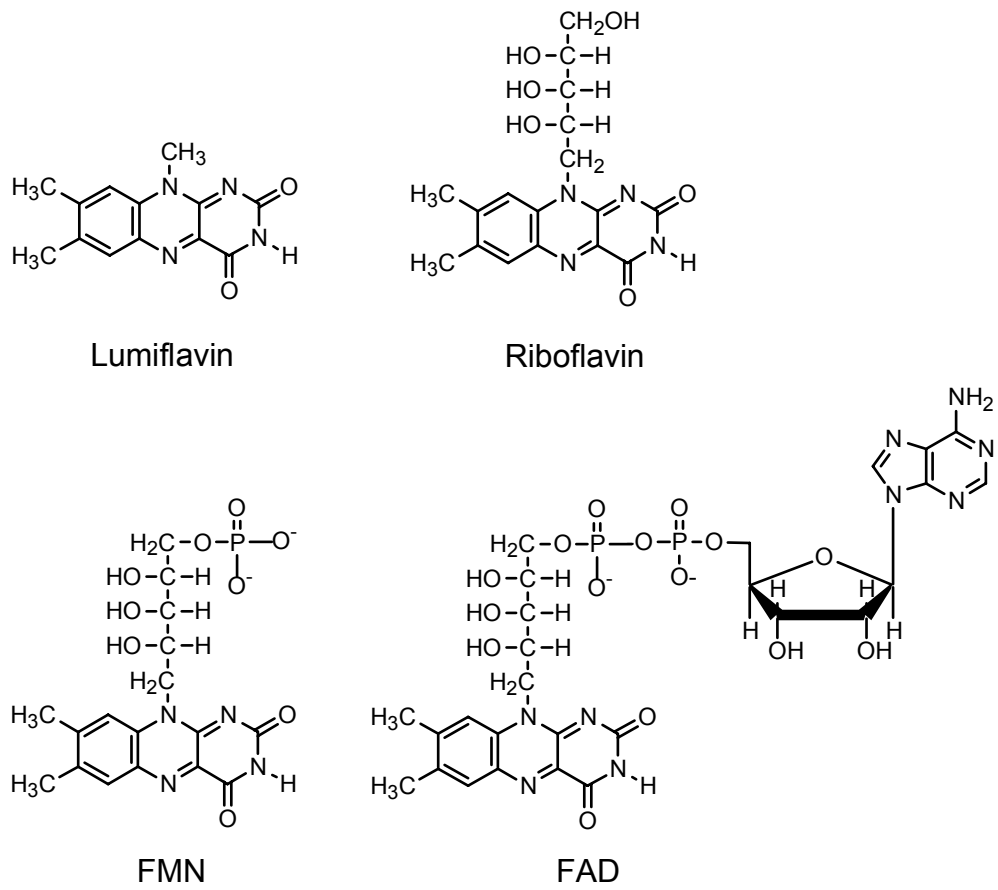


Figure 1.8. Structure of lumiflavin, riboflavin, FMN, and FAD molecules.



a ribityl sugar (Figure 1.8). Riboflavin, the most common flavin in nature, can be biosynthetically produced in lower organisms, but mammals have lost this ability and must obtain this compound from the diet to meet specific metabolic needs [31]. Riboflavin can be converted to FMN (flavin mononucleotide, figure 1.8) by flavokinase or riboflavin kinase (ATP: riboflavin 5'-phosphotransferase) [32]. FMN contains a phosphate residue in an ester linkage at the terminal hydroxyl group of the ribityl side chain. FMN can be further converted to FAD (flavin adenine dinucleotide, figure 1.8) by FAD synthetase (ATP: FMN adenylyltransferase) [32]. FAD is the condensation of FMN with an adenosine monophosphate [33]. The catalytic diversity of different flavin forms is due to specific interactions with the proteins with which they are bound.

Flavins can adopt three oxidation states, which are the oxidized (quinone), one electron reduced (semiquinone), and two electron reduced (hydroquinone) forms (Figure 1.9) [34]. Because of the existence of a semiquinone form, flavins are capable of accepting and donating either one or two electrons. This property endows flavins with catalytic versatility in biocatalysis. The reduced flavin either participates in electron transfer reactions or activates molecular oxygen for the oxygenation of a specific substrate. Interestingly, reduced flavin appears to be an important metal-free system involving the activation of molecular oxygen to generate hydroxylated products (oxygenase activity), peroxide  $\text{H}_2\text{O}_2$  (oxidase activity), or superoxide  $\text{O}^{2\cdot-}$  (electron transfer) [35].

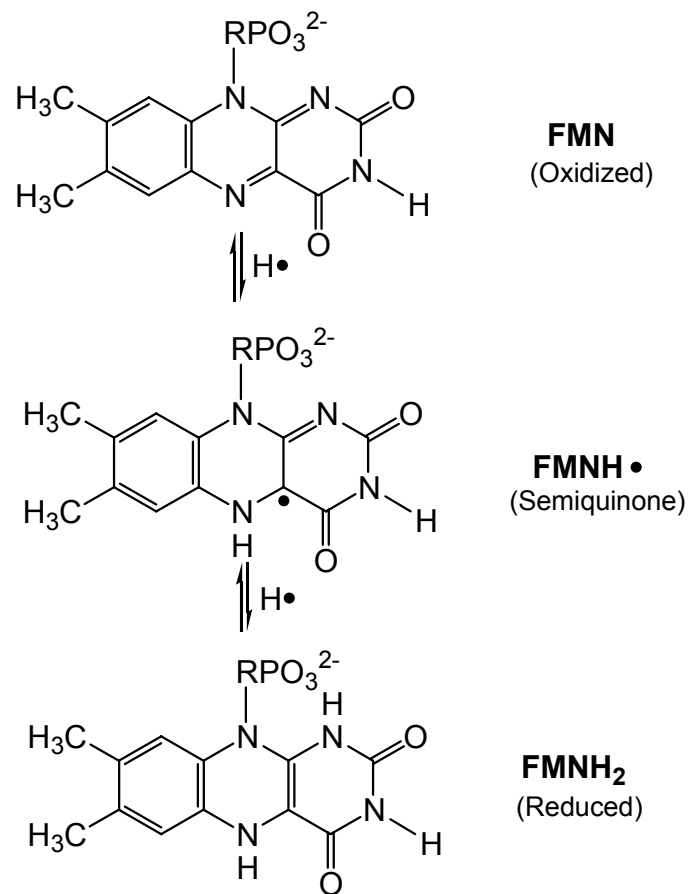


Figure 1.9. Oxidation states of flavin mononucleotide (FMN).

Flavins exhibit three characteristic spectra at different oxidation states (Figure 1.10), which has allowed for the spectroscopic characterization of different flavin intermediates in redox reactions [36]. Spectra in figure 1.10 represent oxidized flavin (spectrum 1), semiquinone flavin (spectrum 2), reduced flavin (spectrum 3), and free flavin (spectrum 4). Free or bound oxidized flavin has a characteristic absorption spectrum at 450 nm, and has fluorescence properties at maximum emission wavelengths of 520 nm. Semiquinone flavin has a weak absorbance at 450 nm and a peak absorbance around 370 nm. Although free semiquinone flavin has no fluorescent properties, fluorescent properties are often observed with flavin bound enzymes [37]. In contrast, the reduced flavin has no apparent absorbance in the visible wavelength range, and it is commonly assumed to be nonfluorescent under most experimental conditions. However, some exceptions are found for flavoenzymes at specific excitation wavelengths [38]. The fluorescence properties of reduced flavin is often determined by the buffer pH, viscosity of the solvent, substitutions on the isoalloxazine ring, and the local active site environment.

### *1.3.1 Physiological roles of flavins*

Apoflavoproteins usually exhibit specificity for a particular flavin form as the prosthetic group based on the enzyme environment. In most flavoproteins, flavin cofactors are tightly but noncovalently bound to the apoflavoproteins. A small number of flavins are covalently attached to the protein through the C(8 $\alpha$ ) or C(6) position of the isoalloxazine ring. The covalent linkage between the flavin and polypeptide is typically

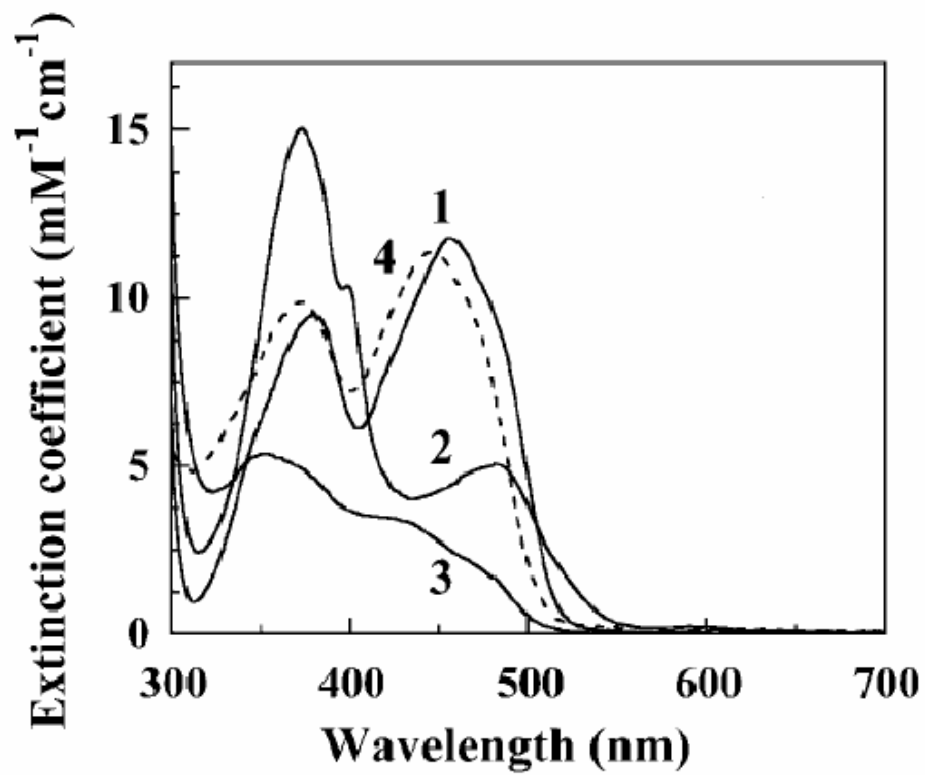


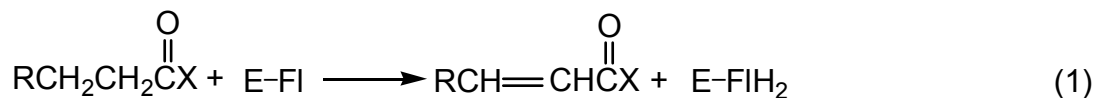
Figure 1.10. Flavin spectra at different oxidation states [36]

bridged by the 8 $\alpha$ -methyl of FMN or FAD linked to Tyr, His, or Cys [31]. The linkage to the C6 position of the flavin is restricted to Cys and FMN [39].

Flavoproteins are able to catalyze a wide variety of reactions. In general, they can be categorized into four classes according to the types of reactions they catalyze: dehydrogenases, oxygenases, oxidases, and reductases.

#### 1.3.1.1 Flavin dehydrogenases

The flavin dehydrogenases are able to catalyze reactions that transfer a pair of electrons and a proton from the substrate to the bound flavin cofactor (E-FI) resulting in the formation of C-C double bonds and the reduced flavoprotein (E-FIH<sub>2</sub>) (Eq. 1) [40].

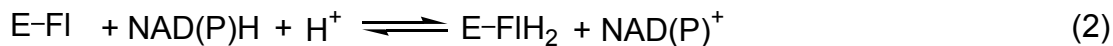


The reduced flavoprotein then donates the reducing equivalents to an electron acceptor. One example of flavoprotein mechanism in this category is acyl-CoA dehydrogenase involved in the oxidation of fatty acids to generate metabolic energy [33]. In the overall reaction, the acyl-CoA dehydrogenase oxidizes acyl-CoA thioesters to the corresponding enoyl-CoA esters, and the flavin cofactor is reduced. The reduced flavin cofactor is reoxidized by a one-electron transfer to another flavoprotein, and the oxidized flavin participates in the next cycle of fatty acid dehydrogenation. Another example is succinate dehydrogenase involved in the oxidation of succinate to fumarate in the Krebs citric acid cycle. Succinate dehydrogenase couples succinate oxidation with the reduction of the FAD cofactor that is covalently bound to the enzyme. The electrons from the

reduced FADH<sub>2</sub> are directly transferred to the iron-sulfur centers of the electron transport chain. Regeneration of oxidized FAD enables succinate dehydrogenase to enter the next round of dehydrogenation reactions.

### 1.3.1.2 Flavin oxygenases

This class of enzymes catalyze oxygen insertion reactions in a broad range of substrates. Generally, the flavin cofactor (E-FI) is reduced first by NAD(P)H (Eq. 2), and then the reduced flavoprotein (E-FIH<sub>2</sub>) activates molecular oxygen to form an active oxygen species to attack the substrate (S) (Eq. 3). As a result of oxygen molecule splitting, one oxygen atom is inserted into the substrate (SO) and the other oxygen atom is incorporated into water [41].



The distinguishing feature of this group of enzymes is that they form and stabilize the peroxyflavin (FI-OO<sup>•</sup>) or hydroperoxyflavin (FI-OOH) intermediate based on the type of reaction catalyzed. The bioluminescence reaction catalyzed by bacterial luciferase is proposed to occur through the formation of a peroxyflavin intermediate, and the peroxyflavin species performs a nucleophilic attack on the substrate to insert oxygen into the substrate (Figure 1.11). Another well-characterized example is cyclohexanone monooxygenase involved in the conversion of a cyclic ketone to lactone, a key step in the biodegradation of cyclohexanol [30, 42]. A series of pH-jump experiments confirmed

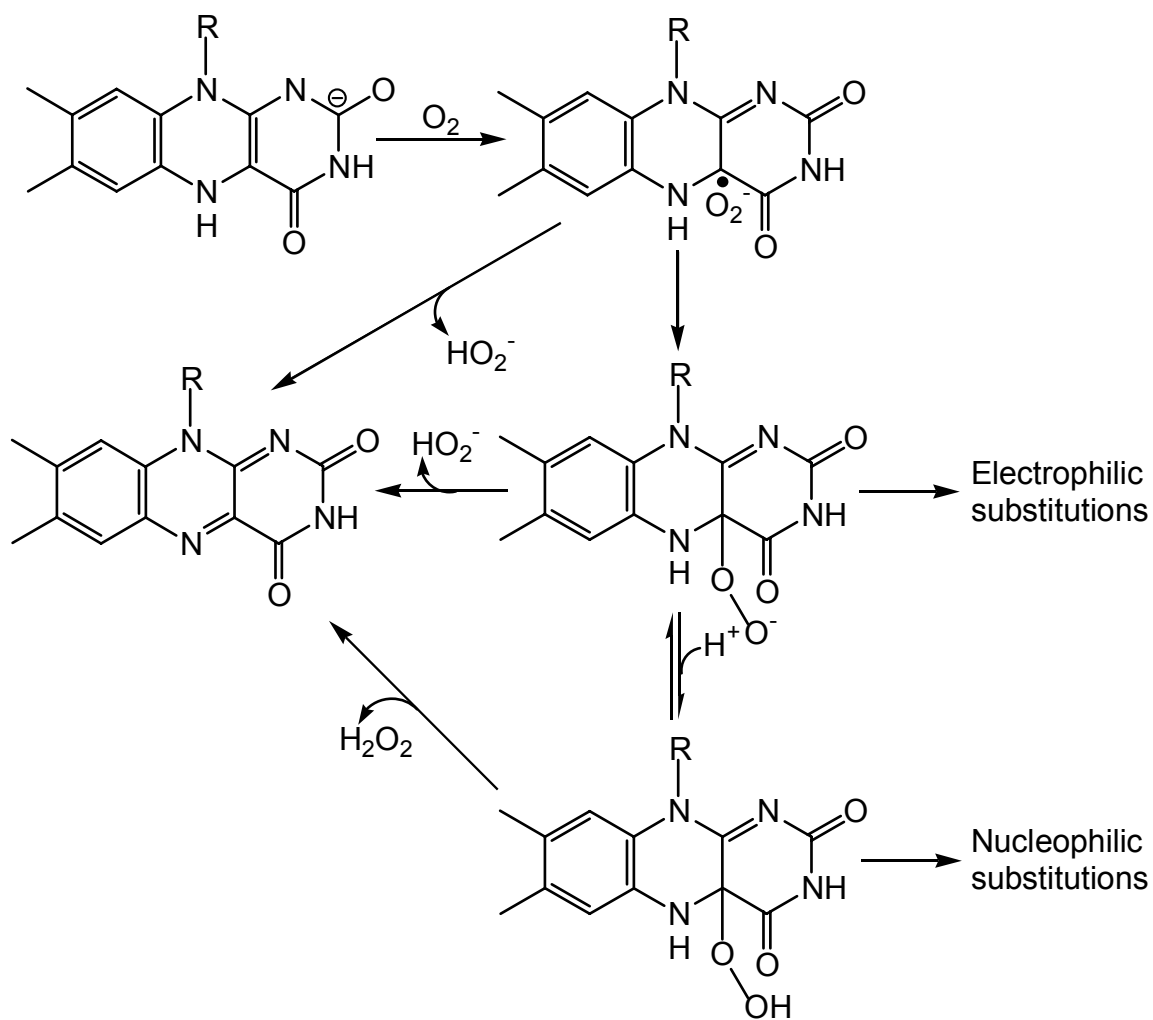


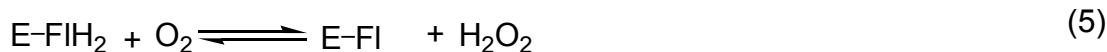
Figure 1.11. Mechanisms of activation of oxygen by reduced flavin [33].

that the anionic peroxyflavin participates in a nucleophilic attack on the substrate cyclohexanone resulting in the production of oxygenated  $\epsilon$ -caprolactone [30]. In contrast, *p*-hydroxybenzoate hydroxylase catalyzes the oxygenation of aromatic compounds, which is an important step in metabolic pathways involved in the degradation of aromatic compounds by microorganisms [43]. This enzyme forms a hydroperoxyflavin intermediate when reduced flavin activates oxygen, and the hydroperoxyflavin makes an electrophilic attack on the aromatic substrate to incorporate one atom of oxygen into the aromatic ring (Figure 1.11) [33, 44]. Another interesting feature of *p*-hydroxybenzoate hydroxylase is the control mechanism to prevent wasteful oxidation of NAD(P)H unless the aromatic substrate is present [42]. This control is exerted at the level of reduction of the flavin cofactor by NAD(P)H, which is 100-100,000 times faster when aromatic substrate is bound to the enzyme than when substrate is absent [42]. The mechanisms catalyzed by oxygenase enzymes is summarized in figure 1.11.

### 1.3.1.3 Flavin oxidases

Flavin oxidases can react with  $O_2$  rapidly, producing a high yield of  $H_2O_2$  in the oxidation of the substrate. Typically, the flavin cofactor (E-FI) of oxidases accepts two electrons from the substrate ( $SH_2$ ) (Eq. 4). The reduced flavin (E-FIH<sub>2</sub>) then forms the anionic flavosemiquinone as an intermediate in the single electron transfer to molecular oxygen with the concomitant formation of  $H_2O_2$  (Eq. 5). The formation of neutral or anionic flavosemiquinone is pH-dependent.

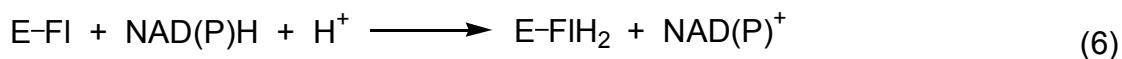




Glucose oxidase catalyzes the oxidation of  $\beta$ -D-glucose to D-glucono-1,5-lactone with the formation of hydrogen peroxide using molecular oxygen as the final electron acceptor. The production of hydrogen peroxide in peroxisomes has a protective effect against microorganisms [45-50]. Glycine oxidase is an oxidase involved in the oxidation of glycine with the formation of  $\text{H}_2\text{O}_2$ . The function of glycine oxidase is the deaminative oxidation of a wide range of amino acids to form the corresponding  $\alpha$ -keto acid [51]. The flavin amine oxidases catalyze the oxidation of amines via an oxidative cleavage of the  $\alpha$ -CH bond of the substrate to form an imine product with the concomitant reduction of the flavin cofactor [52]. The imine product is then hydrolyzed to the corresponding aldehyde and ammonia. The reduced flavin coenzyme reacts with oxygen to form  $\text{H}_2\text{O}_2$  and the oxidized flavin to complete the catalytic cycle.

#### *1.3.1.4 Flavin reductases*

Flavin reductases catalyze flavin (E-FI) reduction by the reduced pyridine nucleotide to form the reduced flavin (E-FIH<sub>2</sub>) and oxidized pyridine nucleotide (Eq. 6).



Flavin reductases are capable of generating reduced flavin by pyridine nucleotides to provide reducing power for diverse reactions. They can utilize flavin as a tightly bound

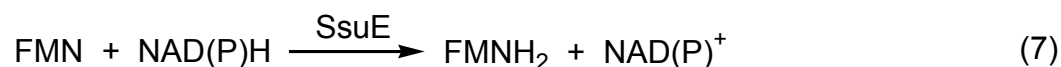
cofactor or a substrate, and they differ in pyridine nucleotide and flavin specificity [21, 26]. Flavin reductases are either specific for NADPH and/or NADH, and they also can utilize FMN and/or FAD [21-23, 53-56].

Bacterial flavin-dependent monooxygenase systems that utilize flavin as a substrate are an emerging class of enzymes. A unique property of this class of flavin reductases is that they do not contain a tightly bound flavin, but utilize flavin as a substrate. The flavin liberated from the polypeptide ensures an easy approach to all flavin reductases, so the living cells can obtain reducing equivalents when needed. The ability of flavin reductases to use flavin as a substrate provides versatility in numerous catalytic reactions. The two-component enzyme systems that have been identified are dependent on a flavin reductase to supply reduced flavin for subsequent reactions.

#### *1.4 Characterization of flavin reductase SsuE*

The SsuE flavin reductase catalyzes flavin reduction to supply reduced flavin to the monooxygenase enzyme SsuD, which is directly involved in the oxygenation of alkanesulfonate. SsuE was initially purified without an N-terminal tag, but the purified SsuE lost its activity [18]. An alternative method to obtain active SsuE was to express the protein as an N-terminal histidine-tagged fusion protein [18]. The SsuE purified by affinity chromatography was more pure and therefore more stable. The histidine-tagged SsuE protein showed no typical flavin spectrum, indicating that SsuE did not contain any flavin prosthetic group. The SsuE protein had a specific activity of 32.4 units/mg when monitoring pyridine nucleotide oxidation with a pH maximum of 7.9 [18]. SsuE

catalyzed an NAD(P)H-dependent reduction of FMN, FAD, or riboflavin (Figure 1. 12) [18], however, FMN was the preferred flavin substrate for SsuE. This is in good agreement with our results from flavin substrate specificity studies. The substrate specificity was also carried out with NADPH or NADH as the pyridine nucleotide substrate. The only difference between NADPH and NADH is the addition of a phosphate group at the 2' position as indicated in figure 1.13, however the catalytic efficiency was increased 300-fold when NADPH was used as a reducing reagent. Based on these observations, the preferred pyridine nucleotide substrate for SsuE was NADPH [18]. Conversely, the results from our group indicated that there is no significant difference in the catalytic efficiency of SsuE with either NADPH or NADH [57]. The SsuE catalyzed reaction is therefore summarized as the following equation (Eq. 7).



### *1.5 Steady-state reaction mechanisms*

The reaction catalyzed by SsuE involves two substrates with the generation of two products. Conventionally, reactions that require two substrates and yield two products are termed Bi Bi reactions. The mechanism of such reactions normally fall into two major mechanistic classifications: sequential and ping-pong reactions. The schematic presentations and diagnostic approaches to differentiate between these mechanisms will be discussed.

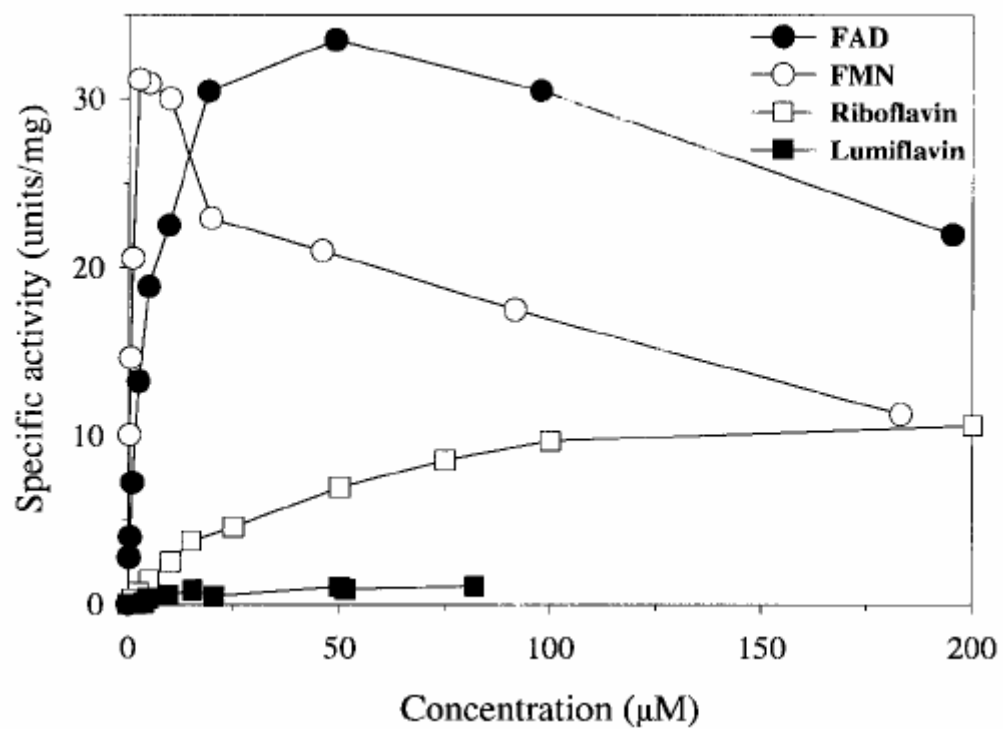


Figure 1.12. Activity of SsuE in the presence of various flavin substrates [18].

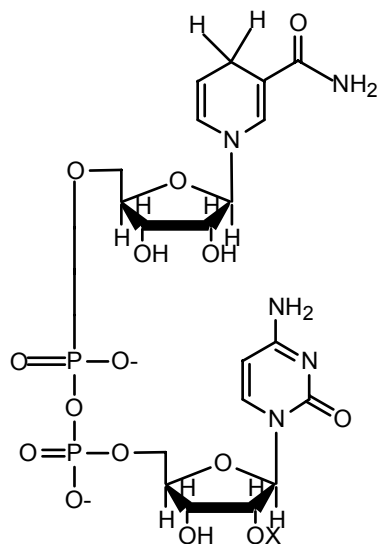


Figure 1. 13. Structure of NADPH ( $X=PO_3^{2-}$ ) and NADH ( $X=H$ ).

### 1.5.1 Sequential Bi Bi reactions

Reactions following sequential mechanisms can only occur after all the substrates bind to the enzyme. The sequential mechanism can be further separated into ordered and random mechanisms. Figure 1. 14 is the schematic description of these two mechanisms [34]. Ordered sequential reactions require substrate A binding to the enzyme first to prepare the binding site for the second substrate B. After the formation of a ternary complex, product P is released first, and Q is the last product to dissociate. If a Bi Bi reaction falls into a random mechanism, substrates A and B bind to the enzyme without a compulsory order. Neither substrate affects the binding of the other and product release can occur in any order. There is no preference for the order of substrate binding and product release.

To determine if a Bi Bi reaction follows a sequential mechanism, the initial rates are plotted versus the substrate concentration. Double-reciprocal plots of the data intersect to the left of the Y-axis (Figure1.15) [34], and the data are further fitted to an equation for a sequential mechanism. If the points intersect on the x-axis, the  $K_s$  (dissociation constant) equals  $K_M$ . Whereas, points above or below the x-axis represent a  $K_s$  value  $>$  or  $<$  than  $K_M$ , respectively. However, they do not distinguish between an ordered or random sequential mechanism. A practical method to differentiate between these two mechanisms is through product inhibition studies. If double-reciprocal plots of the initial rate versus substrate concentration with fixed inhibitor concentrations intersect on the y- axis (Figure 1.16), the inhibitor is competitive. This suggests that the reaction

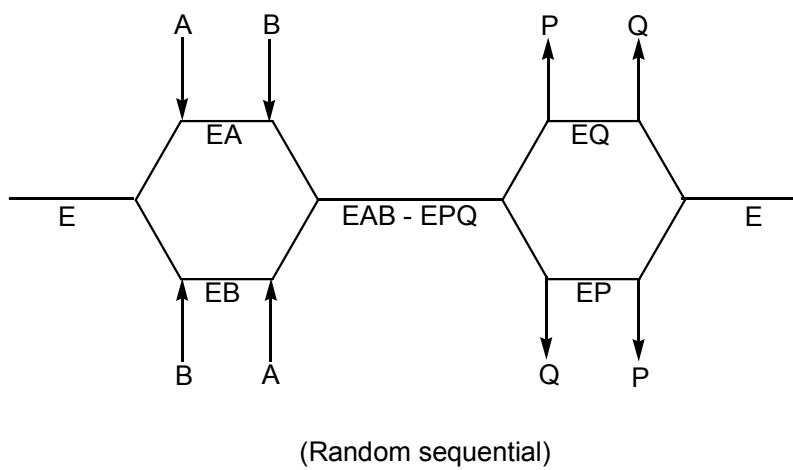
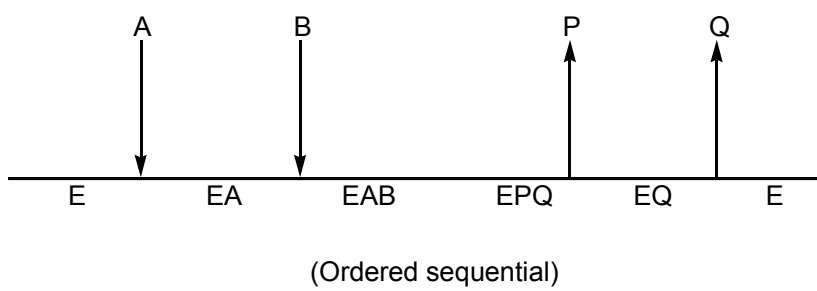


Figure 1.14. Scheme of Bi Bi sequential reaction mechanisms.

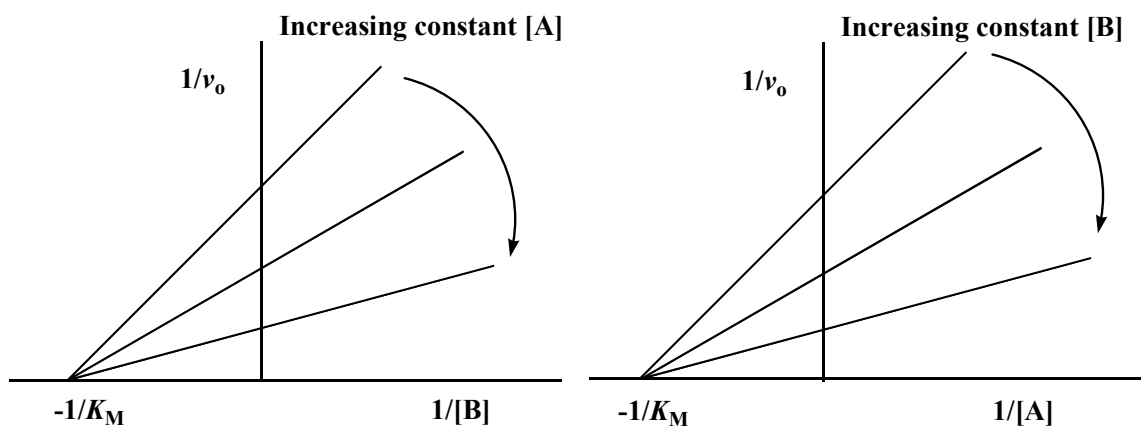


Figure 1.15. Double-reciprocal plots of a sequential mechanism.



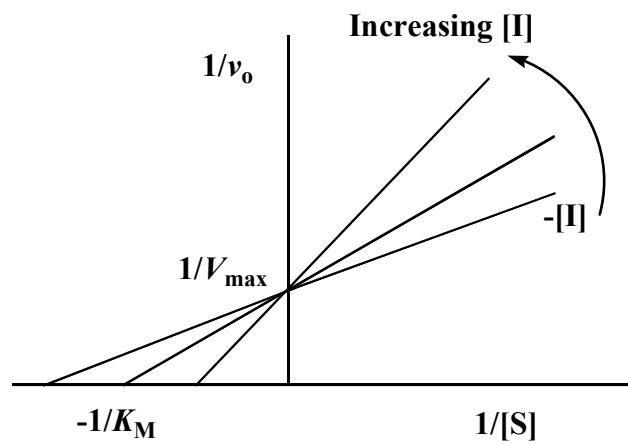


Figure 1. 16. Double-reciprocal plot of a competitive inhibition.

follows an ordered sequential mechanism, and the product which is released last competes with the first substrate for the free enzyme. In contrast, if the double-reciprocal plots of the initial rate versus substrate concentration with fixed inhibitor concentrations are parallel to each other, the inhibitor is a uncompetitive inhibitor. The Bi Bi reaction then follows a random sequential mechanism with no preference for the order of substrate binding and product release.

### *1.5.2 Ping pong Bi Bi reactions*

Ping pong Bi Bi reactions involve the binding of one substrate to the enzyme first, followed by product release. The second substrate then binds to the enzyme, followed by the release of the second product. In a ping pong Bi Bi reaction mechanism, the first product is released prior to the binding of the second substrate [34]. The kinetic diagnostic approach for this type of reaction mechanism is to plot the initial rates against the substrate concentrations. A set of double-reciprocal plots that are parallel to each other represent a ping pong mechanism, and the data are further fitted to an equation for a ping pong mechanism.

### *1.5.3 The steady-state mechanism of flavin reductases*

For flavin reductase catalyzed reactions, steady-state kinetic studies have provided information on the kinetic mechanisms of the reaction. Flavin reductases include standard flavoproteins containing flavin prosthetic groups and proteins utilizing flavin as a substrate rather than a tightly bound cofactor. One example of an FMN

reductase which contains a tightly bound FMN, and utilizes NADPH as the pyridine nucleotide is the flavin reductase, FRP, from *Vibrio harveyi*. The reduced FMNH<sub>2</sub> substrate required by bacterial luciferase is provided by FRP [17]. This enzyme catalyzes the reduction of FMN by NADPH, and exhibits a ping-pong kinetic reaction mechanism [17, 58-60]. In this reaction scheme, NADPH binds to the enzyme first, resulting in the reduction of the flavin cofactor by NADPH. Following the release of NADP<sup>+</sup>, a second FMN binds to the enzyme active site, exchanging the reducing equivalent with the bound FMNH<sub>2</sub> cofactor. The second FMNH<sub>2</sub> is released, and the oxidized enzyme is regenerated [58].

Other FMN reductases do not contain a tightly bound flavin and utilize flavin as a cosubstrate. An example is the flavin reductase, Fre, which is involved in the activation of ribonucleotide reductase. The reduction of riboflavin by NAD(P)H or NADH follows an ordered sequential mechanism (figure 1.17) [61]. In the overall reaction scheme, NAD(P)H binds to the active site first, followed by riboflavin to form a ternary complex. After the reduction of flavin, the reduced flavin is released first, and NAD(P)<sup>+</sup> is the last product to dissociate.

In the strict two-component systems the flavin reductases are directly coupled to the monooxygenase enzyme. Flavin reductases from this group include reductases that contain tightly bound flavin cofactors or utilize flavin as a substrate. EDTA monooxygenase requires the flavin reductase to supply reduced flavin, and this flavin reductase contains a tightly bound flavin cofactor [19]. Whereas, 4-hydroxyphenylacetate 3-monooxygenase is coupled to a flavin reductase that utilizes flavin as a substrate [26]. Although the different classes of flavin reductases follow different reaction mechanisms,

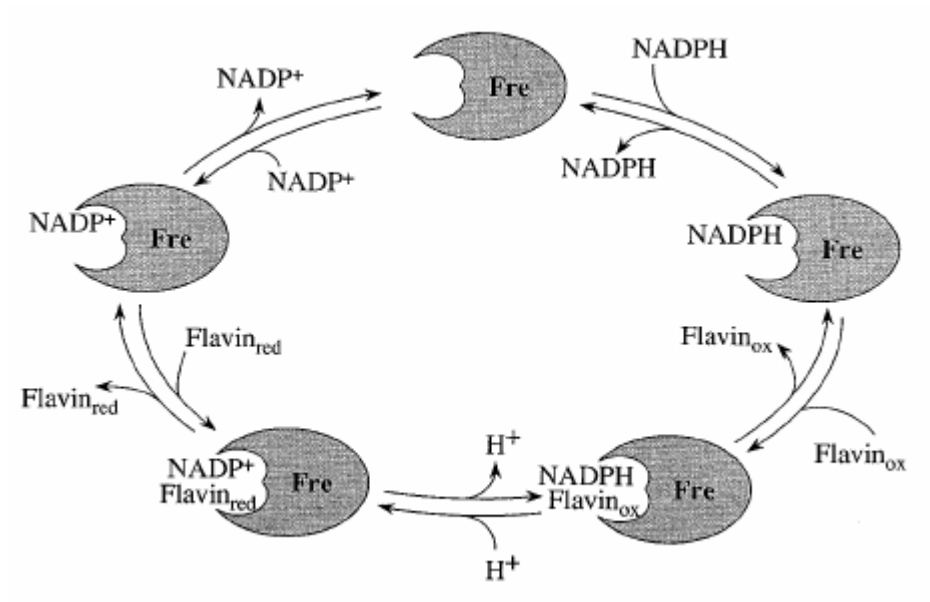


Figure 1.17. Proposed reaction mechanism of the flavin reductase Fre [61].

they are all involved in providing reducing equivalents (FMNH<sub>2</sub>) for a diverse set of reactions.

### *1.6 Pre-steady-state kinetic mechanisms of flavin reductases*

In order to measure the rate constants of individual steps and detect transient intermediates, it is necessary to monitor the reaction as it approaches steady-state [62]. Pre-steady-state kinetic analyses is used to detect transient enzyme-bound species as they form and decay under single enzyme turnover conditions. A method must be employed that allows the rapid mixing of enzyme and substrate(s), as well as, monitoring the spectroscopic properties of reaction intermediate(s). Stopped-flow instrumentation has been designed to allow rapid mixing, and most intermediates demonstrate characteristic absorptions at specific wavelengths.

Rapid reaction kinetic analyses have shown that proteins in the FNR (ferredoxin-NADP<sup>+</sup> reductase) family with a tightly bound flavin prosthetic group form a characteristic charge-transfer complex during flavin reduction [63-67]. Similarly, flavin reduction catalyzed by certain flavin reductases that utilize flavin as a substrate demonstrated the formation of charge-transfer complex [68, 69]. A weak long-wavelength absorption increase was observed when Fre enzyme was mixed with riboflavin and NADPH [68]. Results from single-wavelength studies at 550 nm identified three distinct phases for flavin reduction by Fre (Figure 1.18) [68]. The initial reaction phase represented a charge-transfer complex (CT-1) between riboflavin and NADPH. The next charge-transfer complex (CT-2) is the second reaction phase between reduced riboflavin and NADP<sup>+</sup>. The second charge-transfer complex decays to the Michaelis complex followed by product release from the enzyme. The flavin reductase (ActVB)

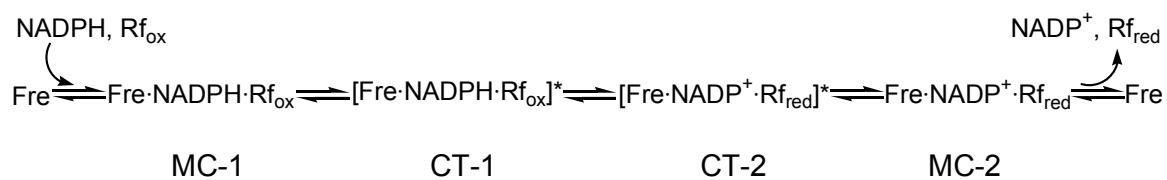


Figure 1.18. Charge-transfer complex formation of Fre [68].

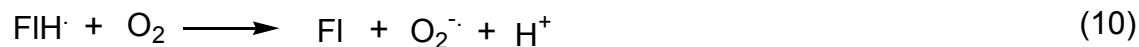
from a two-component system involved in actinorhodin biosynthesis was also shown to produce a broad absorbance band between 550 and 800 nm following titration of the enzyme with reduced FMN in the presence of  $\text{NAD}^+$  [69]. The ActVB protein is responsible for providing reduced flavin to the flavin monooxygenase ActVA. It is evident that flavin reductases that utilize flavin as a substrate rather than a bound prosthetic group share a common mechanism of hydride transfer. Therefore charge-transfer complex formation plays an important role in reductive half-reactions catalyzed by flavin reductase enzymes.

### *1.7 The flavin transfer mechanism in two-component monooxygenase system*

Reduced flavin transfer between two proteins is a rather unique mechanistic model for flavin utilization because flavin cofactors are typically bound to proteins through noncovalent or covalent interactions. Bacterial flavin dependent monooxygenases that utilize reduced flavin as a substrate are continually emerging. All of these two-component enzyme systems rely on a flavin reductase and a monooxygenase enzyme for catalytic activity. An important area of interest in these two-component systems is the mechanism of reduced flavin transfer between the FMN reductase and monooxygenase enzyme.

#### *1.7.1 Flavin stability*

Reduced flavin is very unstable, and it can be oxidized rapidly through autooxidation. When reduced flavin is exposed to oxygen, the formation of oxidized flavin is autocatalytic with the accumulation of more reactive species, especially flavin radicals and superoxide anions,  $\text{O}_2^-$  [42, 70, 71]. The following steps briefly describe the flavin oxidation process (Eqs. 8-11) [70-73].



The reduced flavin (FIH<sub>2</sub>) is initially oxidized by oxygen to generate oxidized flavin (FI) and hydrogen peroxide (H<sub>2</sub>O<sub>2</sub>) (Eq. 8). Even though this step proceeds slowly, as soon as a small percentage of oxidized flavin is formed, a one-electron transfer between FIH<sub>2</sub> and FI leads to the formation of two flavin semiquinone molecules (FIH·) (Eq. 9). One flavin semiquinone subsequently reacts with oxygen to generate oxidized flavin and superoxide radicals (O<sub>2</sub><sup>·-</sup>) (Eq. 10). The other flavin semiquinone then reacts with a superoxide radical to form oxidized flavin and hydrogen peroxide (Eq. 11). The estimated half-life of reduced flavin is only about 25 ms [73]. In order to prevent the generation of harmful radicals, reduced flavin transfer must be tightly controlled between the flavin reductase and monooxygenase enzyme. From previous studies of two-component systems, three flavin transfer mechanisms have been proposed between the two enzyme components: direct flavin transfer, flavin diffusion, and mixed flavin transfer mechanisms. The detailed mechanisms of flavin transfer will be discussed in the following sections.

### 1.7.2 Direct flavin transfer mechanism

Because reduced flavin can be rapidly oxidized generating oxygen radicals, the mechanism involving direct transfer of reduced flavin would be more favorable in a cellular system. Direct protein-protein interactions have been physically identified between *Vibrio harveyi* luciferase and FRP [74]. Fluorescent labeling studies showed



that the monomeric form of FRP was able to form a complex with the luciferase enzyme. Steady-state kinetic analyses were performed with *V. harveyi* luciferase coupled to FRP, and *Vibrio fischeri* luciferase coupled to NAD(P)H-utilizing flavin reductase (FRG) to characterize the mechanism of flavin transfer [17, 58]. The first kinetic evidence for protein-protein interaction was that the  $K_{m,FMN}$  and  $K_{m,NAD(P)H}$  for flavin reductase FRP and FRG in the luciferase-coupled luminescence assay are significantly lower than those observed in single-enzyme assays when measuring NADPH oxidation. The altered kinetic parameter in the coupled assay is an indication of a complex formation between luciferase and flavin reductase. In addition, a ping-pong kinetic pattern in single-enzyme assays of FRP was changed to a sequential pattern when coupled to luciferase [58], further supporting the formation of a protein-protein complex during the catalytic reaction.

Flavin transfer between the flavin reductase (SsuE) and monooxygenase (SsuD) has also been studied by our group through several biophysical approaches [75]. Results from pull-down experiments showed a stable complex is formed between SsuE and SsuD. Fluorescence titrations of FMN-bound SsuE with SsuD monitoring the increase in fluorescent intensity on protein-protein interactions gave a  $K_d$  value of 0.002  $\mu$ M. These results taken together support the formation of static protein-protein interaction between two enzyme components. In addition, the kinetic mechanism of SsuE in the single-enzyme is altered when coupled with SsuD and octanesulfonate [57]. This altered mechanism is indicative of protein interactions between SsuE and SsuD during flavin transfer.

### 1.7.3 Flavin diffusion mechanism

An alternative mechanism for flavin transfer involves the diffusion of reduced flavin between two enzyme components. Results from size-exclusion chromatography and kinetic analysis between FAD reductase and 4-hydroxyphenylacetate 3-monooxygenase ruled out any protein-protein interactions [76]. Flavin transfer for this enzyme system is said to occur through the diffusion of the reduced flavin to the monooxygenase enzyme due to the high affinity of the monooxygenase enzyme for FADH<sub>2</sub> coupled with a high concentration of the monooxygenase enzyme in the cell. The high enzyme concentration and high affinity for FADH<sub>2</sub> ensures the rapid and tight binding of reduced flavin to the monooxygenase to protect the reduced flavin from autooxidation. A flavin diffusion mechanism is further supported by the ability of the monooxygenase to utilize reduced flavin provided by flavin reductases from other systems [77]. Additional support for a diffusion mechanism has been demonstrated with the two-component phenol hydroxylase system from *E. coli* and *A. baumannii* (78-81). Evidence for a diffusion mechanism was based on the ability of the oxygenase component to use chemically reduced flavin for the monooxygenation reaction in the absence of the flavin reductase. Therefore, physical interactions between the reductase and monooxygenase component were not required for substrate hydroxylation [26, 82]. It was further shown through gel filtration and analytical ultracentrifugation studies that the reductase and monooxygenase components do not form stable complexes at equilibrium [27, 76]. Studies on a two-component flavin dependent monooxygenase involved in actinorhodin biosynthesis showed no evidence for complex formation between the two protein components by pull down experiments [77]. In addition, the dissociation

constants of oxidized flavin and reduced flavin with the flavin reductase (ActVB) and monooxygenase (ActVA) demonstrated a strong binding of reduced flavin to ActVA when compared to ActVB. Based on these results a flavin transfer mechanism by a diffusion mechanism was favored [77].

#### *1.7.4 Mixed flavin transfer*

Recent studies on the styrene monooxygenase system demonstrated an alternative flavin transfer mechanism between the NADH-specific flavin reductase (SMOB) and FAD-specific styrene epoxidase (SMOA). Based on the numerical simulation of the steady-state data, a model was established involving both direct flavin transfer and passive diffusion from SMOB to SMOA [83]. The AMP moiety of FAD is a critical structural motif in the recognition and binding of FAD to SMOA, because SMOA only utilizes FAD during catalysis. SMOB may form a transient flavin-transfer complex with SMOA in which the AMP moiety is associated with SMOA and the isoalloxazine ring is associated with SMOB (Figure 1.19). The release of the isoalloxazine ring from SMOB would ensure effective transfer to the active site of SMOA, and reduce the interaction of reduced flavin with molecular oxygen.

Generally, the two-component monooxygenase systems catalyze two separate reactions that can be kinetically studied independently for each component. The single enzymatic assay and the coupled assay with both enzymes could kinetically distinguish how flavin is delivered. If the enzyme kinetic mechanism is altered with the second component present, it indicates that two proteins interact, supporting a channeling mechanism for flavin transfer.

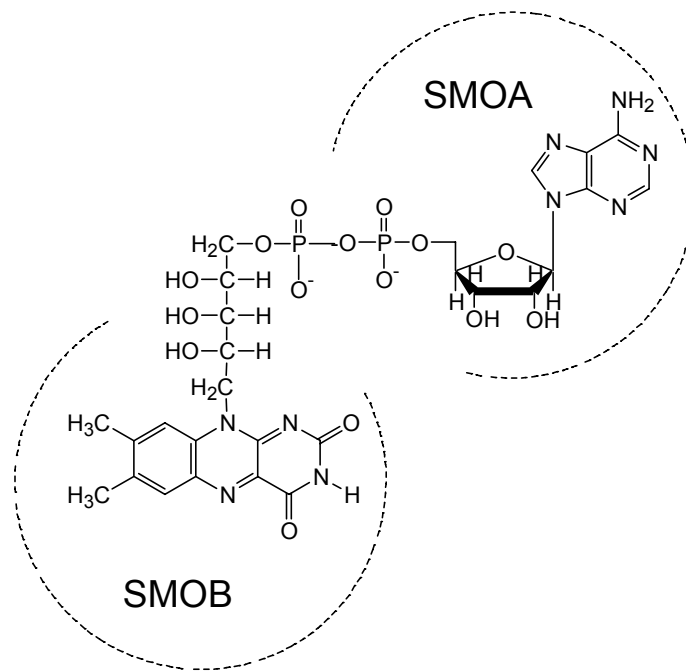


Figure 1.19. Model of transient flavin transfer [83].

### *1.8 Summary*

Flavin, with the characteristic isoalloxazine ring structure, plays an important role in biocatalysis. With respect to flavin binding, flavin either functions as a tightly bound prosthetic group or a diffusible substrate. Flavoenzymes are involved in a broad range of reactions ranging from dehydrogenation, oxidation, oxygenation, and electron transfer. Recently, flavin reductases utilizing flavin as a substrate have emerged, and have been shown to catalyze a broad range of biologically significant reactions. In two-component systems, flavin reductases provide reduced flavin for the oxygenase enzyme. With so many reactions dependent on reduced flavin, kinetic studies on flavin reductase enzymes are of high importance. The two-component alkanesulfonate monooxygenase is a unique system involved in sulfur metabolism. First, this system is involved in the unique cleavage of a C-S bond from a broad range of alkanesulfonate substrates. Second, this two-component system involves the transfer of reduced flavin from the flavin reductase to the monooxygenase enzyme. Single enzyme kinetic studies on the flavin reductase will provide information on the catalytic mechanism of flavin reduction. Coupled assays with the monooxygenase component included in the reaction could reveal the flavin transfer mechanism between the two protein components. The detailed kinetic studies performed on the flavin reductase from the alkanesulfonate monooxygenase system are described in this dissertation.

## CHAPTER TWO

### MATERIALS AND METHODS

#### *2.1 Biochemical and chemical reagents*

FMN, NADPH, NADP<sup>+</sup>, potassium phosphate (monobasic anhydrous and dibasic anhydrous), Tris base, sodium chloride, ampicillin, streptomycin sulfate, glucose, glucose oxidase, dithiothreitol (DTT), 2-propanol-d<sub>8</sub>, NADP<sup>+</sup>-dependent alcohol dehydrogenase from *Thermoanaerobium brockii*, lysozyme, lysine, phenylalanine, threonine, isoleucine, leucine, valine, selenomethionine, riboflavin, nicotinamide, pyridoxine hydrochloride, and thiamine hydrochloride were from Sigma (St. Louis, MO). Isopropyl-β-D-thiogalactoside (IPTG), 2-propanol, absolute ethanol, glycerol, ammonium chloride, calcium chloride, magnesium sulfate, and ammonium sulfate were purchased from Fisher Biotech (Pittsburgh, PA). Octanesulfonate was from Fluka (Milwaukee, WI). LB medium was from BIO 101 Systems (Carlsbad, CA). Phenyl Sepharose column matrix was from Amersham Biosciences (Piscataway, NJ). Macro-prep High Q Support was from BIO-RAD (Hercules, CA). All buffers and media solution were prepared using water purified at a resistance of 18.2 MΩ/cm through a Millipore system (MilliQ, QPAK II). Standard buffer contains 25 mM potassium phosphate, pH 7.5, and 10% glycerol unless otherwise noted.

## 2.2 Construction of expression vectors

### 2.2.1 The T7 RNA polymerase-dependent expression system

The T7 RNA polymerase-dependent expression vector pET21a (Novagen, Madison, WI) was selected for cloning the *ssuE* and *ssuD* genes (Figure 2.1). The pET21a expression plasmid is under control of the T7 promoter and *lac* operator. For selection purposes, the pET21a vector also encodes an ampicillin resistance gene that allows for growth of cells on media containing ampicillin. T7 RNA polymerase is synthesized from the host chromosome, and binds to the T7 promoter upstream of the target gene. The expression of the T7 RNA polymerase is under control of the *lac* operator. Normally, the *lac* repressor binds to the *lac* operator, and physically blocks the transcription of the target gene. Here IPTG is used as a lactose analog which works as an inducer for the transcription of T7 RNA polymerase and the target gene. The transcription of the target gene is further controlled by a *lac* operator engineered between the T7 promoter and the target gene. When the IPTG is introduced into the medium, it binds to the *lac* repressor, resulting in the repressor dissociating from the operator, and then T7 RNA polymerase is expressed. Subsequently, T7 RNA polymerase binds to the T7 promoter permitting the transcription and subsequent translation of the target gene.

### 2.2.2 Construction of expression vectors

The individual cloning of the alkanesulfonate monooxygenase genes into an expression vector was performed utilizing the Seamless Cloning System. For the cloning of *ssuE*, the pET21a was amplified using the primers (5' CAG TCA CTC TTC CCA TAT GTA TAT CTC CTT CTT) and (5' GCT TGC CTC TTC ACT CGA GCA CCA CCA CCA CCA) and included the *Eam*1104 I restriction sites to produce *Nde* I and *Xho* I

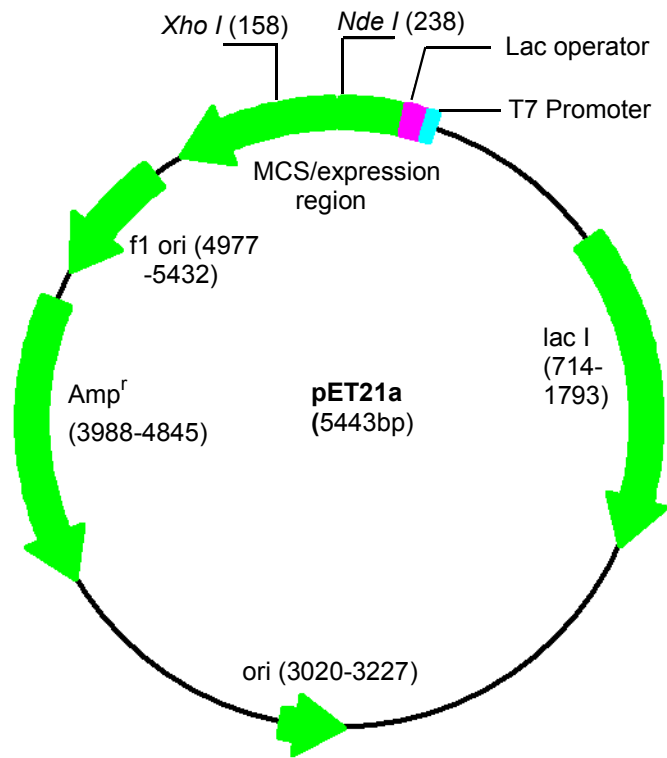


Figure 2.1. The pET21a vector expression system.



overhangs following digestion with the enzyme. The *ssuE* and *ssuD* genes were obtained from genomic DNA prepared from *E. coli* strain K12. The *ssuE* gene was PCR-amplified using the primers (5' ATA AGG CTC TTC TAT GCG TGT CAT CAC CCT G) and (5' CAG TTT CTC TTC GGA GTT ACG CAT GGG CAT T) which included the *Eam1104* I restriction sites and engineered to produce *Nde* I and *Xho* I overhangs following digestion by *Eam1104* I for ligation into the pET21a expression vector. The *ssuD* gene was amplified using the primers (5' AAG GAA CTC TTC TAT GAG TCT GAA TAT G) and (5' TGC CAT CCT TCT GAG TTA GCT TTG CGC CAC) which included the *Eam1104* I restriction sites and engineered to contain *Nde* I and *Xho* I overhangs following digestion by *Eam1104* I for ligation into the pET21a expression vector. The overall process of expression vector construction is represented in Figure 2.2.

DNA vectors containing representative clones were transformed into *E. coli* XL1-Blue supercompetent cells by standard transformation procedures. The *E. coli* XL1-Blue strain was used for amplification and purification of plasmid DNA. Plasmids containing representative clones were submitted for sequence analysis at Davis Sequencing (University of California, Davis). Plasmids containing either *ssuE* or *ssuD* were transformed into BL21(DE3) competent cells for expression of the target gene.

### *2.3 Expression and purification of the alkanesulfonate monooxygenase proteins*

#### *2.3.1 Expression of the alkanesulfonate monooxygenase proteins*

Cells from frozen stocks were isolated on LB-agar plates containing 100 µg/mL ampicillin (LB-Amp). A single colony of *E. coli* BL21(DE3) containing the appropriate expression plasmid was used to inoculate 5 mL LB-Amp media which were incubated 7

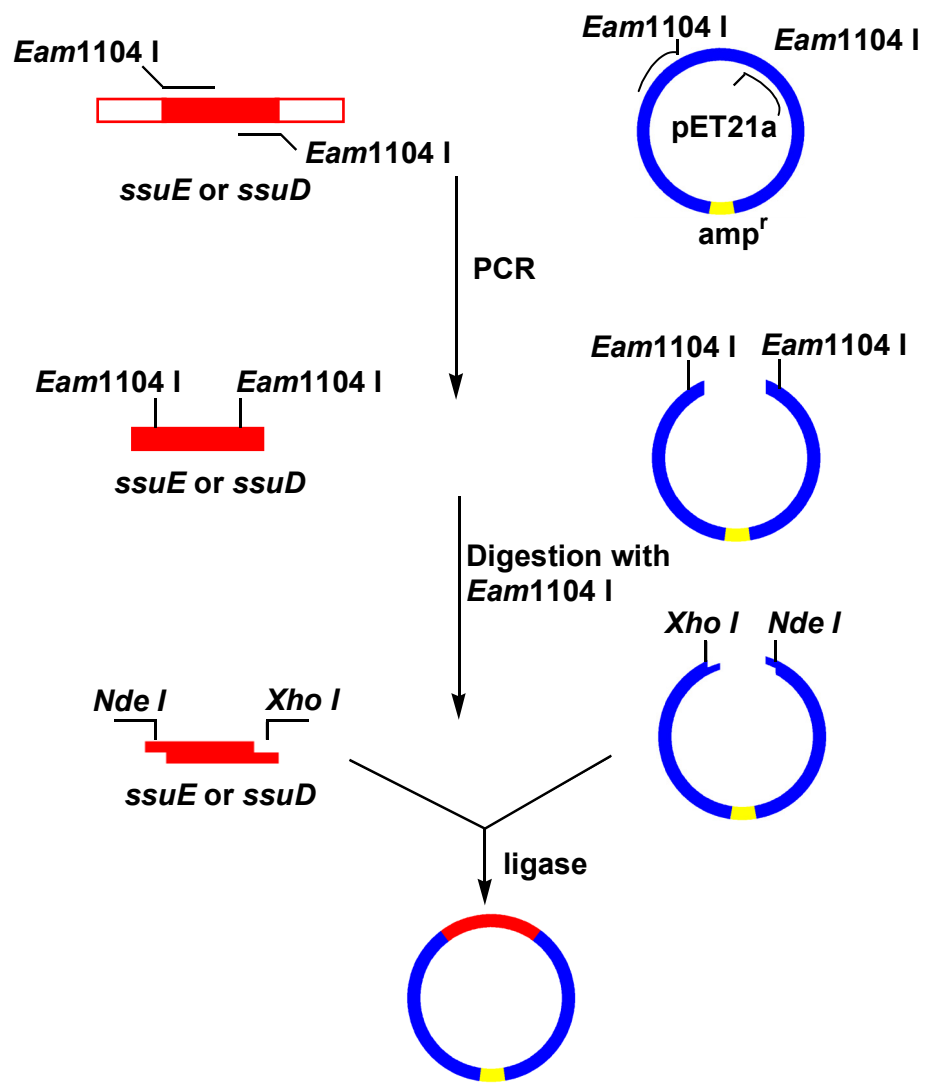


Figure 2.2. Cloning of alkanesulfonate monooxygenase genes (*ssuE* and *ssuD*).

hours at 37 °C. A 1% inoculum of the 5 mL culture was used to inoculate 100 mL of LB-Amp media which was incubated overnight at 37 °C, and used to inoculate two 1 L flasks of LB-Amp media. When the  $A_{600}$  value reached 0.8-0.9 for SsuE and 0.4-0.5 for SsuD the flasks were moved from 37 °C to 18 °C, and isopropyl- $\beta$ -D-thiogalactoside (IPTG) was added to a final concentration of 0.4 mM. The incubation was continued for 6 h and cells were harvested by centrifugation at 5000 x g for 15 min and stored at -80 °C overnight.

### *2.3.2 Purification of SsuE protein*

For the purification of SsuE, cells from the 2 L growth were resuspended in 100 mL standard buffer containing 4  $\mu$ g/mL lysozyme. Cell lysis was performed by sonication, followed by the addition of 1.5% streptomycin sulfate to precipitate nucleic acids. Ammonium sulfate precipitation was from 20% to 45%. The pelleted protein from the 45% ammonium sulfate precipitation was resuspended in 150 mL standard buffer with 20% ammonium sulfate, and loaded onto the phenyl sepharose column. After washing the column with 20% ammonium sulfate buffer, the protein was eluted with a linear gradient from 20% to 0% ammonium sulfate in standard buffer (300 mL total volume), followed by isocratic elution with standard buffer. Fractions containing large  $A_{280}$  values were pooled and loaded onto a macro-prep high Q column. After washing the column with standard buffer, the protein was eluted with a linear gradient from 0 to 300 mM NaCl in standard buffer. Fractions determined to be pure by SDS-polyacrylamide gel electrophoresis (SDS-PAGE) were pooled, precipitated with 45% ammonium sulfate and resuspended in standard buffer containing 100 mM NaCl. The resuspended protein pellet was pooled, dialyzed against standard buffer containing 100 mM NaCl, aliquoted, frozen

and stored at  $-80^{\circ}\text{C}$  until needed.

### *2.3.3 Purification of the SsuD protein*

The procedure for the purification of the SsuD protein was similar to the purification for SsuE with the following modifications. Ammonium sulfate precipitation was from 30% to 60%. The pelleted protein from the 60% ammonium sulfate precipitation was resuspended in 50 mL standard buffer, dialyzed against the standard buffer, and loaded onto a macro-prep high Q column. After washing the column with standard buffer, the protein was eluted with a linear gradient from 0 to 300 mM NaCl in standard buffer. Fractions containing large  $A_{280}$  values were pooled and 20% ammonium sulfate was added before loading onto a phenyl sepharose column. After washing the column with 20% ammonium sulfate buffer, the protein was eluted with a linear gradient from 20% ammonium sulfate to 0% in standard buffer (300 mL total volume), followed by isocratic elution with standard buffer. Fractions determined to be pure by SDS-PAGE were pooled, precipitated with 60% ammonium sulfate, and resuspended in standard buffer containing 100 mM NaCl. The resuspended protein pellet was pooled, dialyzed against standard buffer containing 100 mM NaCl, aliquoted, frozen and stored at  $-80^{\circ}\text{C}$ .

## *2.4 Determination of molecular weight and quaternary structure of SsuE and SsuD*

### *2.4.1 Molecular weight determination of SsuE and SsuD*

Electrospray ionization mass spectrometry, ESIMS, was performed on SsuE and SsuD proteins to determine their precise molecular weights. ESIMS determinations were made on a VG Quattro II triple quadrupole mass spectrometer from Micromass in the GC-Mass Spectrometry Laboratory at Wake Forest University School of Medicine. Samples containing approximately 5 nmol of protein were concentrated and rediluted three times

with deionized water in a Millipore Ultrafree centrifugation filter to replace the buffer components. After the sample preparation, mass spectrometry measurements were recorded for SsuE and SsuD respectively.

#### *2.4.2 Quaternary structure determination of SsuE and SsuD*

Sedimentation velocity experiments of SsuE and SsuD proteins were carried out at 36,000 rpm, and data were collected at 280 nm in a continuous mode. The sample was placed in a sector-shaped cavity sandwiched between two quartz windows. Double sector cells were also used to correct the absorbance of the sample solvent. A series of samples of SsuD (5.3-16  $\mu\text{M}$ ) or SsuE (12.3-47  $\mu\text{M}$ ) were centrifuged, and the absorbance recorded during the sedimentation. Ten consecutive data sets were analyzed by DCDT software to give a  $g^*$  (s) distribution [84], and the data was fit to a single Gaussian to obtain a  $g^*$  value. This value corresponds with the multimeric molecular weight of SsuD or SsuE. The molecular weight combined with the mass spectrometric analysis of the single subunit yielded the number of subunits.

#### *2.5 Substrate specificity assay*

The activity of SsuE was assayed by monitoring the absorbance decrease at 340 nm due to the oxidation of pyridine nucleotides at 25 °C. The initial velocity is defined as nanomoles of NADPH oxidized per minute per nanomole of SsuE protein. Each assay measured the oxidation of pyridine nucleotides by SsuE in the presence of substrates (pyridine nucleotides and flavins). The background rate due to autooxidation of NADPH was taken into account when determining the rate.

To compare the flavin substrate specificity of FMN and FAD, assays were carried out with 0.01  $\mu\text{M}$  SsuE, 200  $\mu\text{M}$  NADPH and varying concentrations of FMN (0.01-1.0

$\mu\text{M}$ ) or FAD (0.05-80  $\mu\text{M}$ ) in 25 mM potassium phosphate buffer, pH 7.5, 10% glycerol, and 100 mM NaCl at 25 °C.

To compare the pyridine nucleotide substrate specificity, assays were carried out with 0.01  $\mu\text{M}$  SsuE, 1  $\mu\text{M}$  or 2  $\mu\text{M}$  FMN, and varying concentrations of NADPH (10-200  $\mu\text{M}$ ) or NADH (10-150  $\mu\text{M}$ ) in 25 mM potassium phosphate buffer, pH 7.5, 10% glycerol, and 100 mM NaCl at 25 °C.

## 2.6 Data analyses

The initial rates calculated from the oxidation of pyridine nucleotides were plotted against each substrate concentration, and fit to the Michaelis-Menten equation (Eq.12) with the Kaleidagraph software.

$$v_o = V_{\max}[\text{S}] / (K_m + [\text{S}]) \quad (12)$$

$v_o$  is the initial rate,  $V_{\max}$  is the maximum rate,  $[\text{S}]$  is substrate concentration, and  $K_m$  is the substrate concentration at half of  $V_{\max}$ .

## 2.7 Flavin binding experiments

### 2.7.1 Fluorescent titrations

Flavin binding to SsuE and SsuD was monitored by spectrofluorometric titration with FMN. Spectra were recorded on a Perkin Elmer LS 55 luminescence spectrometer (Palo Alto, CA) with an excitation wavelength at 280 nm and emission measurements at 344 nm. Both excitation and emission slit widths were set at 5 nm and 2.5 nm for SsuE and SsuD, respectively. For the titration of SsuE with FMN, a 1.0 mL solution of 0.1  $\mu\text{M}$  SsuE (calculated using a molar extinction coefficient of 20.3  $\text{mM}^{-1} \text{cm}^{-1}$  at 280 nm) in standard buffer containing 100 mM NaCl was titrated with between 0.022-0.44  $\mu\text{M}$  FMN ( $\epsilon=12.2 \text{ mM}^{-1} \text{cm}^{-1}$ ), and the fluorescence spectrum recorded following a 2 min

incubation after each addition of FMN. Titration of SsuD was performed with 0.5  $\mu\text{M}$  SsuD (calculated using a molar extinction coefficient of  $46.9 \text{ mM}^{-1} \text{ cm}^{-1}$  at 280 nm) in standard buffer containing 100 mM NaCl (1.0 mL total volume). The fluorescence spectrum was recorded following the addition of aliquots of FMN (5.2-98.6  $\mu\text{M}$ ) to SsuD.

### 2.7.2 Data analysis from FMN titration

The bound FMN concentration was determined by Eq. 13 [27]:

$$[\text{FMN}]_{\text{bound}} = [\text{SsuE}] \frac{(I_0 - I_c)}{(I_0 - I_f)} \quad (13)$$

[SsuE] represents the initial concentration of enzyme.  $I_0$  is the initial fluorescence intensity of SsuE prior to the addition of FMN,  $I_c$  is the fluorescence intensity of SsuE following each addition of FMN, and  $I_f$  is the final fluorescence intensity. The concentration of FMN bound ( $[\text{FMN}]_{\text{bound}}$ , y) was plotted against the total FMN ( $[\text{FMN}]_{\text{total}}$ , x) to obtain the dissociation constant ( $K_d$ ) according to Eq. 14 where n is the binding capacity of SsuE [27].

$$y = \frac{(K_d + x + n) + \sqrt{(K_d + x + n)^2 - 4xn}}{2} \quad (14)$$

## 2.8 Steady-state kinetic measurements of SsuE

### 2.8.1 Determination of kinetic parameters

Enzymatic assays to measure the activity of the SsuE enzyme were performed by monitoring spectrophotometrically the decrease in 340 nm absorbance due to the oxidation of NADPH to  $\text{NADP}^+$  ( $\epsilon=6.22 \text{ mM}^{-1} \text{ cm}^{-1}$ ). Reactions were initiated by the

addition of SsuE (0.01  $\mu\text{M}$ ) enzyme to a reaction mixture (1 mL) containing between 3-60  $\mu\text{M}$  NADPH and 0.01-0.06  $\mu\text{M}$  FMN in standard buffer with 100 mM NaCl at 25 °C. The activity of the SsuE enzyme in the presence of 0.01  $\mu\text{M}$  SsuD enzyme and 200  $\mu\text{M}$  octanesulfonate substrate were monitored as described for single enzyme assays. The octanesulfonate substrate was added prior to the initiation of the reaction with SsuE and SsuD. For each assay, the background rate due to the nonenzymatic oxidation of NADPH was subtracted from the initial velocities determined with SsuE.

### *2.8.2 Product inhibition assays*

Inhibition studies of the SsuE protein with  $\text{NADP}^+$  as inhibitor were performed in a reaction mixture (1.0 mL) containing 0.01  $\mu\text{M}$  SsuE, 0.1  $\mu\text{M}$  FMN, 0-30  $\mu\text{M}$   $\text{NADP}^+$ , and varying concentrations of NADPH between 20-100  $\mu\text{M}$ . The assay was carried out by measuring the decrease in 340 nm due to the oxidation of NADPH to  $\text{NADP}^+$ .

### *2.8.3 Coupled kinetic assays*

Different ratios of SsuD to SsuE were employed in kinetic assays to investigate the impact of SsuD on flavin reduction by SsuE. Assays were carried out with 0.01  $\mu\text{M}$  SsuE only, or a 1:1 and 2:1 ratio of SsuD to SsuE, 150  $\mu\text{M}$  NADPH, and varying concentrations of FMN (0.03-1.0  $\mu\text{M}$ ) in 25 mM potassium phosphate buffer, pH 7.5, 10% glycerol, and 100 mM NaCl at 25 °C. Assays were also carried out with 0.01  $\mu\text{M}$  SsuE, 150  $\mu\text{M}$  NADPH, varying concentrations of FMN (0.01-1.0  $\mu\text{M}$ ), with or without the addition of 0.01  $\mu\text{M}$  SsuD, and 500  $\mu\text{M}$  octanesulfonate in 25 mM potassium phosphate buffer, pH 7.5, 10% glycerol, and 100 mM NaCl at 25 °C.

Assays were also performed to measure the oxidation of NADPH by SsuE with varying concentrations of FMN in the presence of SsuD and the octanesulfonate



substrate. A series of assays were carried out with 0.01  $\mu\text{M}$  SsuE, 0.01  $\mu\text{M}$  SsuD, 200  $\mu\text{M}$  octanesulfonate, 0.01-0.08  $\mu\text{M}$  FMN, and varying fixed concentrations of NADPH at 10  $\mu\text{M}$ , 20  $\mu\text{M}$ , 40  $\mu\text{M}$ , or 60  $\mu\text{M}$  in 25 mM potassium phosphate buffer, pH 7.5, 10% glycerol, and 100 mM NaCl at 25  $^{\circ}\text{C}$ . A separate set of assays were carried out with 0.01  $\mu\text{M}$  SsuE, 0.01  $\mu\text{M}$  SsuD, 200 $\mu\text{M}$  octanesulfonate, varying fixed concentration of FMN at 0.02  $\mu\text{M}$ , 0.04  $\mu\text{M}$ , 0.06  $\mu\text{M}$ , or 0.1  $\mu\text{M}$ , and varying concentrations of NADPH (5-80  $\mu\text{M}$ ) in 25 mM potassium phosphate buffer, pH 7.5, 10% glycerol, and 100 mM NaCl at 25  $^{\circ}\text{C}$ . The background rate due to autooxidation of NADPH was taken into account when determining the rate, and each experiment was performed in triplicate.

### 2.9 Data analyses for the steady-state kinetic mechanism of SsuE

The data from the assays were fit with the Enzfitter program (Biosoft, Cambridge, UK) using three possible mechanisms (Eq. 15-17). Initial reaction rates of the SsuE protein in the presence or absence of the SsuD enzyme and alkanesulfonate substrate were fit to the following equations: sequential mechanism (Eq. 15), ping-pong mechanism (Eq. 16), and equilibrium ordered mechanism (Eq. 17).

$$\frac{v}{e} = \frac{k_{\text{cat}}AB}{K_aB + K_bA + AB + K_{ia}K_b} \quad (15)$$

$$\frac{v}{e} = \frac{k_{\text{cat}}AB}{K_aB + K_bA + AB} \quad (16)$$

$$\frac{v}{e} = \frac{k_{\text{cat}}AB}{K_aK_b + K_bA + AB} \quad (17)$$

For these equations  $K_a$  and  $K_b$  are the  $K_m$  values for substrate A and B, respectively. A and B are the substrate concentrations.  $K_{ia}$  is the dissociation constant for substrate A.  $k_{\text{cat}}$

is the turnover number of the enzyme.

The data from the steady-state inhibition studies were fit with the Enzfitter program to the three following inhibition equations: competitive (Eq. 18), noncompetitive (Eq. 19), and uncompetitive (Eq. 20).

$$\frac{v}{e} = \frac{k_{\text{cat}}A}{K_a(1+I/K_{\text{is}})} + A \quad (18)$$

$$\frac{v}{e} = \frac{k_{\text{cat}}A}{[A(1+I/K_{\text{is}})] + [A(1+I/K_{\text{ii}})]} \quad (19)$$

$$\frac{v}{e} = \frac{k_{\text{cat}}A}{K_a + [A(1+I/K_{\text{ii}})]} \quad (20)$$

The  $K_a$  represents the Michaelis constant for substrate A. A and I are the substrate concentration and inhibitor concentration, respectively.  $K_{\text{is}}$  is the slope inhibition constant, and  $K_{\text{ii}}$  is the intercept inhibition constant.  $k_{\text{cat}}$  is the turnover number of the enzyme.

### 2.10 Synthesis of [4(R)-<sup>2</sup>H]NADPH

[4(R)-<sup>2</sup>H]NADPH was synthesized as previously described with slight modifications [85, 86]. The pro-*R* hydrogen in the stereo structure of NADPH was replaced with deuterated hydrogen (Figure 2.3). The reaction was initiated with 35 mg of NADP<sup>+</sup>, 1.2 mL of 2-propanol-d<sub>8</sub>, and 48 units of NADP<sup>+</sup> dependent alcohol dehydrogenase (*Thermoanaerobium brockii*) in 15 mL of 25 mM Tris buffer, pH 9.0. The reaction was performed at 42 °C, and monitored at 340 nm. At approximately 40 min the reaction was bubbled with nitrogen for one hour to evaporate the acetone. The alcohol dehydrogenase enzyme was separated from [4(R)-<sup>2</sup>H]NADPH by centrifugation at 2000 g

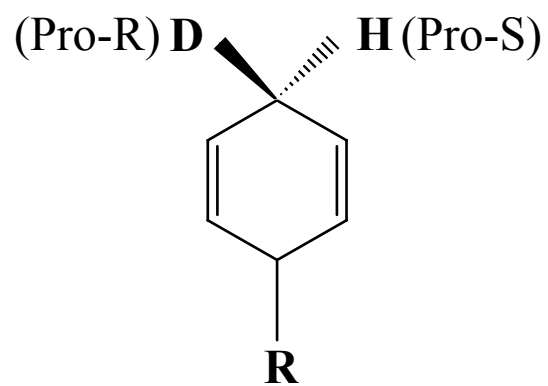


Figure 2.3. Location of deuterated hydrogen in NADPH.

in a 10,000 molecular weight Amicon Ultra-4 centrifugation filter from Millipore (Bedford, MA). The [4(*R*)-<sup>2</sup>H]NADPH was precipitated with absolute ethanol at a ratio of 12:1 (ethanol to product solution), cooled at -20 °C for 20 min, and centrifuged at 10,000 g for 30 min. The synthesized product [4(*R*)-<sup>2</sup>H]NADPH was resuspended in 1.5 mL of 10 mM Tris buffer, 10% glycerol, pH 8.5, 100 mM NaCl, and stored at -20 °C for later use. The product absorbance ratio of A<sub>260</sub>/A<sub>340</sub> was 2.3. NADPH was synthesized from NADP<sup>+</sup> using the same procedure to standardize the experimental results obtained with [4(*R*)-<sup>2</sup>H]NADPH. The ratio of A<sub>260</sub>/A<sub>340</sub> corresponding to the product absorbance was 2.3. Both newly synthesized [4(*R*)-<sup>2</sup>H]NADPH and NADPH were used in single-wavelength stopped-flow kinetic analyses.

### *2.11 Stopped-flow kinetic experiments*

Stopped-flow kinetic analyses were carried out with an Applied Photophysics SX.18 MV stopped-flow spectrophotometer. All reactions were measured in single mixing mode (Figure 2.4).

#### *2.11.1 Establishment of anaerobiosis*

The stopped-flow instrument was made anaerobic by repeated filling and emptying of the drive syringes with an oxygen scavenging system containing 25 mM potassium phosphate buffer, pH 7.5, 10% glycerol, 100 mM NaCl with 20 mM glucose and 10 units of glucose oxidase in one drive syringe and 10 mM Tris buffer, pH 8.5, 10% glycerol, 100 mM NaCl with 20 mM glucose and 10 units of glucose oxidase in the other drive syringe. The protein solution was made anaerobic in a tonometer by vacuum gas

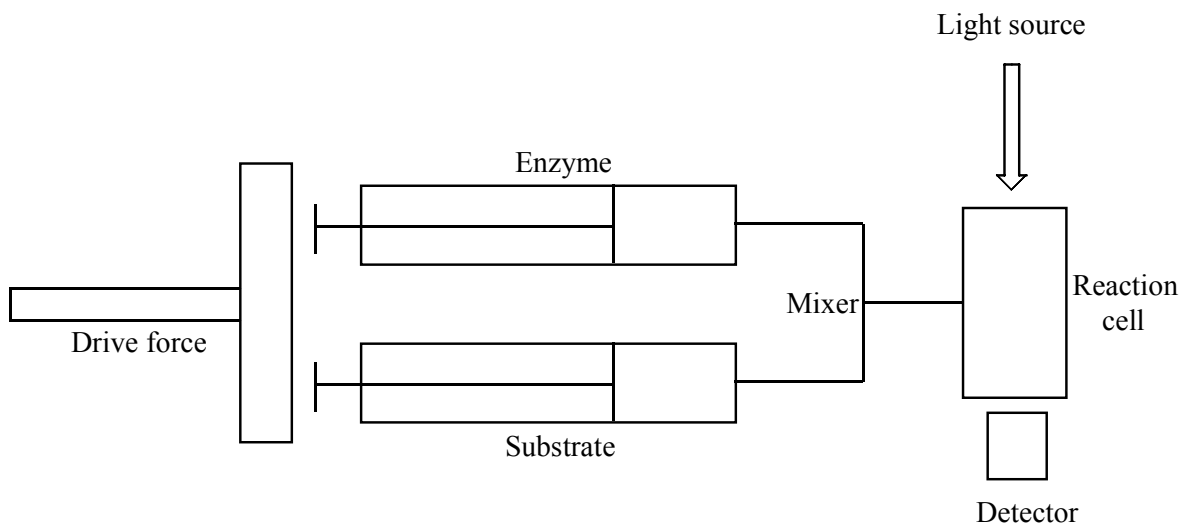


Figure 2.4. Illustration of stopped-flow single mixing mode.

exchange followed by saturation with oxygen free argon. Solutions containing FMN and NADPH were made anaerobic with 20 mM glucose and 10 units of glucose oxidase by bubbling the solutions with oxygen free argon for 15 min in a gas-tight syringe. All experiments were carried out in single-mixing mode and monitored by multiple wavelength photodiode array detection or single wavelength analyses at 450 and 550 nm.

### *2.11.2 Photodiode array detection analyses*

Measurements by photodiode array detection were carried out anaerobically with 20  $\mu\text{M}$  FMN, 22  $\mu\text{M}$  SsuE, and 200  $\mu\text{M}$  NADPH (final concentration after mixing) in 25 mM potassium phosphate buffer, pH 7.5, 10% glycerol, and 100 mM NaCl at 4 °C. Spectra were recorded at a wavelength range of 300 to 700 nm in log time base.

### *2.11.3 Assay by monitoring single wavelength*

Flavin reduction and charge-transfer complex formation were monitored at 450 nm and 550 nm. Single wavelength measurements monitoring NADPH dependence were carried out anaerobically with 30  $\mu\text{M}$  FMN, 30  $\mu\text{M}$  SsuE, and NADPH concentrations between 150-500  $\mu\text{M}$  (final concentration after mixing) in 25 mM potassium phosphate buffer, pH 7.5, 10% glycerol and 100 mM NaCl at 4 °C. FMN dependent measurements were carried out anaerobically with 200  $\mu\text{M}$  NADPH, 33  $\mu\text{M}$  SsuE, and FMN concentrations between 10-50  $\mu\text{M}$  (final concentration after mixing) in 25 mM potassium phosphate buffer, pH 7.5, 10% glycerol and 100 mM NaCl at 4 °C. The assays with [4(*R*)-<sup>2</sup>H]NADPH or NADPH as reducing reagents were carried out anaerobically with 30  $\mu\text{M}$  FMN, 30.5  $\mu\text{M}$  SsuE, and 200  $\mu\text{M}$  NADPH or [4(*R*)-<sup>2</sup>H]NADPH (final

concentration after mixing) in 25 mM potassium phosphate buffer, pH 7.5, 10% glycerol, and 100 mM NaCl at 4 °C.

### 2.12 Data analyses of pre-steady-state complexes

Initial analyses of the single wavelength stopped-flow traces at 450 and 550 nm were performed with the PROKIN software (Applied Photophysics, Ltd.). Firstly, global analysis was applied to discern the steps involved in the flavin reduction. Secondly, a three-step sequential reversible model of  $A \rightarrow B \rightarrow C \rightarrow D$  was adopted during the fitting, and the kinetic traces were resolved into three distinct phases. All single wavelength traces at 450 and 550 nm were imported and fitted with EnzFitter (Biosoft, Cambridge, UK) or Kaleidagraph software (Abelbeck Software, Reading, PA). The single-wavelength traces were best fitted to a triple-exponential using the following equation:

$$A = A_1 \exp(-k_1 t) + A_2 \exp(-k_2 t) + A_3 \exp(-k_3 t) + C \quad (21)$$

where  $k_1$ ,  $k_2$  and  $k_3$  are apparent rate constants for the three phases,  $A$  is the absorbance at time  $t$ ,  $A_1$ ,  $A_2$ ,  $A_3$  are amplitudes of each phase, and  $C$  is the absorbance at the end of the reaction.

The data for the concentration dependence of NADPH or FMN on  $k_{1\text{obs}}$  was fitted with a simplified hyperbolic equation:

$$k_{\text{obs}} = k_{\text{lim}}[S]/(K_d + [S]) \quad (22)$$

where  $k_{\text{obs}}$  is the observed rate constant for the formation of the charge-transfer complex,  $k_{\text{lim}}$  is the limiting rate constant in the flavin reductive reaction,  $K_d$  is the dissociation constant of enzyme-substrate complex, and  $S$  is the substrate concentration.

### 2.13 Mutagenesis of double displacement of leucines to methionines

The mutations were generated utilizing site-directed mutagenesis. Two leucine residues at positions 114 and 165 of the SsuE protein underlined (Figure 2.5) were substituted with methionine residues using the QuikChange Site-Directed Mutagenesis Kit (Stratagene, La Jolla, CA, USA). The leucine at position 114 is a methionine residue in the homologous SsuE proteins from *Pseudomonas aeruginosa* and *P. putida*, making this residue ideal for conservative substitutions. The SsuE/pET21a plasmid was used as the template with L114M (5'-ACC GTG GCC CAT ATG CTG GCG GTC GAT-3') and L165M (5'-CGT CTT GATAACC GCG ATG GAA ACT TTC TGG CAG-3') as forward primers and L114M (5'-ATC GAC CGC CAG CAT ATG GGC CAC GGT-3') and L165M (5'-CTG CCA GAA AGT TTC CAT CGC GGT ATC AAG ACG-3') as reverse primers. The PCR amplified products were purified with QIAquick PCR Purification Kit Protocol, and digested with DpnI restriction enzyme to remove parental DNA. The L114,165M *ssuE* mutant construct was transformed into *E. coli* XL-1 Blue supercompetent cells for amplification of plasmid DNA and storage. Plasmids were extracted following the QIAprep Miniprep protocol (QISGEN, Valencia, CA) from a 5 mL growth of *E. coli* XL-1 Blue cells incubated overnight in LB-Amp media at 37 °C. The generated mutations were verified by DNA- sequence analysis at Davis Sequencing (University of California, Davis). Plasmids containing the L114,165M *ssuE* substitution were transformed into BL21(DE3) expression cells for expression of the mutant protein.



```
1 MRVITLAGSP RFPSRSSLL EYAREKLNGL 30
31 DVEVYHWNLQ NFAPEDLLYA RFDSPALKTF 60
61 TEQLQQADGL IVATPVYKAA YSGALKTLTD 90
91 LLPERALQ GK VVLPLATGGT VAHLLLAVDYA 120
121 LKPVLSALKA QEILHG VFAD DSQVIDYHHR 150
151 PQFTPNLQTR LDTALETFWQ ALHRRDVQVP 180
181 DLLSLRGNAH A 191
```

Figure 2.5. The SsuE sequence with mutation sites underlined.

### *2.14 Preparation of M9 media*

1 M MgSO<sub>4</sub>, 1 M CaCl<sub>2</sub>, and 20% glucose solutions were separately prepared first and filtered under a SterilGard hood. The 5x M9 salts was prepared with Na<sub>2</sub>HPO<sub>4</sub>•7H<sub>2</sub>O, KH<sub>2</sub>PO<sub>4</sub>, NaCl, NH<sub>4</sub>Cl, and autoclaved. The stock solution of 100x trace elements with EDTA, FeCl<sub>3</sub>, ZnCl<sub>2</sub>, CuCl<sub>2</sub>, CoCl<sub>2</sub>, H<sub>3</sub>BO<sub>3</sub>, MnCl<sub>2</sub>, Ni<sub>2</sub>SO<sub>4</sub>, and molybdcic acid was prepared, and brought to a pH value of 7.0 with NaOH solution, filter sterilized and stored at 4 °C. The 1000x vitamin stock with riboflavin, niacinamide, pyridoxine monohydrate, and thiamine was prepared, filter sterilized and stored at 4 °C. Finally, a 1 L M9 medium was prepared by mixing 770 mL of H<sub>2</sub>O (autoclaved in advance), 200 mL of 5x M9 salts, 2 mL of 1M MgSO<sub>4</sub>, 20 mL of 20% glucose, 0.1 mL of 1M CaCl<sub>2</sub>, 10 mL of 100x trace elements, and 1 mL of 1000x vitamins under UV-ultra light chamber, and used immidiately.

### *2.15 Expression and purification of Selenomethionyl SsuE*

Selenomethionyl SsuE (L114,165 SeMet SsuE) protein was expressed under conditions of methionine pathway inhibition. A single colony of BL21(DE3) containing the L114,165M SsuE vector was used to inoculate 5 mL LB media containing 100 mg/mL ampicillin. Following a 7 h incubation at 37 °C, the cells were harvested and resuspended in 4 mL M9 media containing 22.2 mM glucose as the carbon source. The resuspended culture (1 mL) was used to inoculate four 1 L flasks containing M9 media with 100 mg/mL ampicillin and was incubated at 37 °C until the absorbance at 600 nm reached 0.7. Specific amino acids (lysine, phenylalanine and threonine at 100 mg/L;

isoleucine, leucine and valine at 50 mg/L) were added to block methionine biosynthesis and selenomethionine (60 mg/L) was added to replace methionine during cell growth. Induction with 0.4 mM IPTG was performed 15 min after the addition of the amino acids and the cultures were incubated for an additional 5 h at 18 °C before harvesting. The purification protocol for the expressed protein followed the same procedure as previously described for wild-type SsuE except the addition of 5 mM dithiothreitol to all buffers keeping a reducing environment during the purification process.

### *2.16 Circular Dichroism of wild-type SsuE and SeMet SsuE*

The spectra were recorded on a Jasco J-810 Spectropolarimeter (Easton, MD). All measurements were carried out with 0.05 mg/mL of SsuE or SeMet SsuE in 25 mM potassium phosphate buffer, pH 7.5 at 25 °C. Measurements were taken in 0.1 nm increments from 300 to 180 nm in a 0.1 cm path length cuvette. Each data is the average of four scans. Smoothing of the data was performed by Jasco-720 software.

### *2.17 Activity assay of SeMet SsuE*

The activity assay was carried out by measuring the oxidation of pyridine nucleotides with wild-type or selenomethioninyl SsuE protein. The reaction took place with 120 μM NADPH, 0.5 μM FMN, 0.01 μM SsuE or selenomethioninyl protein in 25 mM potassium phosphate buffer, pH 7.5, 10% glycerol, and 100 mM NaCl at 25 °C. The background rate due to autooxidation of NADPH was taken into account when determining the rate.

### 2.18 Crystallization of wild-type SsuE and SeMet SsuE

The crystallization of wild-type SsuE protein and selenomethionyl SsuE protein was accomplished by our collaborator Dr. T. Conn Mallett from Wake Forest School of Medicine. Purified wild-type SsuE protein at 8 mg/mL in 10 mM HEPES buffer pH 7.0 was screened for crystallization by vapor diffusion at 293 K using sitting drops (containing 2 mL protein sample and 2 mL reservoir solution) and the sparse-matrix strategy [87] as implemented in Crystal Screens I and II and the PEG/Ion Screen (Hampton Research, Inc.). Large single SsuE crystals grew as hexagonal rods from 15–20% PEG 3350, PEG 4000 and PEG 8000 with 0.1–0.3 M lithium citrate in hanging-drop vapor-diffusion experiments (8 mL total drop size over a 1.0 mL reservoir solution). Crystals appeared within a day and grew to full size ( $\sim 0.15 \times 0.15 \times 0.5$  mm) in two weeks. SsuE protein crystals containing oxidized flavin were obtained by both crystal soaking and cocrystallization with FMN. Crystals were transferred to a cryoprotectant solution containing 20% glycerol, 20% PEG 8000 and 0.2 M lithium citrate prior to flash cooling at 100 K in the cold stream.

Initial X-ray diffraction data from the SsuE crystals were collected in the laboratory using a Rigaku/ MSC Saturn92 CCD detector with Cu  $K\alpha$  radiation from a Micro007 rotating-anode X-ray generator. The crystals diffracted weakly ( $\sim 3.5$  Å) using the laboratory X-ray diffraction facility, but several complete data sets were collected. Diffraction data were indexed, integrated and scaled using d\*TREK [88]. A complete data set to 2.9 Å resolution was collected using beamline X26C of the National Synchrotron Light Source, Brookhaven National Laboratory. The SeMet SsuE was crystallized employing similar methods used for the wild-type SsuE protein.

## CHAPTER THREE

### RESULTS

#### *3.1 Protein expression and purification*

The *ssuD* and *ssuE* genes PCR amplified from genomic *E. coli* K12 were cloned independently into the T7 RNA polymerase-dependent expression vector pET21a (Novagen), and the proteins were expressed in *E. coli* BL21(DE3). Initial expression of each protein at 37 °C resulted in the location of the protein in inclusion bodies. To minimize the formation of insoluble protein aggregation, a lower temperature was used to slow down protein expression during cell growth. The optimal temperature for protein expression was 18 °C following induction with IPTG. Proteins were purified by applying a combination of ammonium sulfate fractionation, hydrophobic chromatography, and anionic exchange chromatography to the supernatant after treatment with streptomycin sulfate. We were able to achieve greater than 90% purity for both SsuE and SsuD judged by SDS-PAGE. Figure 3.1 shows the different stages of purification for the SsuE and SsuD proteins. The purification of SsuE or SsuD protein yielded 30-50 mgs of protein from a 2 L growth.

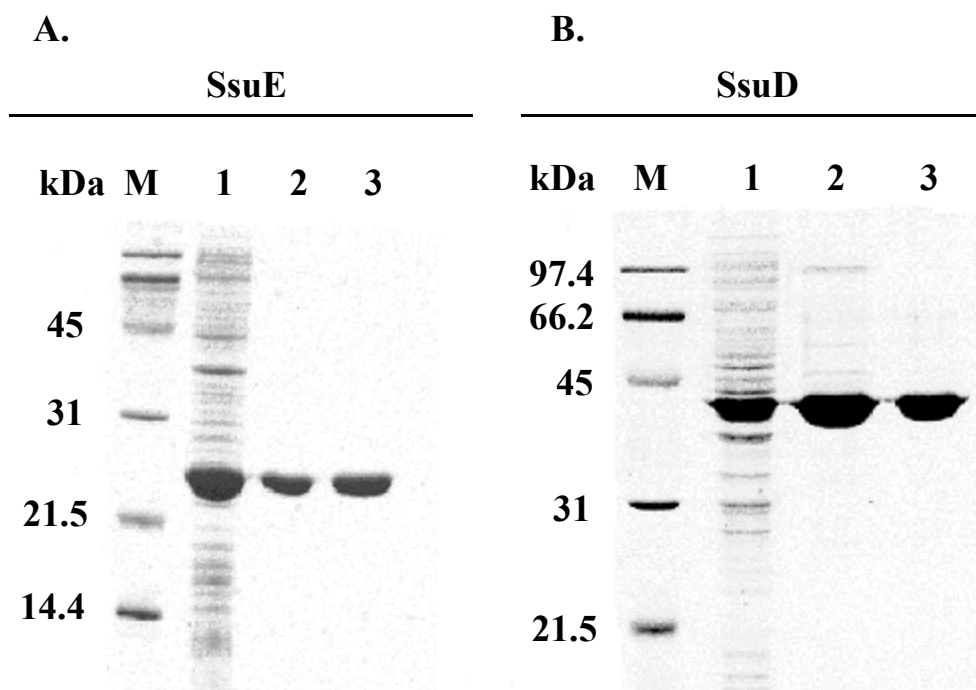


Figure 3.1. SDS-PAGE of samples from alkanesulfonate monooxygenase proteins (A. Lane M, Protein standard; Lane 1, Cell lysate; Lane 2, Sample after phenyl sepharose column; Lane 3, Sample after anionic exchange column. B. For SsuD the order of the column for lane 2 and lane 3 were switched).

## *3.2 Biophysical characterization of SsuE and SsuD*

### *3.2.1 Determination of molecular weight of SsuE and SsuD*

The purified SsuE and SsuD proteins were analyzed by ESIMS to determine their precise molecular weights (Figure 3.2). Initial studies with the SsuE and SsuD proteins reported the molecular weight as higher than the calculated molecular weight from the amino acid sequence by gel filtration [18]. The mass of each protein determined by mass spectrometric analysis was  $41,605 \pm 2.6$  and  $21,253 \pm 1.5$  for SsuD and SsuE, respectively, which was similar to the calculated molecular weight.

### *3.2.2 Quaternary structural determination of SsuE and SsuD*

The quaternary structure of each protein was determined by sedimentation velocity experiments. Data from sedimentation equilibrium analyses using multiple concentrations of SsuD was fit to a single Gaussian at 7.7 S (Figure 3.3). This value corresponds with a weight averaged molecular weight of 165,610. Based on the results from mass spectrometric analysis the single monomeric subunit of SsuD has an atomic mass unit of  $41,615 \pm 2.6$ . These combined results indicate that SsuD has an oligomeric state consisting of four subunits. Results from similar analytical methods showed that the SsuE protein exists as a dimeric structure (data not shown).

## *3.3 Substrate specificity studies of SsuE*

### *3.3.1 Flavin dependent assays*

The SsuE enzyme catalyzes flavin reduction by pyridine nucleotides. In order to determine the flavin specificity, assays were carried out with saturating concentrations of NADPH, and varying FMN or FAD concentrations. The initial velocities versus substrate

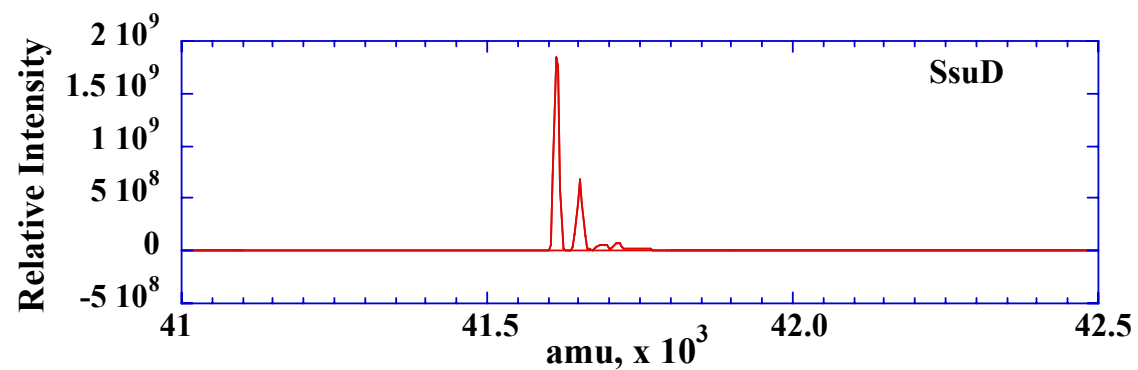
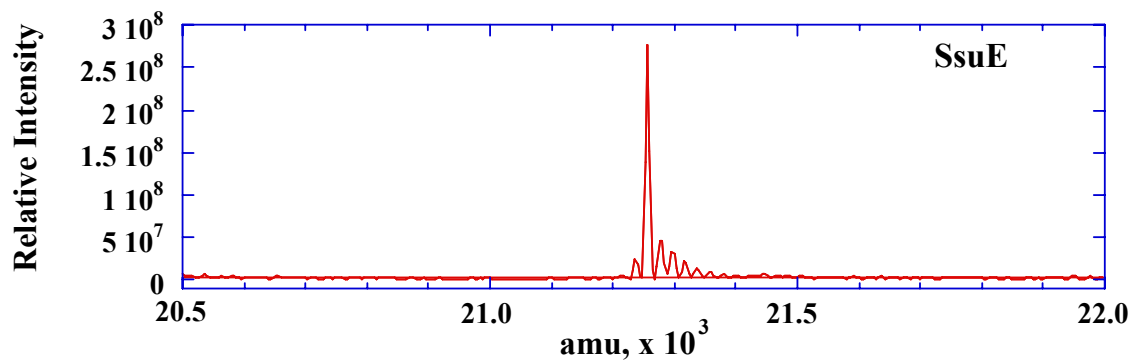


Figure 3.2 Mass spectrometric analyses of SsuE and SsuD.



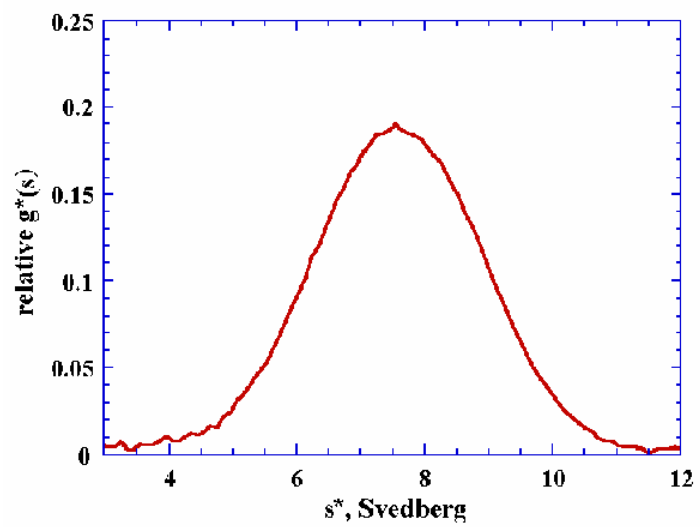


Figure 3.3. The  $g^*(s)$  value distribution of SsuD protein.

concentrations were plotted, and fitted to the Michaelis-Menten equation (Figure 3.4). FMN showed a 92-fold increase in catalytic efficiency when compared with FAD, demonstrating FMN as the preferred flavin substrate (Table 3.1). This result is consistent with previous reports on the flavin specificity of SsuE [18].

### *3.3.2 NADPH and NADH dependent assays of SsuE enzyme*

Assays were carried out with saturating concentrations of FMN with varying concentrations of NADPH or NADH. The initial velocities versus substrate concentrations were plotted, and fitted to the Michaelis-Menten equation (Figure 3.5). The kinetic parameters for these two substrates were essentially identical with similar catalytic efficiencies (Table 3.1). These results suggest that NADPH and NADH are both effective substrates for SsuE, which conflicted with previous reports that NADPH was the preferred substrate for SsuE [18]. Based on our results and previous studies, the NADPH pyridine nucleotide substrate was used in all subsequent kinetic assays.

### *3.4 FMN affinity assays*

The affinity of each alkanesulfonate monooxygenase enzyme for oxidized FMN was determined through fluorescence spectroscopy. To identify the affinity of the SsuE enzyme for FMN, aliquots of an FMN solution were added to SsuE and the decrease in protein intrinsic fluorescence at 344 nm due to flavin binding was monitored (Figure 3.6). The concentration of flavin bound to the SsuE enzyme was plotted against the total concentration of FMN added with each aliquot (Figure 3.7), and the data fitted to Eq. 14. The average  $K_d$  value for FMN binding to SsuE was  $0.015 \pm 0.004 \mu\text{M}$  with one FMN binding site per SsuE monomer. Similar experiments were performed with SsuD titrating with oxidized FMN, and monitoring the decrease in emission intensity at 340 nm. The

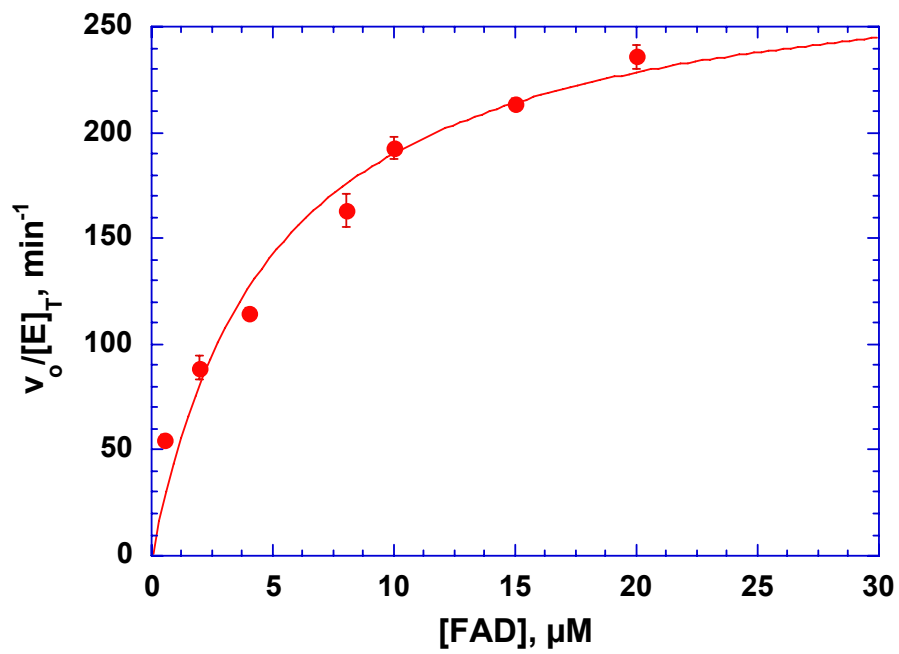
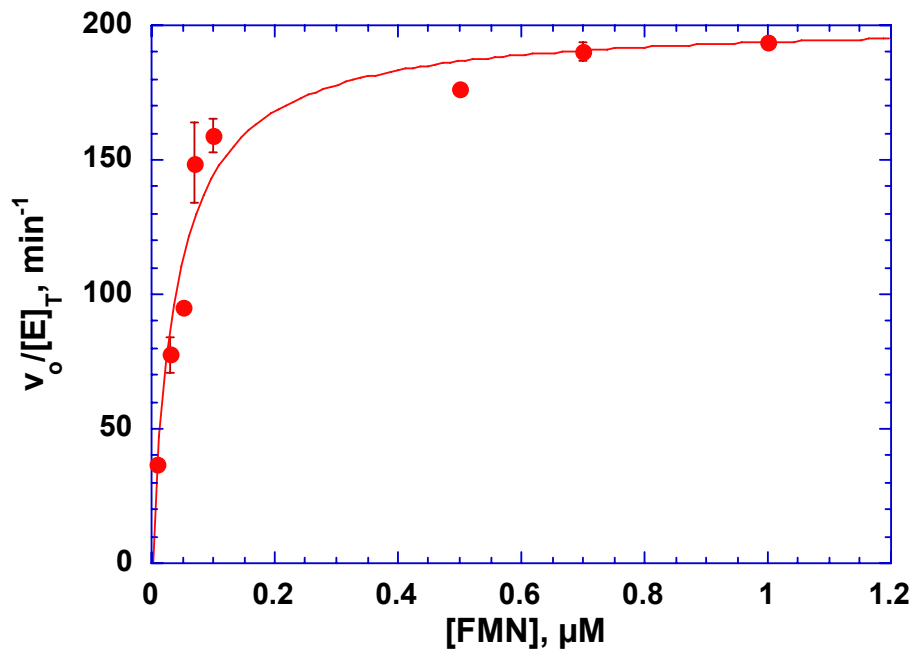


Figure 3.4. Initial velocities with flavin substrates.

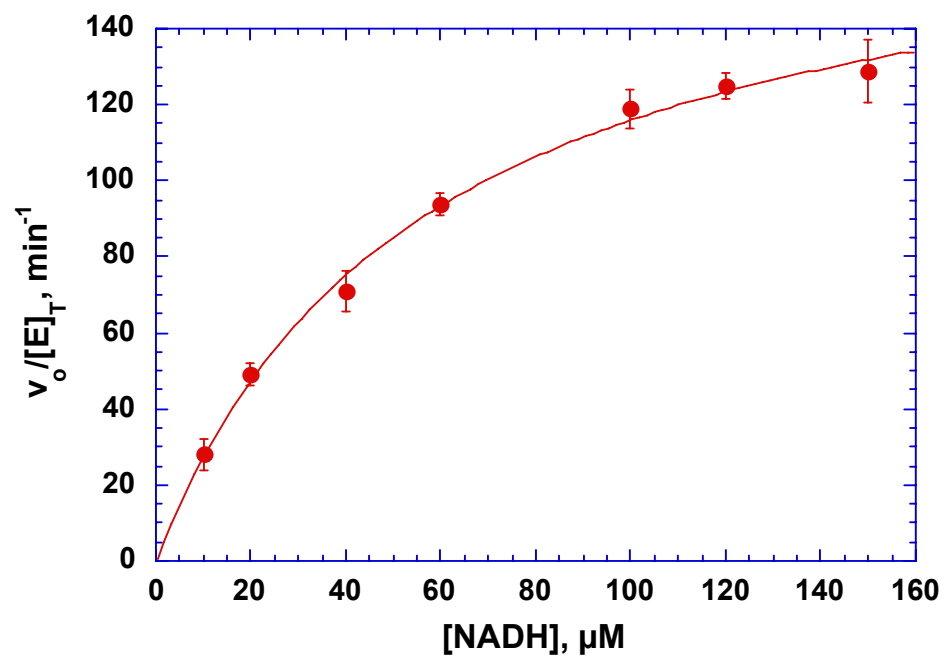
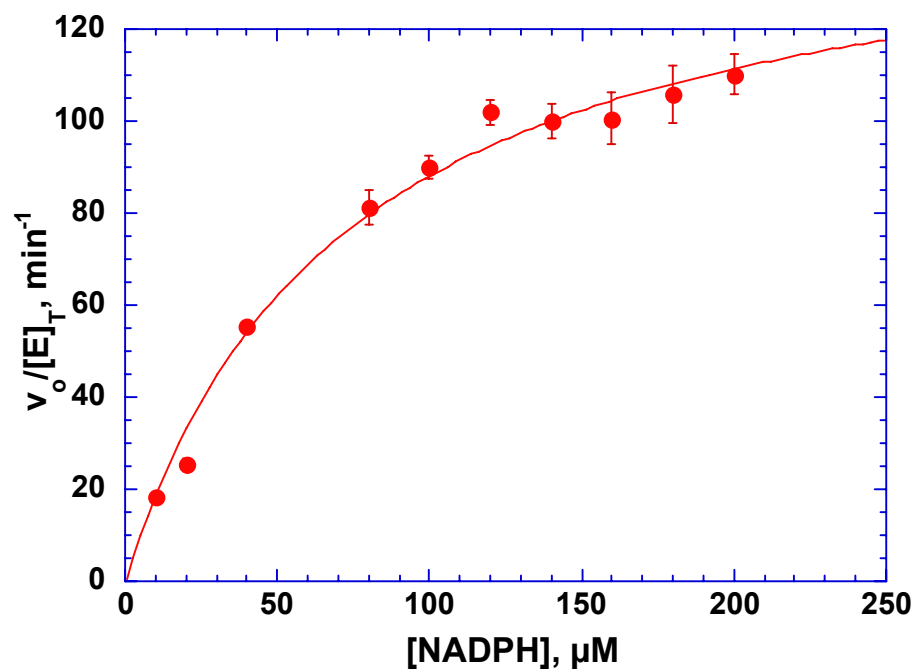


Figure 3.5. Initial velocities with pyridine nucleotide substrates.

Table 3.1. Kinetic parameters for SsuE.

	$K_m$ ( $\mu\text{M}$ )	$k_{\text{cat}}$ ( $\text{min}^{-1}$ )	$k_{\text{cat}}/K_m$ ( $\text{min}^{-1}/\mu\text{M}$ )
FMN	$0.039 \pm 0.01$	$201 \pm 10$	$5153 \pm 25$
FAD	$5.1 \pm 0.9$	$285 \pm 27$	$55.9 \pm 1.2$
NADPH	$42 \pm 5$	$232 \pm 9$	$5.5 \pm 0.4$
NADH	$57 \pm 5$	$181 \pm 7$	$3.2 \pm 0.2$

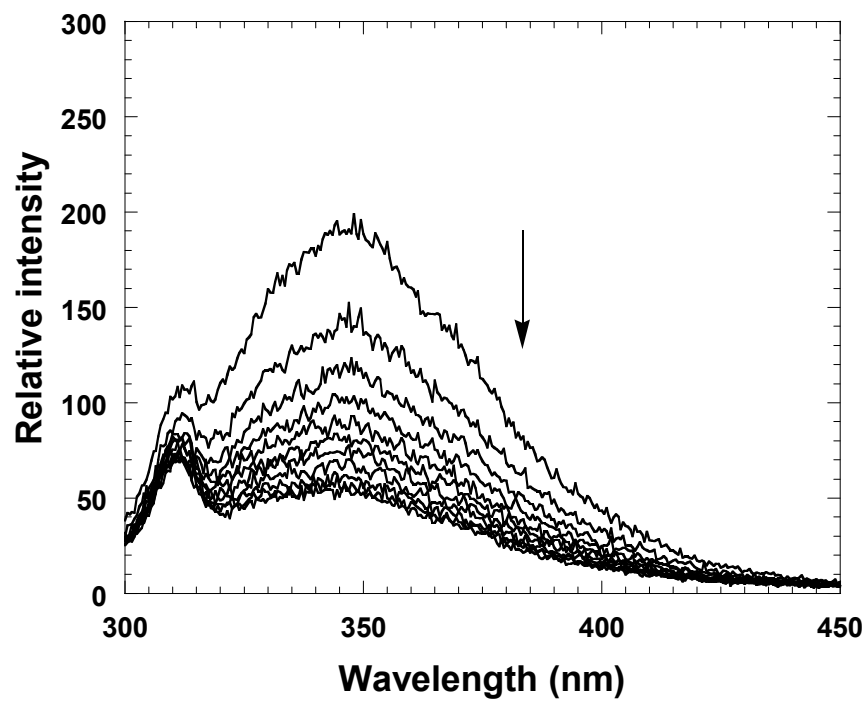


Figure 3.6. Fluorescence quenching of SsuE by the addition of FMN.

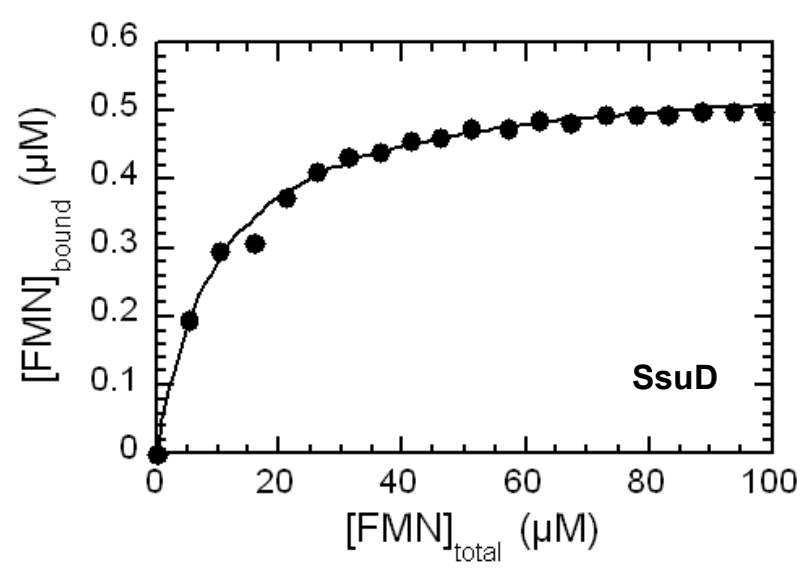
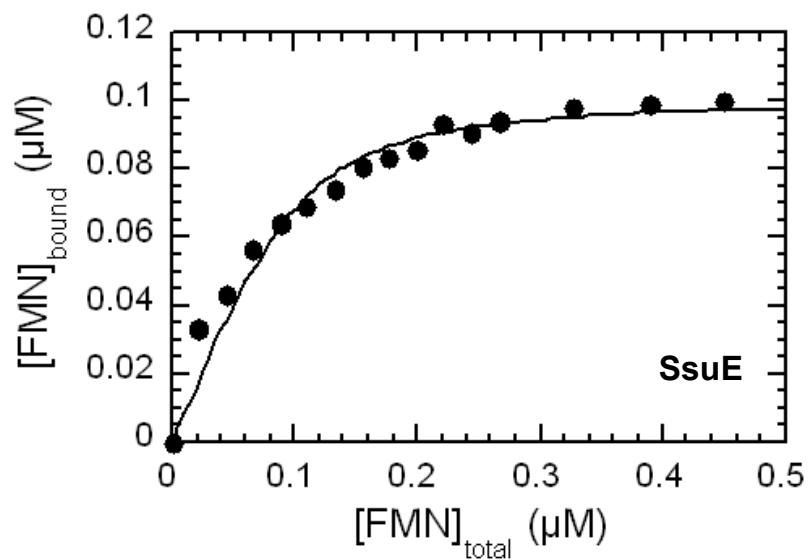


Figure 3.7. Fluorimetric titration of the SsuE or SsuD with FMN.

concentration of flavin bound to the SsuD enzyme was plotted against the total concentration of FMN added with each aliquot (Figure 3.7), and the data fitted to Eq. 14. The average  $K_d$  value for FMN binding to SsuD was  $10.2 \pm 0.4 \mu\text{M}$  with a stoichiometry of  $1.2 \pm 0.1$  for FMN bound to SsuD.

### *3.5 Steady-state kinetic analysis of the SsuE enzyme*

#### *3.5.1 The kinetic patterns of Bi Bi reaction of SsuE enzyme*

The bisubstrate reaction mechanism of SsuE involves the reduction of FMN by the pyridine nucleotide NADPH. Steady-state kinetic studies were performed to investigate the kinetic mechanism of SsuE in the absence of SsuD. Varying concentrations of FMN at several fixed concentrations of NADPH gave an intersecting pattern to the left of the  $e/v$  axis (Figure 3.8). A second set of experiments was performed varying NADPH at fixed levels of FMN (Figure 3.9). The intersection point was again to the left of the  $e/v$  axis. Both sets of experiments were best fit to an equation for a sequential mechanism, however they did not distinguish between an ordered or random sequential mechanism. Steady-state kinetic parameters determined from the fit of the data to Eq. 15 gave  $K_m$  values of  $0.016 \pm 0.002 \mu\text{M}$  and  $5.4 \pm 0.9 \mu\text{M}$  for FMN and NADPH, respectively. A  $K_{ia}$  value for NADPH of  $3.9 \pm 2.4$ , and an apparent  $k_{cat}$  value of  $116.0 \pm 6.3 \text{ min}^{-1}$  was obtained.

#### *3.5.2 Inhibition studies with $\text{NADP}^+$ as product inhibitor*

Inhibition studies on SsuE were performed with  $\text{NADP}^+$  as the inhibitor to discern between an ordered or random mechanism and to determine the order of substrate binding and product release. For these experiments the concentration of NADPH was varied at different concentrations of  $\text{NADP}^+$  and fixed nonsaturating levels of FMN.



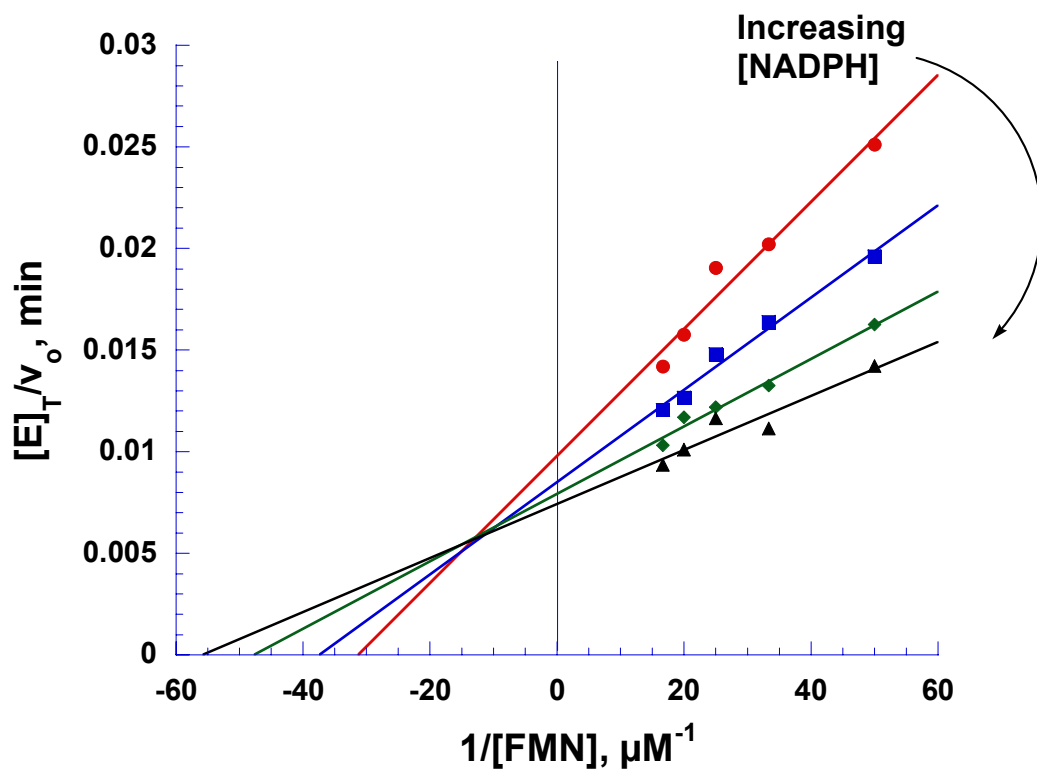


Figure 3.8. Initial velocity patterns of the SsuE catalyzed reduction of FMN.

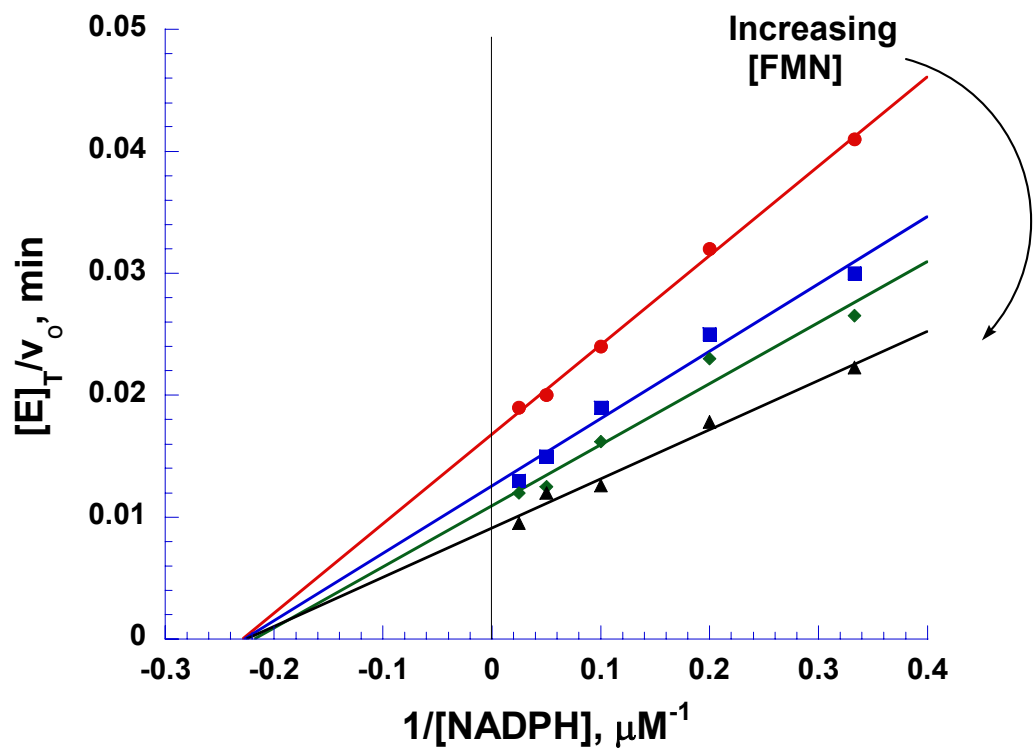


Figure 3.9. Initial velocity patterns of the SsuE catalyzed reduction of FMN.

Double reciprocal plots of the data intersected on the  $e/v$  axis (Figure 3.10), and the data were best fit to the equation for competitive inhibition (Eq. 18) which gave a  $K_i$  value of  $13.6 \pm 6 \mu\text{M}$  for  $\text{NADP}^+$ . In addition, there was no apparent inhibition with saturating levels of NADPH, varying concentrations of FMN, and different fixed concentrations of  $\text{NADP}^+$ . These results indicate that high substrate concentrations were able to reverse the effects of the inhibitor leading to the formation of the  $\text{E}\cdot\text{NADPH}$  complex. An ordered sequential mechanism for a bisubstrate system shows competitive inhibition when the substrate and product are competing for the same form of the enzyme. For these experiments the NADPH substrate and  $\text{NADP}^+$  product are competing for the free enzyme. The results from the  $\text{NADP}^+$  inhibition experiments confirm that the mechanism of SsuE proceeds by an ordered sequential mechanism with NADPH binding first followed by FMN to form a ternary complex. Following reduction of the flavin, the reduced  $\text{FMNH}_2$  product is released first followed by  $\text{NADP}^+$  (Figure 3.11).

### *3.6 Steady-state kinetic parameters with varying ratios of SsuD:SsuE*

Steady-state kinetic analysis was performed to determine if the kinetic parameters of SsuE were altered in the presence of SsuD. For these experiments either NADPH or FMN was held constant at saturating levels while varying the alternate SsuE substrate in the presence of varied stoichiometric ratios of SsuE to SsuD. The rate was determined by monitoring the decrease in 340 nm absorbance due to the oxidation of NADPH. Under these conditions there was no significant change in the steady-state kinetic parameters or mechanism of SsuE (Figure 3.12, Table 3.2).

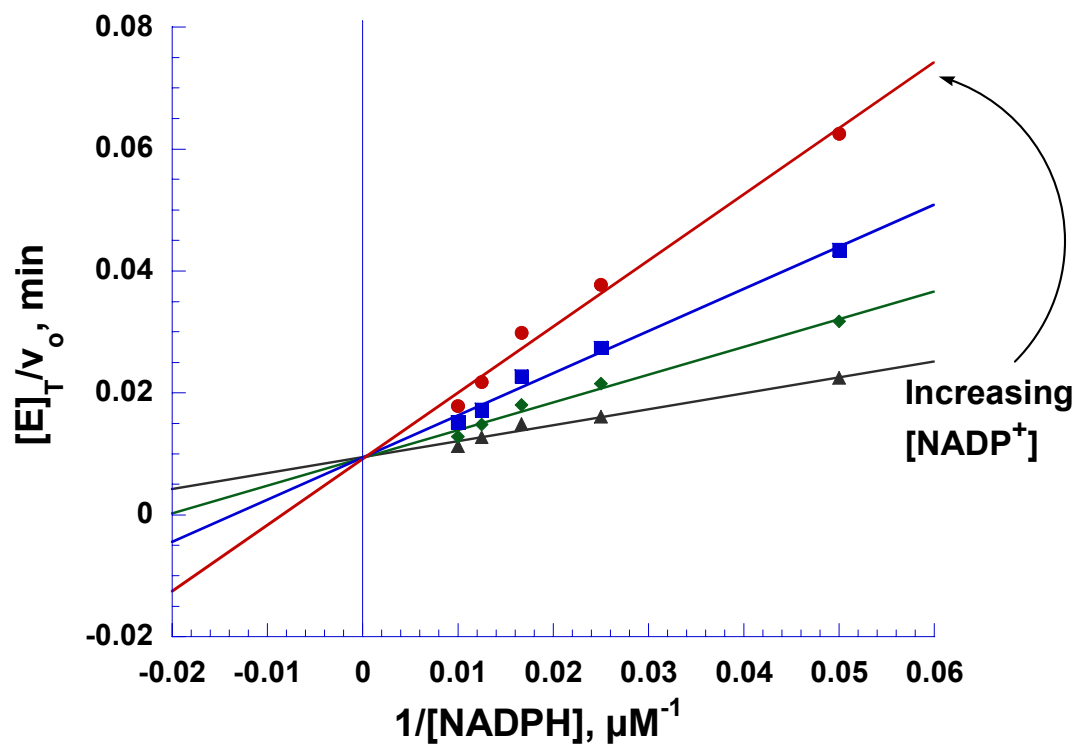


Figure 3.10. Inhibition of the SsuE enzyme with the product inhibitor NADP<sup>+</sup>.

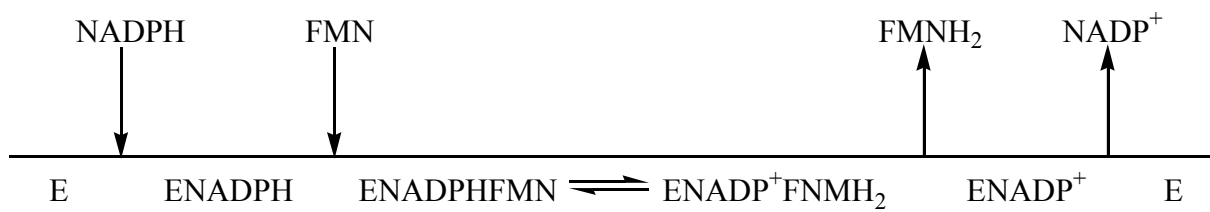


Figure 3.11. Reaction mechanism for SsuE catalyzed reduction of FMN.

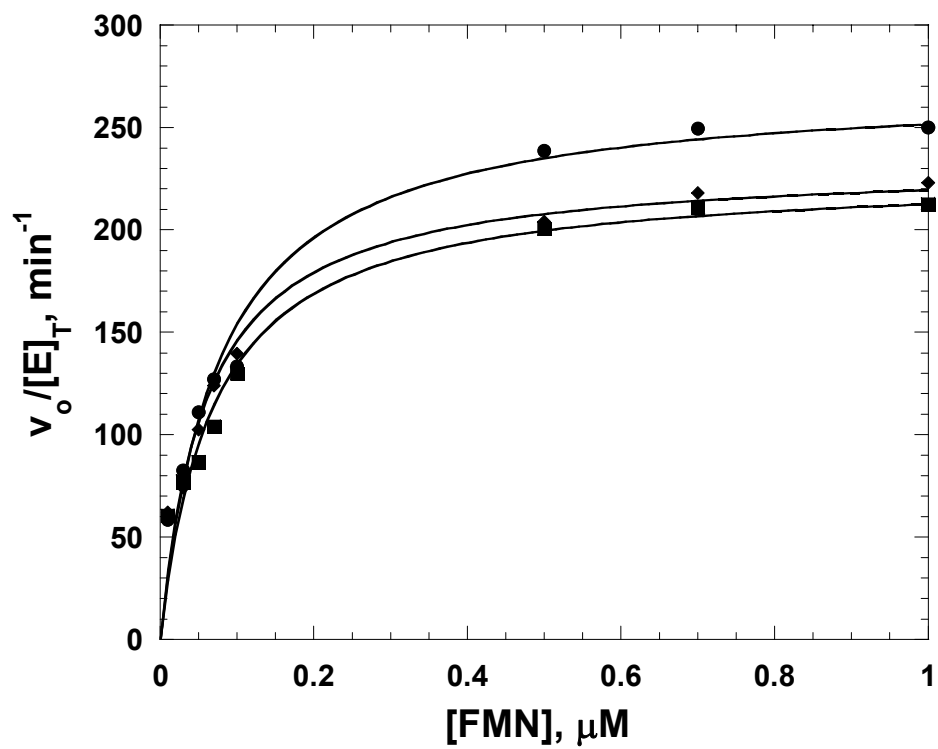


Figure 3.12. Kinetic analyses with varying ratios of SsuD:SsuE.

SsuE only ( $\diamond$ ), SsuE:SsuD=1:1 ( $\bullet$ ), SsuE:SsuD=1:2 ( $\blacksquare$ )

Table 3.2. Kinetic parameters for SsuE with SsuD.

	$K_{m, \text{FMN}} (\mu\text{M})$	$k_{\text{cat}} (\text{min}^{-1})$	$k_{\text{cat}}/K_{m, \text{FMN}} (\text{min}^{-1}/\mu\text{M})$
SsuE	$0.059 \pm 0.008$	$232 \pm 9$	$3900 \pm 20$
SsuD:SsuE = 1:1	$0.076 \pm 0.01$	$270 \pm 11$	$3500 \pm 10$
SsuD:SsuE = 2:1	$0.069 \pm 0.01$	$227 \pm 12$	$3300 \pm 20$

### *3.7 Steady-state kinetic mechanism of the SsuE enzyme in the presence of the SsuD enzyme and alkanesulfonate substrate*

Although there was no significant change in the kinetic parameters of SsuE in the presence of SsuD only, we were interested in determining if the kinetic parameters and mechanism of the SsuE enzyme were altered with the addition of the SsuD enzyme and saturating alkanesulfonate substrate. Experiments were performed similar to those already described with the addition of octanesulfonate and a stoichiometric amount of SsuD enzyme relative to SsuE. The octanesulfonate substrate was previously shown to be a preferred substrate for the SsuD enzyme [18]. Double reciprocal plots of initial reaction rates against varying concentrations of FMN at several fixed concentrations of NADPH intersected on the  $e/v$  axis (Figure 3.13). Double reciprocal plots of reaction rates against NADPH concentration at different fixed concentrations of FMN intersected to the left of the  $e/v$  axis above the x-axis (Figure 3.13). These results were best fit to Eq. 17 for a rapid equilibrium ordered mechanism with NADPH binding first followed by FMN to form the ternary complex to give a  $K_m$  value for FMN of  $0.13 \pm 0.01 \mu\text{M}$ , a  $K_{ia}$  value of  $3.5 \pm 0.1 \mu\text{M}$ , and a  $k_{\text{cat}}$  value of  $104.0 \pm 0.5 \text{ min}^{-1}$  (Table 3.3). A rapid equilibrium ordered mechanism indicates that the  $K_m$  value for the first substrate is appreciably lower than the  $K_{ia}$  value, and can typically be confirmed by analyzing the data from Figure 3.13 as a secondary plot of the slopes versus  $1/[\text{FMN}]$  concentration [89]. For a bireactant equilibrium ordered mechanism a replot of the data should be linear and extrapolate through the origin. It was difficult to verify this mechanism further because FMN is inhibitory at high concentrations which limits the analysis of the slope effects. The inhibitory effect of increased flavin concentrations on the specific activity was previously



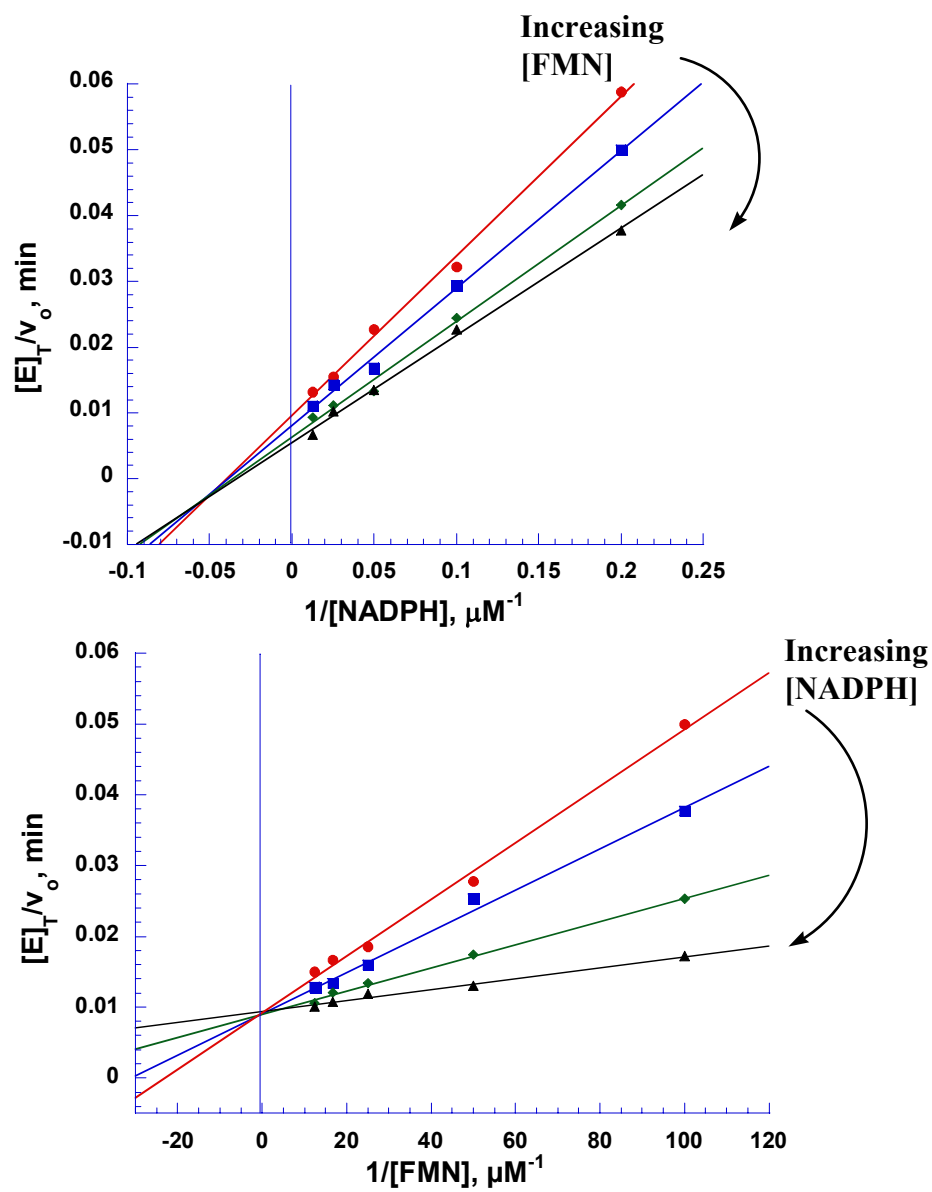


Figure 3.13. Initial velocity patterns of the SsuE catalyzed reduction by FMN with SsuD and octanesulfonate.

Table 3.3. Steady-state kinetic parameters for SsuE.

	SsuE	SsuE + SsuD and octanesulfonate
$k_{\text{cat}}$ ( $\text{min}^{-1}$ )	$116.0 \pm 6.3$	$104.0 \pm 0.5$
$K_{\text{FMN}}$ ( $\mu\text{M}$ )	$0.016 \pm 0.002$	$0.13 \pm 0.01$
$K_{\text{NADPH}}$ ( $\mu\text{M}$ )	$5.4 \pm 0.9$	0.00
$K_{\text{iNADPH}}$ ( $\mu\text{M}$ )	$3.9 \pm 2.4$	$3.5 \pm 0.1$

observed with the alkanesulfonate monooxygenase system [18]. However, the data strongly suggests that the mechanism of the SsuE protein is modified from an ordered to a rapid equilibrium ordered kinetic mechanism and a 10-fold increase in the  $K_m$  value for FMN is observed in the presence of SsuD and the octanesulfonate substrate. Figure 3.14 is the representation of the modified kinetic mechanism of SsuE with SsuD and octanesulfonate present. With the modified mechanism, NADPH binds to SsuE enzyme in rapid equilibrium, and ensures the reaction is driven in the forward direction even with low concentrations of NADPH.

### *3.8 Pre-steady-state kinetic analysis of SsuE enzyme*

#### *3.8.1 Reduction of oxidized flavin by NADPH.*

The reaction mechanism of SsuE involves the reduction of the flavin by NADPH. Rapid reaction kinetic analyses were performed using photodiode array detection to monitor the overall reduction of the flavin. Representative absorption spectra following the mixing of SsuE with FMN and NADPH are shown from 1 ms to 10 s (Figure 3.15). There was an observable decrease in the flavin spectra that was complete by one second. Closer examination of the absorbance spectra showed a broad absorbance band between 520 and 650 nm (Figure 3.16). A long-wavelength absorbance band is indicative of charge-transfer complexes between flavin and the pyridine nucleotide. Two charge transfer complexes can be generated; one between oxidized flavin and NADPH (CT-1), and the other between reduced flavin and  $\text{NADP}^+$  (CT-2). The weak absorbance increase in the long-wavelength absorbance region (520-650 nm) occurred at the beginning of the reaction and was complete upon full reduction of the flavin. The first spectrum was taken

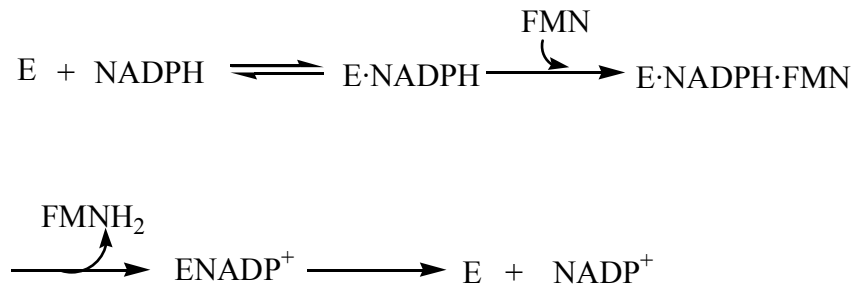


Figure 3.14. Rapid equilibrium ordered sequential mechanism.

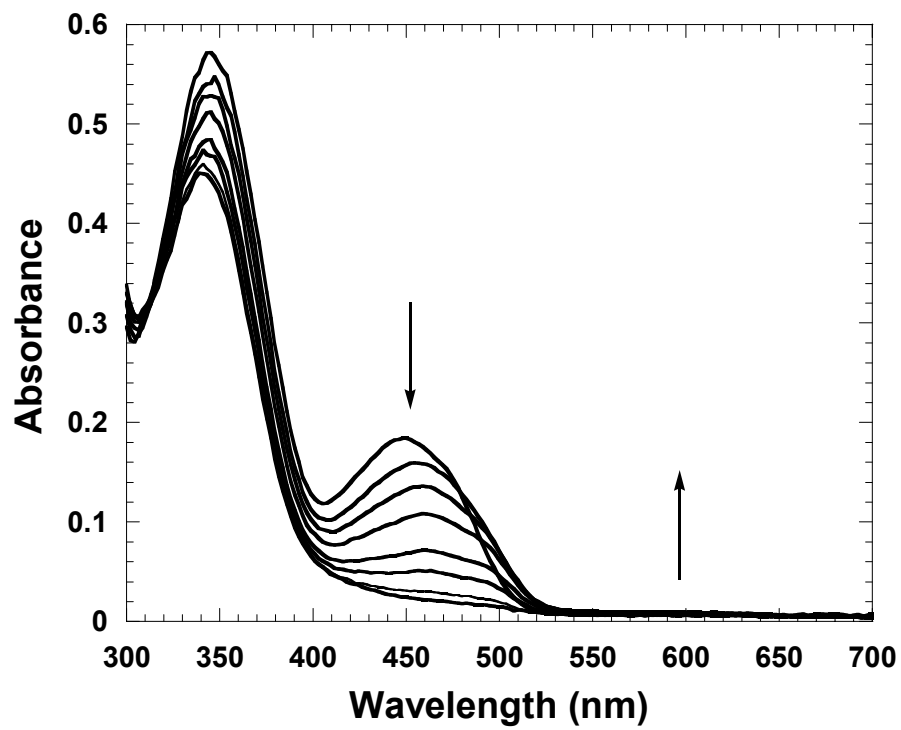


Figure 3.15. Diode array spectra monitoring the absorbance change (from 1 ms to 10 s).

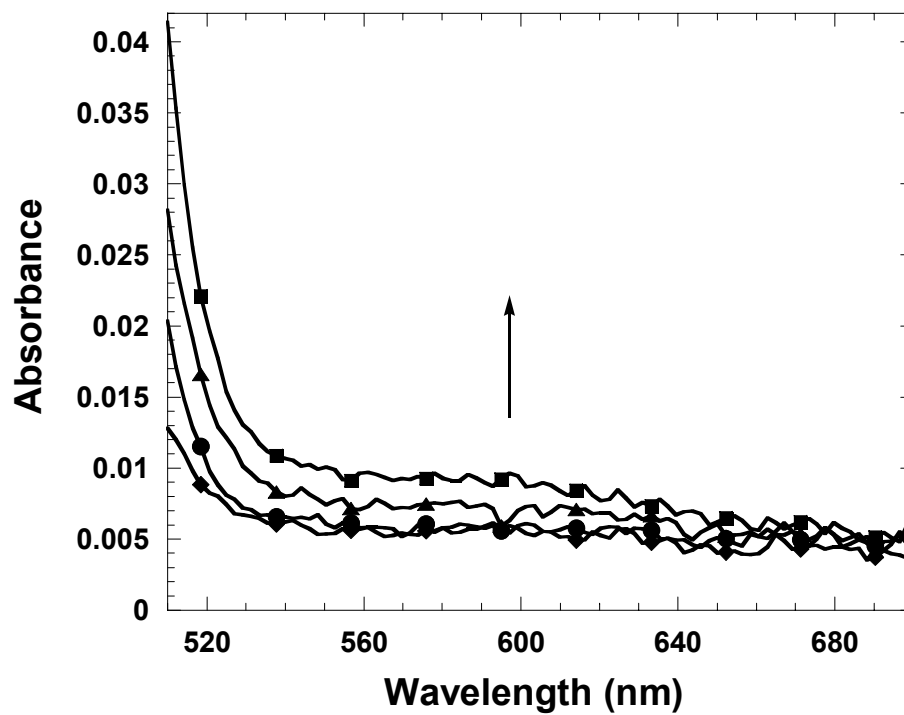


Figure 3.16. Charge-transfer complex formation during flavin reduction (the data shown were recorded at 1 (●), 76 (■), 227 (▲), and 536 (◆) ms after the initiation of the reaction).

immediately after mixing SsuE with FMN and NADPH, and there was no appearance of a broad absorbance band. By 76 ms a weak absorption band was formed in the long wavelength range, that had diminished back to baseline after 0.6 s. These results indicate that a weak charge-transfer complex is formed between the enzyme bound flavin and pyridine nucleotide, however it was difficult to discern between the two charge-transfer complexes (CT-1 and CT-2).

### 3.8.2 *Flavin reduction and charge-transfer complex formation.*

Stopped-flow single wavelength measurements were carried out at 450 and 550 nm to further examine the formation of the charge-transfer complex in SsuE catalyzed flavin reduction. The traces obtained at 450 and 550 nm were superimposed to identify the individual phases associated with flavin reduction (Figure 3.17), and plotted in log time to observe the absorbance changes at the start of the reaction. An absorbance decrease at 450 nm representing the flavin reduction process was observed and was complete by 0.6 second. Data obtained at 550 nm showed a distinct increase followed by a decrease in absorbance with a similar time course as the absorbance trace obtained at 450 nm corresponding to flavin reduction. Both spectra at 450 and 550 nm were best fit to the sum of three exponentials representing three distinct phases for the reaction (Eq. 21). The trace at 550 nm showed a rapid initial absorbance increase followed by a phase with a much slower absorbance increase. In the final phase, a decrease in the absorbance at 550 nm back to baseline was observed. These results from the single-wavelength studies at 550 nm were consistent with the formation of a charge-transfer complex. The initial fast phase at 550 nm had an observed rate of  $241.4 \pm 5.7 \text{ s}^{-1}$  ( $k_{1\text{obs}}$ ). When compared to the spectra obtained at 450 nm, this initial fast phase corresponded to the

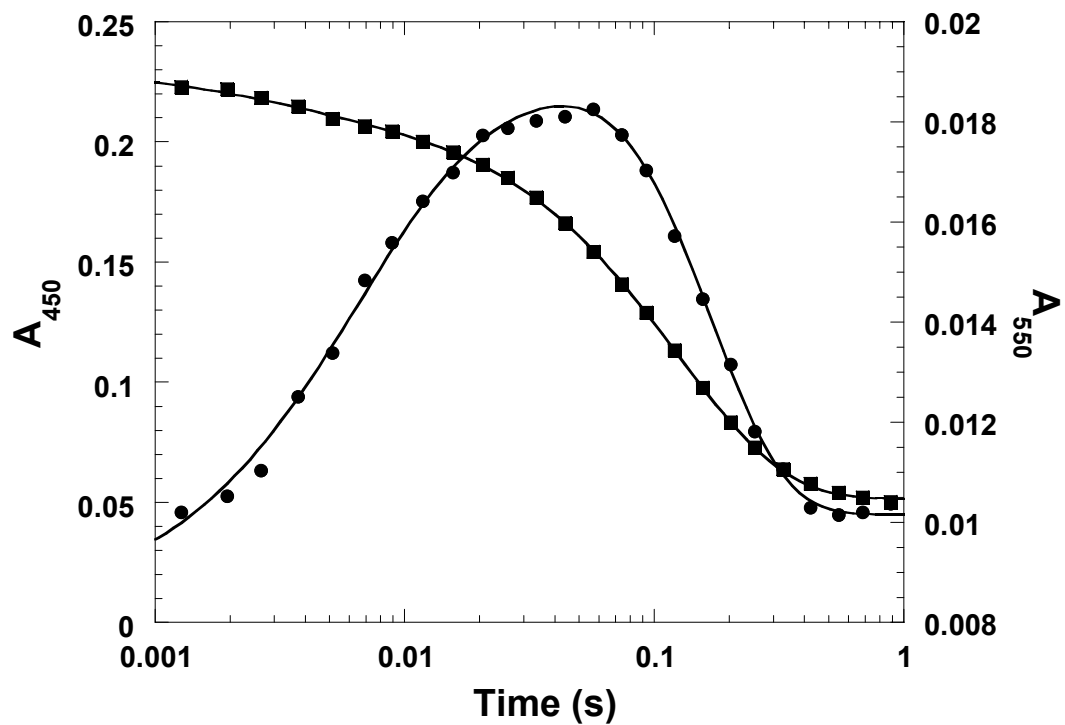


Figure 3.17. Single wavelength absorbance traces at 450 (■) and 550 (●) nm.



majority of flavin still in the oxidized form. The slower second phase relative to the first fast phase at 550 nm, had an observed rate of  $11.0 \pm 0.4 \text{ s}^{-1}$  ( $k_{2\text{obs}}$ ). An observed rate of  $19 \pm 1 \text{ s}^{-1}$  ( $k_{3\text{obs}}$ ) was obtained for the third phase, which represented a decrease in the absorbance at 550 nm. The decrease in absorbance at 550 nm corresponded to the third phase at 450 nm representing flavin reduction.

### *3.8.3 Rapid flavin reduction of SsuE enzyme with SsuD*

Previous studies had shown that the kinetic mechanism of SsuE was altered from an ordered mechanism to a rapid equilibrium ordered mechanism in the presence of SsuD and the octanesulfonate substrate [57]. Whereas, there was no significant change in steady-state kinetic parameters in coupled assays with only SsuD. The rapid reaction kinetic experiments described above were also performed in the presence of SsuD to explore the effect of SsuD on the SsuE catalyzed reductive half-reaction. The results showed that there were no significant changes in the individual rate constants between the single enzyme assay and the coupled assay (Figure 3.18) suggesting that SsuD had no observable influence on the individual rates of flavin reduction or charge-transfer formation by SsuE.

### *3.8.4 Dependence of flavin reduction on NADPH concentration*

In order to investigate the dependence of flavin reduction on the concentration of NADPH, stopped-flow experiments were performed with varying concentrations of NADPH monitoring flavin reduction at 450 nm. Traces obtained from 450 nm were best fit to triple exponentials, and only  $k_{1\text{obs}}$  showed a dependence on NADPH concentrations. Figure 3.19 revealed that the rate of flavin reduction was directly dependent on NADPH concentrations. This observation is consistent with results from steady-state studies.

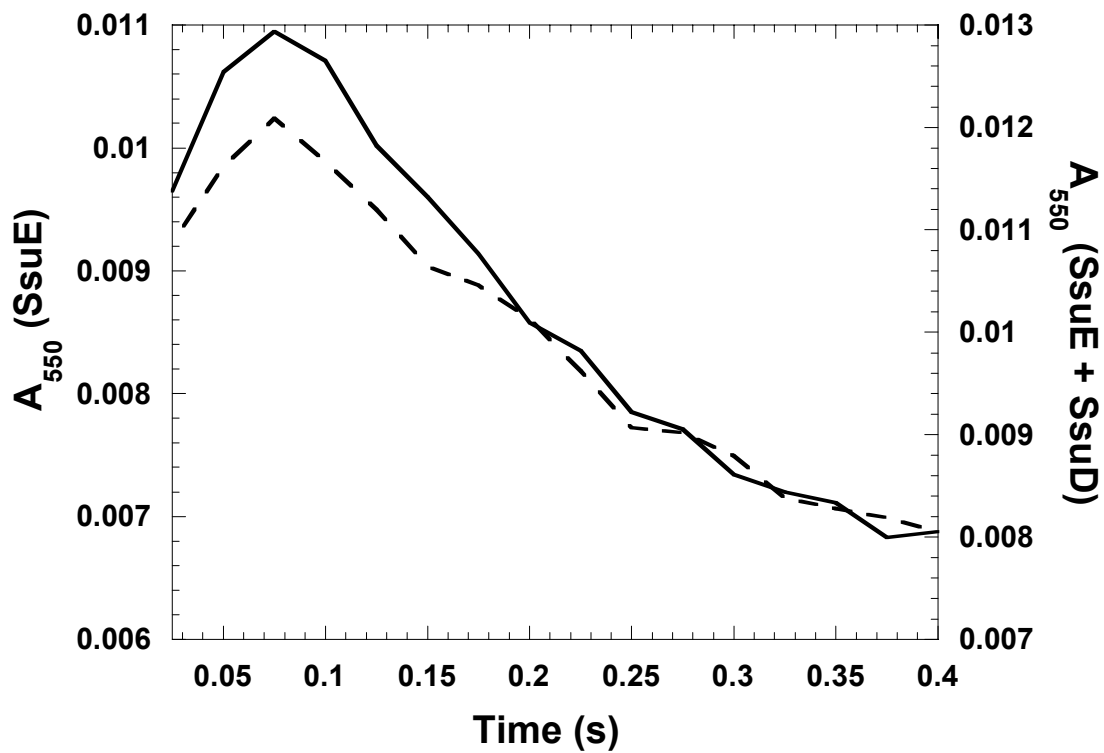


Figure 3.18. Charge-transfer complex formation with SsuE only (solid line) or SsuE + SsuD (dashed line).

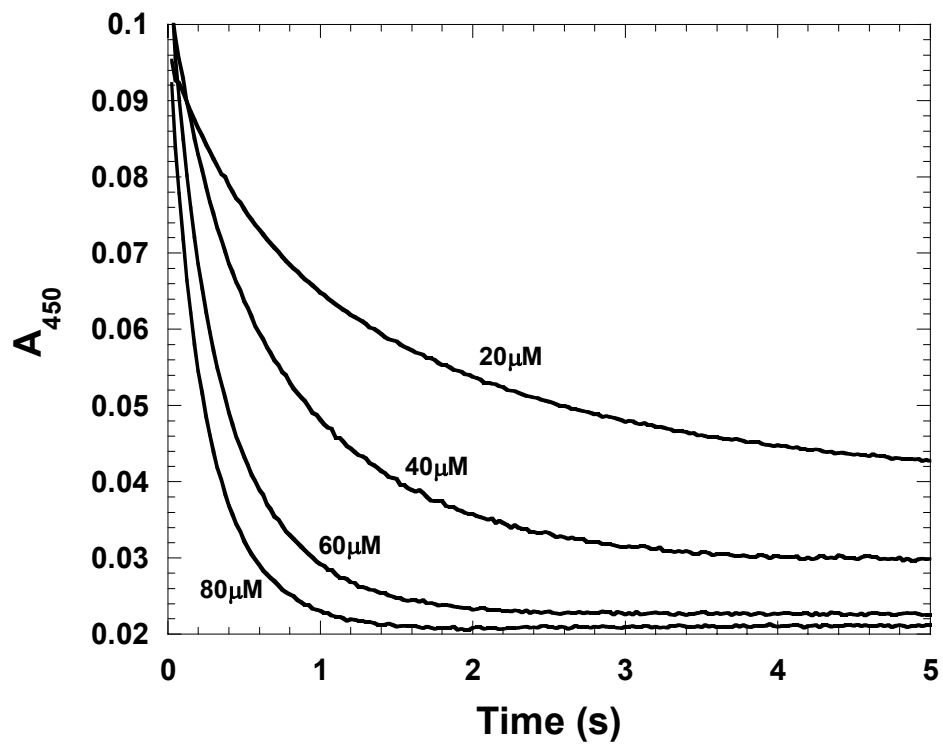


Figure 3.19. Flavin reduction dependence on NADPH concentrations.

### 3.8.5 Dependence of charge-transfer complex formation on NADPH concentration

Studies from single-wavelength experiments with SsuE at 550 nm suggested that NADPH forms a charge-transfer complex during flavin reduction. The dependence of charge-transfer complex formation on the concentration of NADPH was performed to determine if any of the individual rates were dependent on the concentration of the pyridine nucleotide substrate. There was a hyperbolic dependence on the NADPH concentration for  $k_{1\text{obs}}$  at 550 nm with a value for the y-intercept of zero (Figure 3.20). This is consistent with NADPH binding in rapid equilibrium to the enzyme followed by the essentially irreversible formation of a charge-transfer complex. A fit of the data to Eq. 22 gave a  $K_d$  of  $0.29 \pm 0.03$  mM for the binding of NADPH to SsuE with a limiting rate constant for  $k_1$  of  $364 \text{ s}^{-1}$ . Interestingly, the observed second and third phases were independent of NADPH concentration (Figure 3.21). The dependence of the initial fast phase on NADPH concentration would be expected for a charge-transfer complex representing the oxidized flavin associated with the reduced pyridine nucleotide as observed with previously characterized flavin reductases [38, 69]. Based on these results the formation of a charge-transfer complex between FMN and NADPH (CT-1) is assigned to the rate constant for  $k_{1\text{obs}}$ .

### 3.8.6 Dependence of charge-transfer complex formation on FMN concentration

For most flavoproteins the flavin is tightly bound to the protein so monitoring the dependence of the flavin on the reaction rate is typically not determined. Because SsuE utilizes flavin as a substrate, the rate dependence on the flavin concentration for charge-transfer complex formation could be monitored at 550 nm. Figure 3.22 demonstrates the dependence of the flavin concentration on charge-transfer complex formation during

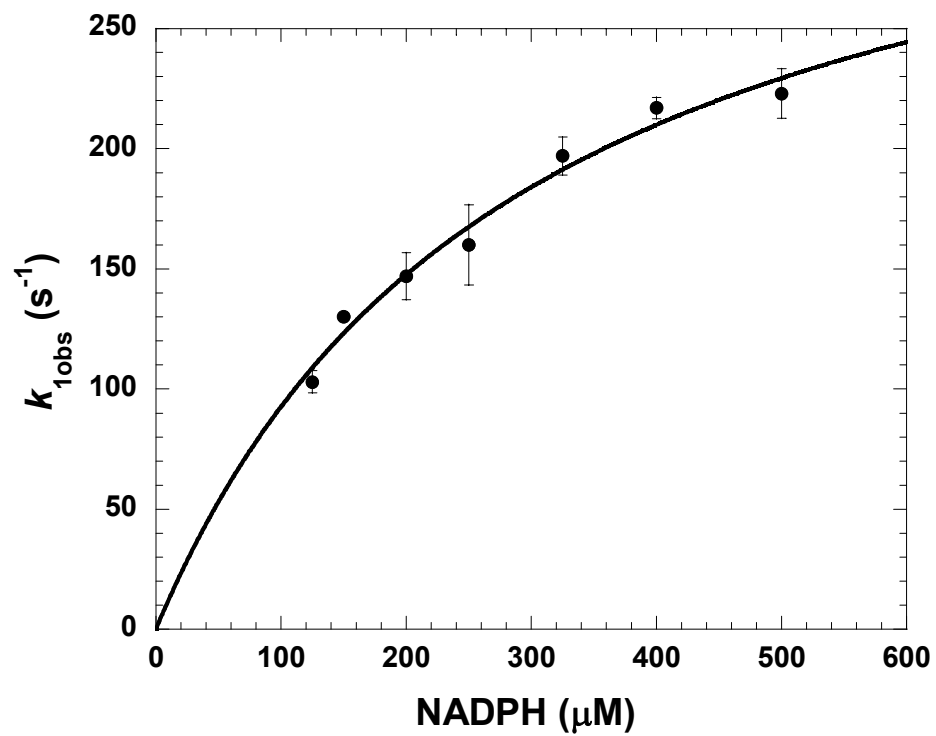


Figure 3.20. The dependence of the observed rates on NADPH concentration in SsuE catalyzed flavin reduction.

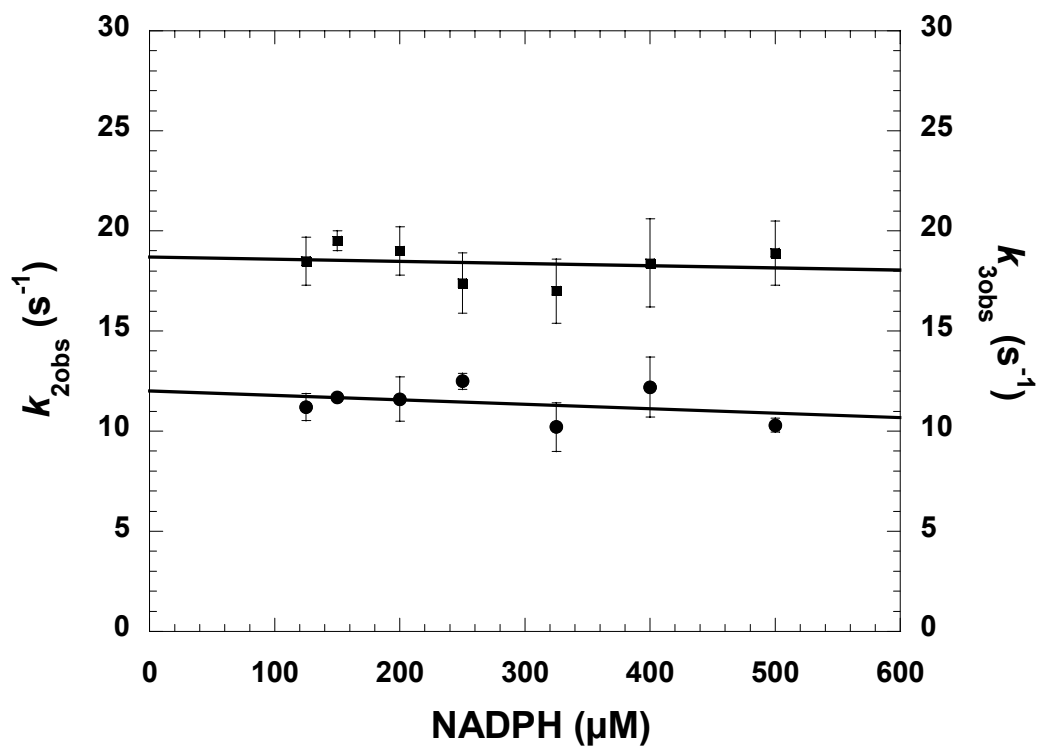


Figure 3.21. The dependence of the observed rates on NADPH concentration in SsuE catalyzed flavin reduction.  $k_{2\text{obs}}$  (●),  $k_{3\text{obs}}$  (■).

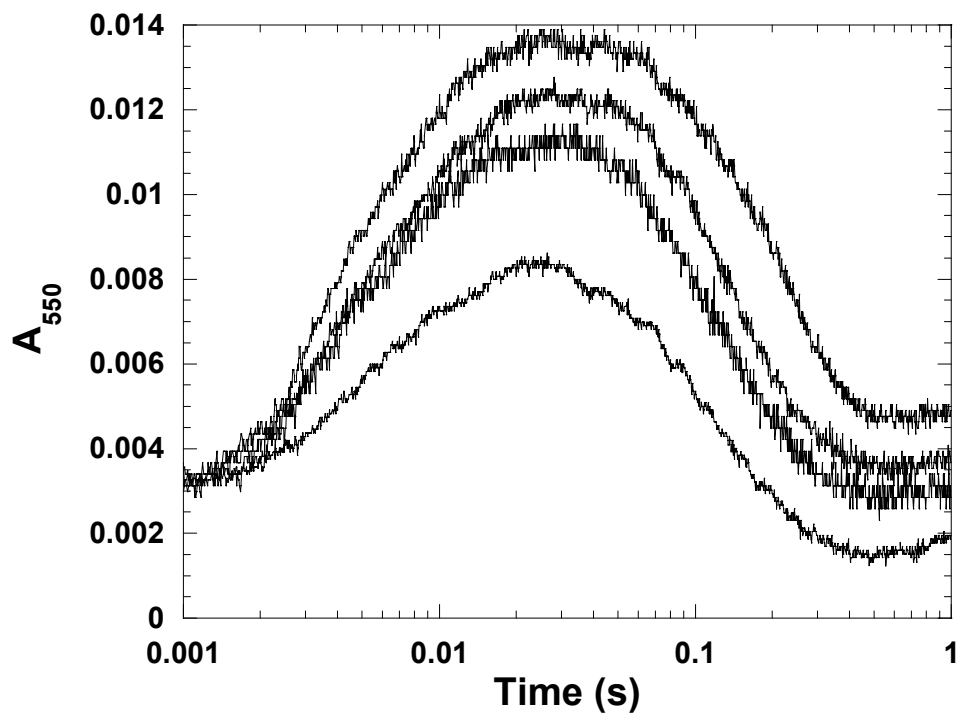


Figure 2.22. FMN-dependence on charge-transfer complex formation (FMN concentration from top to bottom spectra: 50, 30, 20, and 10  $\mu\text{M}$ ).

flavin reduction. Higher flavin concentrations resulted in an increase in charge-transfer complex formation. Figure 3.23 shows a plot of the dependence of the initial fast phase ( $k_{1\text{obs}}$ ) on FMN concentration. The  $k_{1\text{obs}}$  showed a clear hyperbolic dependence on the flavin concentration with a zero y-intercept. The data were fitted to Eq. 22 to give a  $K_d$  of  $7.9 \pm 0.2 \mu\text{M}$  for the binding of FMN to SsuE with a limiting rate constant for  $k_1$  of  $199.0 \pm 2.3 \text{ s}^{-1}$ . The dependence of  $k_{1\text{obs}}$  on the flavin concentration confirmed the fast phase at 550 nm as CT-1. The observed second and third reaction phases were independent of low flavin concentrations. However, as the concentration of flavin increased there was a clear decrease in the rates for both phases (Figure 3.24). This demonstrated that substrate inhibition occurred at a charge-transfer conversion step. Similar FMN-dependent inhibition has been observed for the SsuE protein by steady-state kinetic analysis [18, 57], and in coupled reactions with FMN reductases associated with bacterial luciferase [58].

### 3.8.7 Isotope effects with deuterated pyridine nucleotide substrate.

Deuterated [(4*R*)-<sup>2</sup>H]NADPH was synthesized and utilized in rapid kinetic reactions to further investigate the step corresponding to hydride transfer to the flavin. Previous studies have shown that flavin reductases are selective for reduced pyridine nucleotides at the pro-*R* position [90, 91]. The reduced pyridine nucleotide NADPH was also synthesized as a control to ensure that the reaction of [(4*R*)-<sup>2</sup>H]NADPH did not contain contaminants that could inhibit the reaction. Each reaction was monitored at 550 nm to determine if an isotope effect was observed with any of the individual phases. Single-wavelength absorbance spectra showed a similar pattern with either [(4*R*)-<sup>2</sup>H]NADPH or NADPH for the formation of the charge-transfer complex (Figure 3.25). A



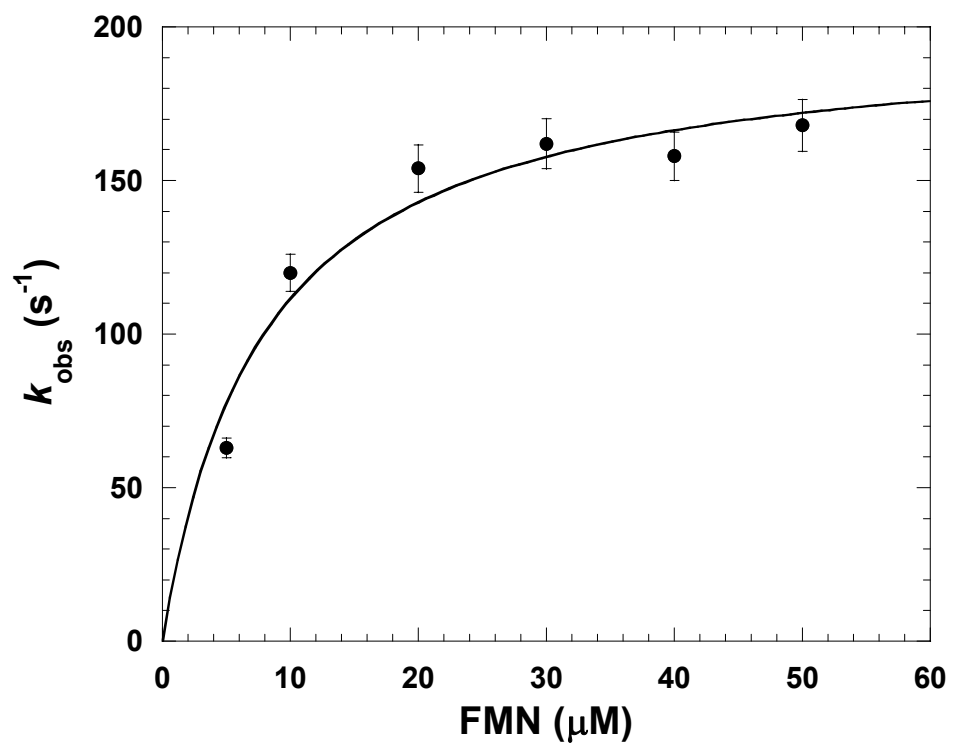


Figure 3.23. The dependence of the observed rates on FMN concentration in SsuE catalyzed flavin reduction.

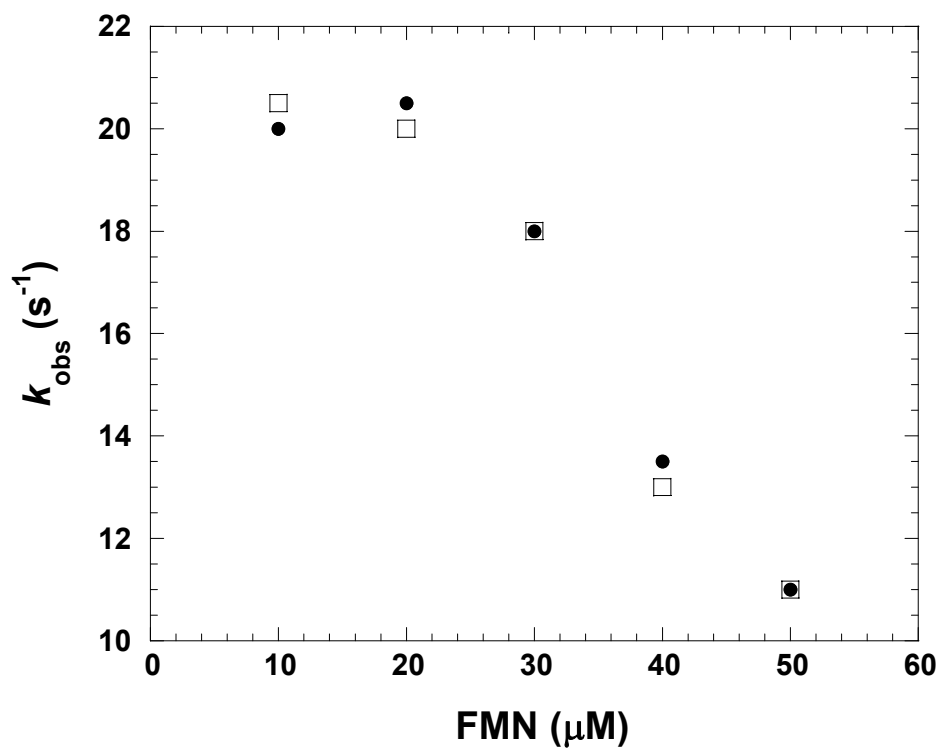


Figure 3.24. Flavin inhibition on charge-transfer complex formation,  $k_{2\text{obs}}$  (●),  $k_{3\text{obs}}$  (□).

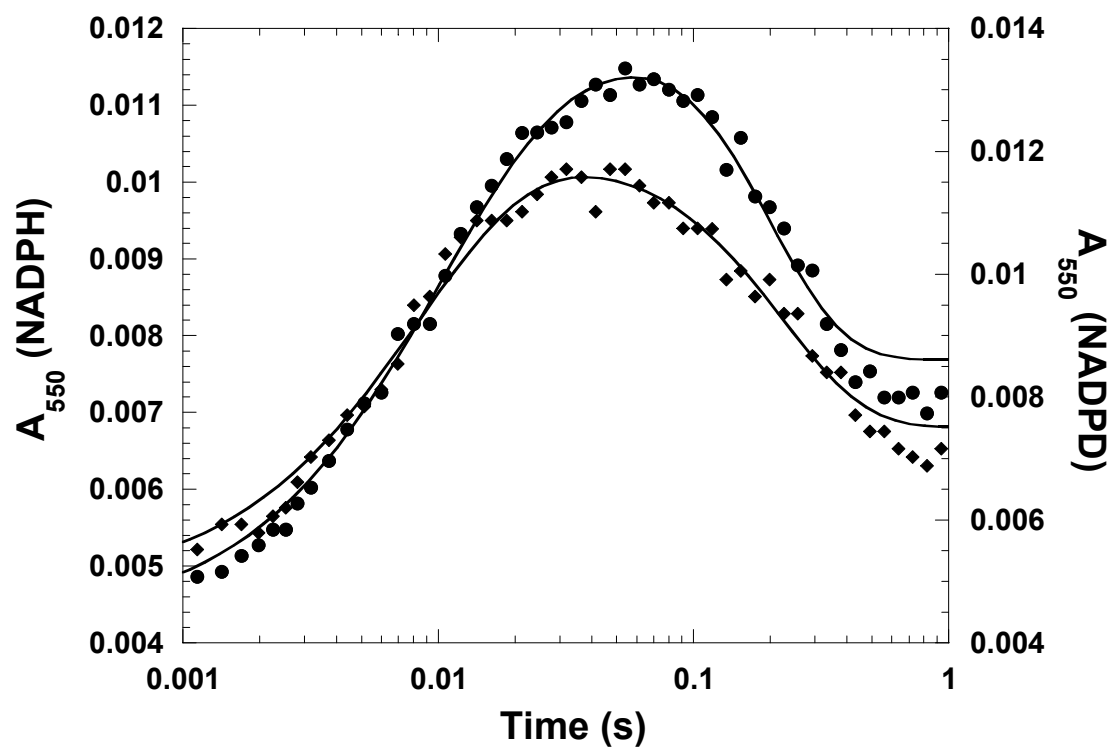


Figure 3.25. Single wavelength absorbance traces at 550 nm with NADPH (●) and [4(R)-<sup>2</sup>H]NADPH (◆).

similar trace was observed with [(4*R*)-<sup>2</sup>H]NADPH that was best fit to a triple exponential. The first rate ( $k_1$ ) was almost identical with [(4*R*)-<sup>2</sup>H]NADPH or NADPH as the reducing reagent. Interestingly, the rate calculation demonstrated an isotope effect of 1.3 on the second ( $k_2$ ) and third ( $k_3$ ) phases. These results suggested that the conversion of CT-1 to CT-2 is the rate-limiting step by which electron transfer takes place, and assigns this conversion to  $k_2$ . Not only was the rate affected by deuterated substrate, but the amplitude was also altered. The charge-transfer complex with [(4*R*)-<sup>2</sup>H]NADPH did not reach the same maximal absorbance level as with NADPH. The heavier substrate slowed the charge-transfer complex conversion from CT-1 to CT-2, and reduced the amount of charge-transfer formed during flavin reduction.

### 3.9 Site-directed mutagenesis of *SsuE*

Determining the structure of *SsuE* will provide a basis for further studies aimed at analyzing the catalytic mechanism of flavin reduction and flavin transfer. The *SsuE* protein lacks cysteine and methionine residues, consistent with its role in scavenging sulfur from alternate sources during sulfur starvation. The lack of methionine residues in this protein ruled out standard expression protocols to obtain selenomethionyl protein for MAD (multi-wavelength anomalous diffraction) phasing. An alternative approach for derivatization is to substitute leucine residues with methionine for MAD phasing analysis [92]. The preliminary idea was that the replacements will not interfere with crystal growth, and leave the crystal structure isomorphous with the wild-type protein [92]. Amino acid residues L20 and L165 were replaced with methionine, however, when the mutant was purified, it was difficult to obtain significant quantities for analysis. Results from amino acid sequence analysis identified a leucine residue at a position in *E. coli*

substituted with methionine in *Pseudomonas aeruginosa* and *P. putida*, making this residue ideal for conservative substitution. The substitution of L114M, L165M was confirmed by DNA-sequence analysis at Davis Sequencing (University of California, Davis).

Selenomethionyl SsuE (L114,165SeMet SsuE) protein was expressed under conditions of methionine pathway inhibition. The purification protocol for the expressed protein followed the same procedure as previously described for wild-type SsuE [57] except that 5 mM DTT was added to buffers during the entire purification process. The purified L114,165SeMet SsuE protein separated at the same molecular weight as wild type SsuE on SDS-PAGE (Figure 3.26), and possessed similar activity to the wildtype protein.

Circular dichroism experiments were performed to verify the secondary structures of the L114,165SeMet and wild-type SsuE proteins. The result revealed that these two spectra overlapped each other (Figure 3.27), and suggested that selenomethionyl substitutions did not cause any major perturbations in secondary structure.

### *3.10 Single crystal of native SsuE and SeMet SsuE*

The wild type SsuE was successfully crystallized by hanging-drop vapor-diffusion experiments within two weeks. A large single hexagonal rod crystal was formed for SsuE protein (Figure 3.28). A similar method was used for the crystallization of SeMet SsuE cocrystallized with oxidized flavin substrate. A yellow crystal was formed for SeMet SsuE (Figure 3.29), and will be further analyzed to determine if X-ray diffraction data can be collected for this crystal.

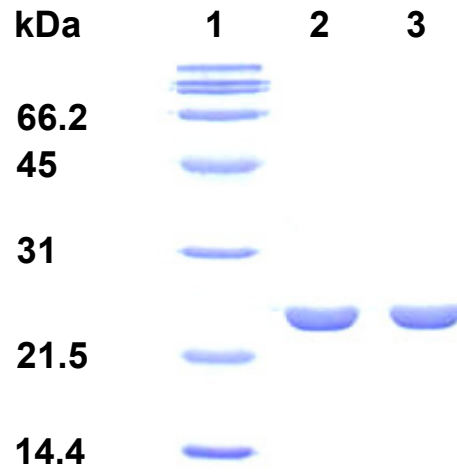


Figure 3.26. SDS-PAGE of purified SeMet SsuE and wild-type SsuE  
(Lane 1, protein marker; Lane 2, SeMet SsuE; Lane 3, wild-type SsuE).

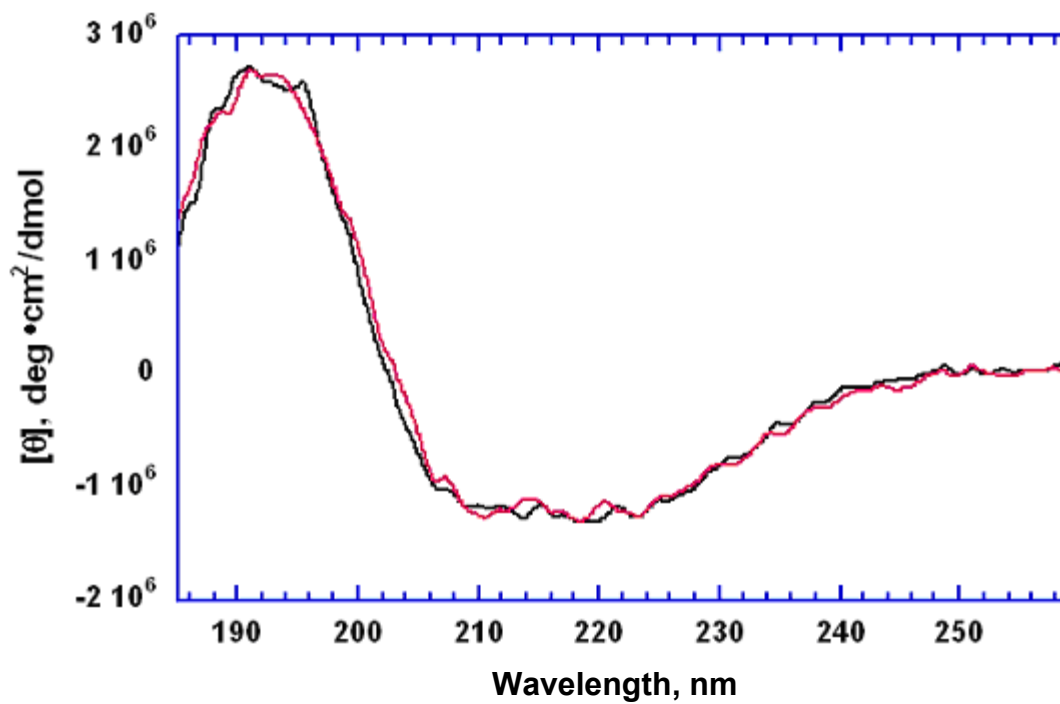


Figure 3.27. CD spectra of SeMet SsuE and wild-type SsuE (Black: wild-type SsuE; Red: SeMet SsuE).

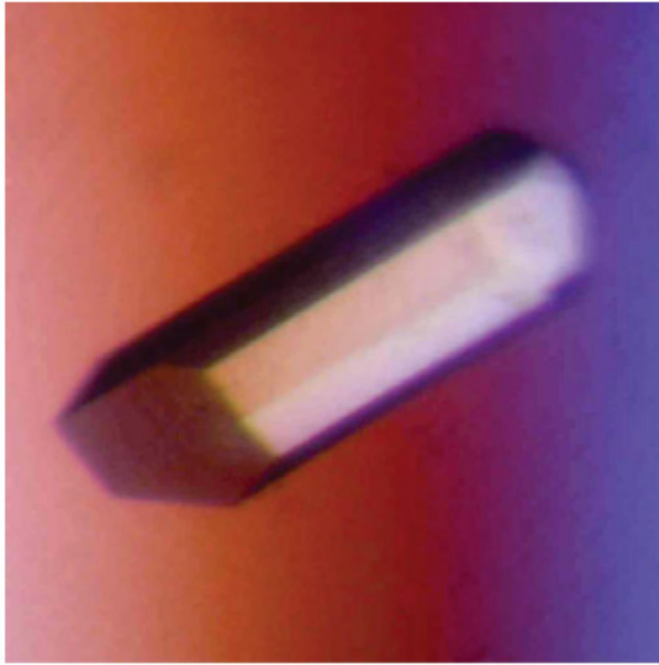


Figure 3.28. The hexagonal rod crystal of SsuE protein.



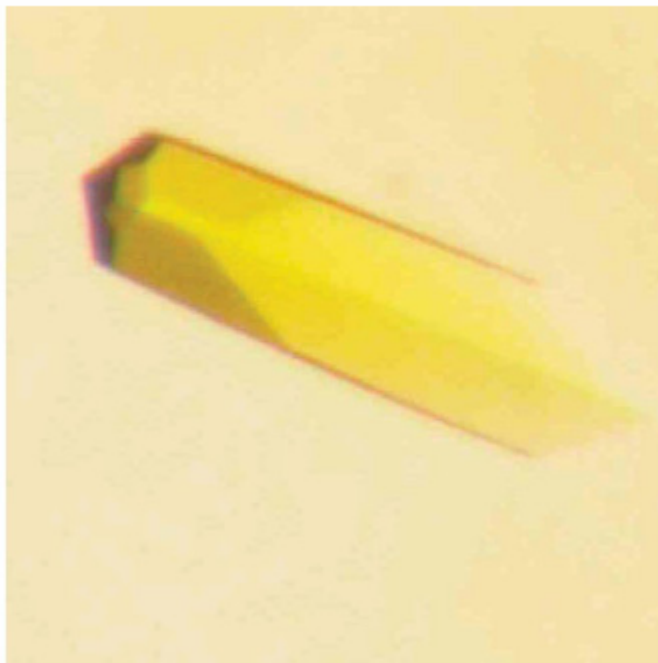


Figure 3.29. The SeMet SsuE crystal co-crystalized with FMN.

### 3.11 The X-ray pattern and Pseudo-precession image of native SsuE

The SsuE crystal was subjected to X-ray diffraction with Cu  $K\alpha$  radiation. Several complete diffraction data were collected, indexed, integrated, and scaled using d\**TREK* program [88]. The X-ray diffraction pattern and pseudo-precession image were shown in figure 3.30 and 3.31. A 2.9 Å resolution defines the SsuE crystal to a space group of *P622*, with unit-cell parameters  $a = b = 183.8$ ,  $c = 181.5$  Å,  $\alpha = \beta = 90$ ,  $\gamma = 120^\circ$ . The calculated monomeric volume of the crystal is 2.60 Å<sup>3</sup>/Da, representing eight SsuE monomers in the asymmetric unit. Further crystallographic studies are under way with L114, 165SeMet SsuE to solve the three-dimensional structure by MAD phasing.

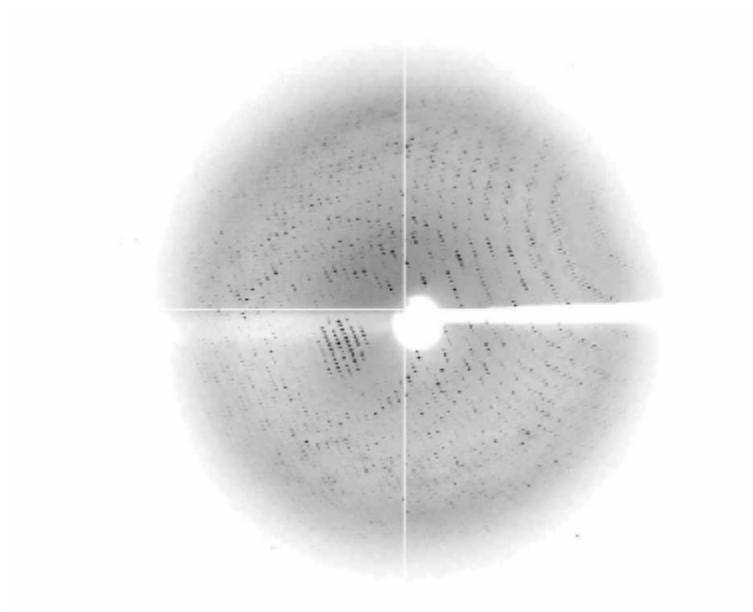


Figure 3.30. X-ray diffraction pattern of the native SsuE protein.

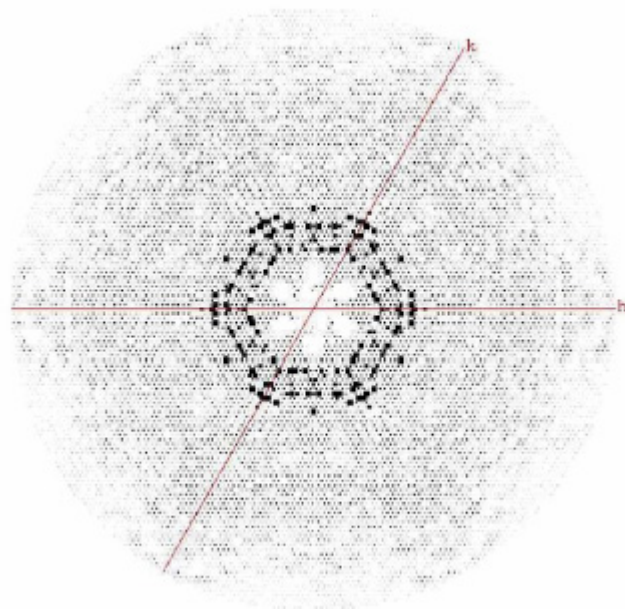


Figure 3.31. The Pseudo-precession image of the native SsuE protein.

## **CHAPTER FOUR**

### **DISCUSSION**

Flavoproteins in prokaryotic and eukaryotic organisms are a diverse group of enzymes that participate in many vital biological reactions in living cells. From a structural view, they range from single enzymes to complex systems. Most flavoenzymes accommodate both flavin reduction and oxidation on the same enzyme. Because the flavin is a tightly bound prosthetic group, this group of flavoenzymes has tight control over redox reactions. In some flavoenzymes, the active sites contain more than one flavin cofactor and an iron-sulfur cluster is often included to facilitate the electron transfer reaction. The reactions catalyzed by flavin-dependent two-component systems are commonly composed of a flavin reductase coupled with a monooxygenase enzyme. The two-component enzyme systems catalyze various reactions including oxygenation, light emission, and detoxification of recalcitrant compounds.

A strictly coupled flavin dependent two-component system involved in desulfonation is expressed on a single operon. It is comprised of a flavin reductase and a flavin-dependent monooxygenase. The flavin reductase supplies reduced flavin for the monooxygenase to activate molecular oxygen for C-S bond cleavage. Organosulfur is considered a stable compound that is difficult to eliminate from the environment. Many

efforts have been applied to eradicate this detrimental pollutant. The chemical methods employed are either expensive or produce equally harmful compounds. The two-component alkanesulfonate monooxygenase system from *E. coli* is a good candidate for bioremediation to desulfonate a broad range of organosulfur compounds. In addition, the sulfur chemistry of the C-S bond cleavage and flavin transfer is novel in this system. An in depth investigation was carried out in our lab to characterize the catalytic mechanism of the FMN reductase from the alkanesulfonate monooxygenase system.

#### *4.1 Biophysical and biochemical characterization of SsuE and SsuD proteins*

The SsuE protein and SsuD protein were expressed by cloning the genes for *ssuE* and *ssuD* onto a pET21a vector, followed by transformation into the *E. coli* expression strain BL21(DE3). A purification protocol for SsuE and SsuD was developed, applying both ammonium sulfate fractionation and column chromatography. The purification of SsuE and SsuD yielded 30-50 mgs of protein from a 2 L growth, and achieved greater than 90 % purity for both proteins.

ESI-mass spectrometry was used to obtain an accurate molecular weight for each protein. The molecular weight determined by mass spectrometry was  $21,257.0 \pm 1.5$  for SsuE, which is similar to the calculated molecular weight of 21,253. The molecular weight of SsuD was  $41,615.4 \pm 2.6$ , compared to the calculated molecular weight of 41,605. Results from analytical ultracentrifugation studies showed the quaternary structure of SsuE as a homodimer and SsuD as a homotetramer, respectively.

SsuE catalyzes the reduction of flavin by pyridine nucleotides. Experiments were performed to determine the substrate specificity of SsuE. The structure of FAD and FMN differ from each other by an adenosine monophosphate group (Figure 1.8). FAD is an

FMN molecule structurally attached to an AMP moiety. Results from flavin specificity studies for SsuE showed a higher catalytic efficiency value for FMN when compared with FAD. The pyridine nucleotide substrates NADPH and NADH differ from each other by a 2' phosphate group (Figure 1.13). Results from pyridine nucleotide specificity studies showed equal catalytic efficiency values for NADPH and NADH. These results differed from previous studies which showed NADPH as the preferred pyridine nucleotide substrate [18]. Based on these substrate specificity studies and previous studies, FMN and NADPH were used for kinetic analyses through out this study.

#### *4.2 Steady-state kinetic mechanism of SsuE*

The two-component alkanesulfonate monooxygenase catalyzes two distinct reactions, so kinetic studies can be performed independently on each enzyme component. An interesting feature of this system is the presence of a flavin-dependent reductase involved in flavin reduction followed by the transfer of reduced flavin to the monooxygenase component. The mechanism of flavin transfer could either occur through a diffusion mechanism or by direct flavin transfer involving protein interactions between the reductase and monooxygenase enzyme. The goal of these studies was to first establish the kinetic mechanism and parameters of SsuE in single-enzyme assays and then compare these results with the kinetic behavior of SsuE in the presence of the SsuD enzyme with and without the alkanesulfonate substrate.

Initial studies focused on determining the affinity of each enzyme for oxidized FMN. These studies were central in establishing the specificity of each enzyme for oxidized flavin, and to determine if oxidized FMN binding to SsuD would interfere with further kinetic analysis with both SsuE and SsuD enzymes. The SsuE enzyme bound one

FMN per monomer, and had a 1000-fold lower  $K_d$  value than SsuD for oxidized flavin (Figure 3.7). Based on these results the flavin reductase has a greater affinity for the oxidized flavin than the monooxygenase enzyme. Similar results were obtained for the flavin reductase in the two-component enzyme system involved in styrene degradation that also relies on flavin transfer between a flavin reductase and monooxygenase enzyme in the kinetic mechanism [27]. While specific for FAD, the flavin reductase enzyme was shown to have a 10-fold lower  $K_d$  value for FAD when compared to the monooxygenase enzyme. The higher affinity of the flavin reductase for the oxidized form of the flavin species in this two-component family appears to play an important role in promoting flavin specificity between the FMN reductase and monooxygenase enzyme.

Data from the steady-state kinetic analysis of SsuE alone strongly support a sequential mechanism with the formation of a ternary complex before any chemistry occurs (Figure 3.8, 3.9). Formation of the ternary complex likely results in the transfer of electrons directly from NADPH to the flavin. Product inhibition studies with  $\text{NADP}^+$  (Fig. 3.10) further specify an ordered sequential mechanism with NADPH binding first followed by FMN as diagrammed in figure 3.11. Following reduction of the flavin, the reduced flavin product is released first and transferred either directly or by diffusion to SsuD. These results seem inconsistent with binding assays which demonstrate the ability of FMN to bind without the pyridine nucleotide substrate. However, the kinetic mechanism does not suggest that the second substrate cannot bind without the first substrate, but dictates that the reaction can only occur if the enzyme follows an ordered mechanism. An ordered sequential kinetic mechanism is consistent with other characterized flavin reductases that utilize flavin as a substrate, and further establishes



SsuE as a flavin reductase that lacks a bound flavin prosthetic group [61]. Interestingly, the flavin reductases that contain flavin as a bound cofactor typically follow a ping-pong mechanism in single-enzyme assays [27, 93].

#### *4.3 Steady-state kinetic mechanism with SsuD monooxygenase*

There was no observable change in the steady-state kinetic parameters of SsuE with varying ratios of the SsuD enzyme (Table 3.2), however the kinetic mechanism of SsuE was altered to an equilibrium ordered mechanism in the presence of SsuD and saturating levels of octanesulfonate. With this mechanism the NADPH substrate and  $\text{NADP}^+$  product are in equilibrium with free enzyme. At saturating levels of FMN, the rate of the reaction will not be dependent on the concentration of NADPH, and the equilibrium is displaced toward the ternary complex. These results suggest that SsuD and the octanesulfonate substrate ensure that the reaction is driven in the forward direction even in the presence of low concentrations of NADPH. Thus, there is no  $K_m$  value determined from the fit of the data for NADPH. Interestingly, the  $K_m$  value for FMN determined from the plot of the initial reaction rates was increased 10-fold over the  $K_m$  value for SsuE in the single-enzyme assay (Table 3.3).

There are several reports of observed changes in the kinetic parameters for the two-component monooxygenase family of enzymes when comparing single-enzyme flavin reductase assays to luciferase-coupled assays. The flavin reductases FRP and FRG of bacterial luciferase have been shown to follow a ping-pong mechanism when monitoring single-enzyme reductase activity [17, 58]. The FRP flavin reductases contain a bound FMN cofactor that is reduced by NADPH, oxidized  $\text{NADP}^+$  is released, and a second flavin binds and is reduced by the bound flavin cofactor. The reduced flavin

product in the absence of luciferase is oxidized in an unproductive dark reaction. Alternatively, in the coupled luminescence reaction measuring light emission, that includes luciferase and the decanal substrate in the reaction, the ping-pong mechanism is altered to a sequential mechanism. In addition, the  $K_m$  values for FMN and NADPH are decreased significantly in the coupled luminescence reaction when compared to the single-enzyme assay. In the coupled luminescence reaction the luciferase enzyme preferentially utilizes the FMNH<sub>2</sub> cofactor and directly competes with the FMN substrate in reacting with the reduced flavin cofactor. The change in the steady-state kinetic parameters and mechanism strongly support a model involving direct flavin transfer from the reductase to the luciferase enzyme. Conversely, there was no change in the steady-state kinetic parameters of the 4-hydroxyphenylacetate 3-monooxygenase system when monitoring the activity of the monooxygenase component in a coupled assay [76]. Instead, the mechanism of flavin transfer was proposed to occur through a diffusion mechanism due to the high affinity of the monooxygenase enzyme for reduced flavin.

Based on previous data and our current analysis, there are several possible explanations for the observed changes in the steady-state kinetic parameters and mechanism for SsuE. The  $K_m$  value of  $0.016 \pm 0.002 \mu\text{M}$  for flavin binding to SsuE in the single-enzyme assays is nearly equal to the  $K_d$  value, suggesting the  $K_m$  value essentially represents the dissociation constant. Therefore, the 10-fold increase in the  $K_m$  value for SsuE in the presence of SsuD and the alkanesulfonate substrate can be attributed to a decrease in the binding affinity for oxidized flavin. Because flavin transfer between proteins is an essential step in catalysis, a lower affinity for oxidized or reduced FMN by SsuE would likely increase the rate of reduced flavin transfer to SsuD. In addition, a

change to a rapid equilibrium ordered mechanism displaces the reaction towards the ternary complex and subsequent flavin transfer. The change in mechanism and observed increase in the  $K_m$  value for the oxidized flavin with SsuE in the presence of SsuD and the alkanesulfonate substrate ensures that the critical flavin transfer step in the pathway is preserved. Therefore flavin reduction by SsuE would lead to desulfonation of the alkanesulfonate substrate by SsuD as opposed to a nonproductive reaction leading to the generation of oxygen radicals.

An alternative explanation for the differences in the  $K_m$  values and steady-state mechanism is that there are two flavin binding sites in SsuE similar to that observed for bacterial luciferase FRG and FRP. The first site would result in nonproductive flavin reduction while the second site provides the reduced flavin utilized by SsuD. Although there is no bound flavin cofactor in SsuE, this does not exclude the existence of a second flavin binding site. One could envision that in the absence of SsuD and the octanesulfonate substrate the flavin binds to SsuE at the nonproductive FMN binding site that possesses a higher affinity for oxidized flavin. However, during catalytic turnover with SsuD the flavin binds to the second binding site with the higher  $K_m$  value for oxidized flavin. The reduced flavin located at the second binding site would be the preferred flavin substrate transferred to SsuD similar to the flavin transfer mechanism of bacterial luciferase. This may also explain why inhibition of SsuE at FMN concentrations above 0.2  $\mu\text{M}$  were observed in the experiments with SsuD and octanesulfonate. The excess flavin may be binding to the nonproductive binding site and competing with SsuD in reacting with the reduced flavin involved in flavin transfer. The observed kinetic change to a rapid equilibrium ordered mechanism would correspond with the second

flavin binding site. The necessity for the two binding sites in the bacterial luciferase FMN reductases has not been fully defined, and further experiments will be performed to explore the possibility of two flavin binding sites in SsuE.

The results are the first to define an altered kinetic mechanism in the FMN reductases while solely monitoring flavin reduction. There are still several questions to be addressed regarding the mechanism of reduced flavin transfer in this family of enzymes, however our work provides a basis for future studies aimed at evaluating the mechanism of flavin transfer between the alkanesulfonate monooxygenase enzymes.

#### *4.4 Pre-steady-state kinetic mechanism of SsuE*

The steady-state mechanism for many flavin reductases associated with two-component systems are known, however the reaction intermediates have not been characterized. The SsuE enzyme from the alkanesulfonate system was characterized by pre-steady-state kinetics to further understand the mechanistic role of this enzyme in flavin reduction and transfer.

Results from rapid reaction kinetic experiments demonstrated the formation of a charge-transfer complex during flavin reduction by SsuE. The generation of the relatively weak absorbance increase in the long-wavelength absorbance region is consistent with previous studies on flavoproteins in the FNR family. These results demonstrate that flavin reductases with low amino acid sequence identities to standard flavoproteins share similar mechanistic properties [63-69]. Compared to the proteins with a tightly bound flavin, the flavin reductases show a relatively weak formation of the charge-transfer complex. This may be caused by loose flavin binding to the active site of flavin reductases. Given the role of these enzymes in flavin reduction and transfer, a mechanism

involving a tightly bound flavin would not be as effective. However, a common mechanism involving the charge-transfer complexes between the donor (usually the reduced nicotinamide) and acceptor (oxidized flavin) may apply to flavin reductases. The formation of the charge transfer complexes is more complicated for proteins that utilize two flavins as cofactors, or a flavin and [2Fe-2S] center [94-96]. These flavoproteins require additional steps to reach the electron acceptor, and the intramolecular electron transfer often acts as the rate-limiting step in the overall reductive reaction [86, 96-101].

Further analyses of flavin reduction by SsuE at 550 nm showed a distinct increase and decrease in absorbance, characteristic of a charge transfer complex (Figure 3.17). The data was best fit to the sum of three exponentials with two of the phases associated with the initial formation of the charge transfer complex and the third phase assigned to complex decay. The initial fast phase ( $k_{1\text{obs}}$ ) showed a clear dependence on NADPH concentration, which would be expected for the formation of a complex between NADPH and FMN (Figure 3.20). The second ( $k_{2\text{obs}}$ ) and third ( $k_{3\text{obs}}$ ) phases were not dependent on the concentration of NADPH (Figure 3.21). These results indicate that three individual steps are involved in flavin reduction following the initial binding step to form MC-1. Formation of a charge-transfer complex between NADPH and FMN (CT-1) represents the initial fast phase ( $k_{1\text{obs}}$ ) at 550 nm due to the dependence of this phase on NADPH concentration. The phases for the formation of the charge-transfer complexes correlate with the absorbance changes monitoring reduction of the flavin at 450 nm (Figure 3.17).

The  $k_{1\text{obs}}$  representing the initial fast phase also showed a dependence on the flavin concentration at 550 nm (Figure 3.23), which was not observed for the second and third phases. Thus, further confirming the initial fast phase as the formation of the CT-1

complex. The rate of conversion from CT-1 to CT-2 and the final decay of CT-2 were inhibited at high flavin concentrations. Flavin inhibition has been reported with several flavin reductase enzymes [18, 57, 58, 102], but the inhibition mechanism has not been clearly defined. To our knowledge this is the first report to assign flavin inhibition to an individual reaction step for the flavin reductase enzymes. From previous steady-state kinetic studies, an ordered sequential mechanism has been determined with NADPH binding first and FMN binding second to form MC-1 before any chemistry occurs. Because FMN binds SsuE tightly with a  $K_d$  value of 0.015  $\mu\text{M}$ , the higher FMN concentration results in FMN occupying the active site of SsuE blocking NADPH from binding. The coupled assay with SsuD was also performed to understand the SsuE reduction mechanism as a complete system, and was very similar with respect to the single enzyme assay. As stated, the major rate-limiting step for hydride transfer is at the conversion of CT-1 to CT-2. Therefore, even with SsuD present to bind reduced flavin, it does not effect the conversion of CT-1 to CT-2, because the major rate-limiting step does not occur during product release even if the product release step is partially rate-limiting.

From the single wavelength stopped-flow studies, a rate-limiting step was observed in the charge-transfer conversion step between CT-1 to CT-2. Deuterated [4(*R*)- $^2\text{H}$ ]NADPH was utilized in these studies to further probe the rate-limiting step in flavin reduction. An isotope effect of 1.3 was observed in the conversion of CT-1 to CT-2 (Figure 3.25). In addition, the concentration of CT-1 simulated by Specfit program accumulates relative to CT-2 with [4(*R*)- $^2\text{H}$ ]NADPH as the pyridine substrate. These combined results with [4(*R*)- $^2\text{H}$ ]NADPH reflects a rate-limiting step on hydride transfer. The isotope effect of 1.3 on the decay of CT-2 may imply a rapid equilibrium or partial

rate-limiting step on the conversion of CT-2 to MC-2 or product release. There was no significant isotope effect on the first step defined as the conversion of MC-1 to CT-1. This observation can be explained if NADPH and FMN bind to SsuE to form a ternary complex in preparation for hydride transfer. After the binding of both substrates, SsuE may undergo a slow conformational change to assist the hydride transfer from NADPH to FMN. The isotope studies showed that this step is not deuterium sensitive. The three-dimensional structure of phthalate dioxygenase reductase showed that a phenylalanine (Phe225) stacks with the isoalloxazine ring of flavin, and serves as a gate between the flavin and NADH binding site (Figure 4.1) [103]. The phenylalanine ring must move out of the way to allow the nicotinamide ring to approach and interact with the oxidized flavin in preparation for hydride transfer [103]. Conserved Phe181 plays an important role in stabilizing FMN binding during P450 reductase catalysis [104]. Similarly, Tyr314 in FNR serves as the gating system between the nicotinamide ring of NADPH and the isoalloxazine ring of FAD [105]. The hypothesis is that aromatic residues are involved in hydrophobic interactions with the isoalloxazine ring of the flavin, and impede hydride transfer from the nicotinamide ring of the pyridine nucleotide. Additional evidence can be found in the flavin reduction of human cytochrome P450 reductase which showed a Trp676 near the isoalloxazine ring of the FAD during NADPH binding [94, 106]. As mentioned, the conserved RXXS sequence found in the FNR family and Fre proteins has also been identified in SsuE (Figure 4.2) [107]. This conserved sequence contains a Phe residue at position 54 within the conserved motif. Substitution of this residue to Ala resulted in an 18-fold increase in the  $K_m$  value (unpublished results). Therefore, this Phe residue may play a direct role in flavin stacking and further studies are being performed

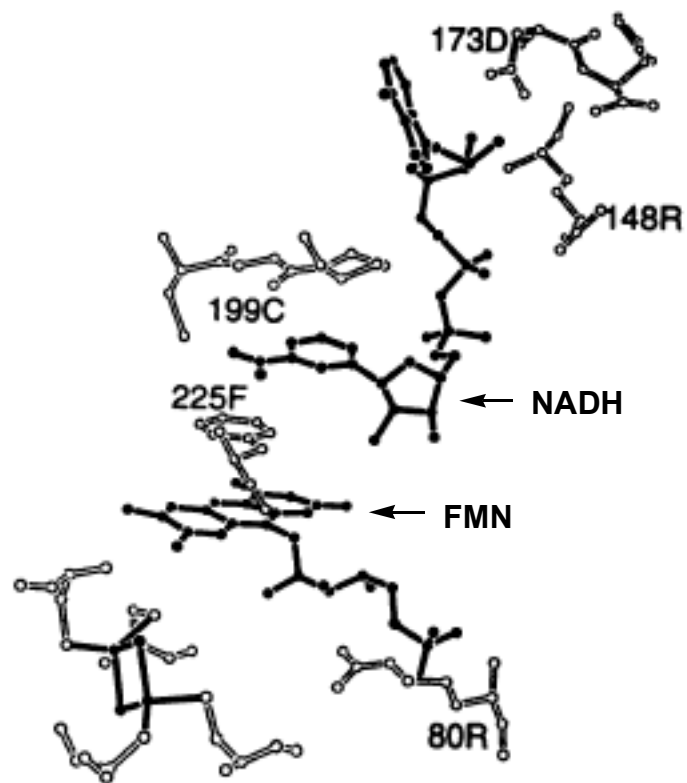


Figure 4.1. Structure showing Phe225 stacks between FMN and NADH in phthalate dioxygenase reductase [103].



	51 54
SsuE	R F D S
Fre E.c	R P F S
Fre P. 1	R P F S
Fre V. f	R P F S
FNR	R L Y S

Figure 4.2. Alignment of the RXXS motif of SsuE with flavin reductases.

to evaluate the importance of this residue in the mechanism of flavin reduction.

Based on these results, a reaction mechanism to define flavin reduction by SsuE was developed (Figure 4.3). In the scheme, NADPH and FMN bind in rapid equilibrium to SsuE to form a ternary Michaelis complex (MC-1). Rapid equilibrium binding would explain why the formation of MC-1 was not clearly detectable in these kinetic studies, and established that both substrates must bind in order to form the charge-transfer complexes. The rate constant  $k_1$  describes the charge-transfer complex formation from the MC-1 complex to CT-1. As stated, formation of CT-1 represents the formation of the charge-transfer complex between NADPH and FMN. Following the fast phase a slower conversion ( $k_2$ ) of CT-1 to CT-2 occurs to form a charge-transfer complex of  $\text{NADP}^+$  associated with  $\text{FMNH}_2$ . This conversion is the deuterium-sensitive step, and hydride transfer is the major rate-limiting step. The final phase ( $k_3$ ) is the decay of the charge transfer complex generating MC-2, or it may represent the release of product from CT-2. The slower third step was likely due to the partial rate-limiting decay of CT-2.

Mechanistic studies of the SsuE flavin reductase have led to the characterization of the individual steps involved in flavin reduction. Flavin reductases that belong to strict two-component systems are continually being identified, and appear to play an important role in diverse physiological functions. As the flavin is not tightly bound to the enzyme, the free flavin distributed in the cell solution is highly accessible for flavin reductases. The liberated reducing power in solution may serve as a general electron source to cope with varied reaction mechanisms. The increased flexibility of flavin reductases may have evolved from standard flavoproteins to adapt to more complex environments during electron transfer, but are still capable of utilizing a similar mechanism to accomplish

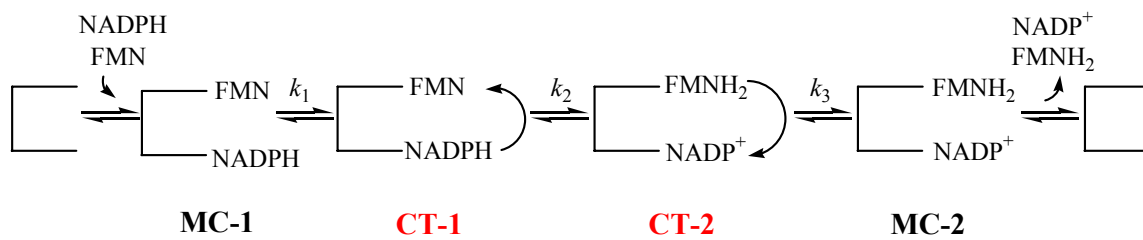


Figure 4.3. Proposed reaction scheme for SsuE catalyzed reaction.

flavin reduction.

#### *4.5 Crystallization of SsuE*

Of flavin reductases that utilize flavin as cosubstrate, only the three-dimensional structure of the Fre enzyme involved in the reactivation of the iron center in ribonucleotide reductase has been determined [108]. Interestingly, the Fre enzyme is structurally similar to the ferredoxin reductase family, even though there is no significant amino acid sequence identity between Fre and other enzymes in this family. Although there is a low overall amino acid sequence identity between SsuE and other flavin reductase enzymes, there are highly conserved regions within this family of enzymes that may be involved in substrate binding or protein interactions with the monooxygenase component. This may also explain why flavin reductase proteins unique to a specific two-component system can be substituted with unrelated flavin reductase proteins belonging to other systems [76]. Determining the structure of SsuE will provide a basis for further studies aimed at analyzing the catalytic mechanism of flavin reduction and transfer. In addition, the structural role of conserved regions common to all flavin reductases may be deduced from the SsuE structure.

The vapor-diffusion technique yielded single crystals that grow as hexagonal rods and diffract to 2.9 Å resolution using synchrotron X-ray radiation. The protein crystallizes in the primitive hexagonal space group P622. The SsuE protein lacks any cysteine or methionine residues owing to the role of the SsuE enzyme in the acquisition of sulfur during sulfate starvation. Therefore, substitution of two leucine residues (Leu114 and Leu165) to methionine was performed to obtain selenomethionine-containing SsuE for MAD phasing. The selenomethionine derivative of SsuE has been

expressed and purified and crystals of the protein have been obtained with and without bound FMN. These preliminary studies should lead to the structure solution of SsuE. It is anticipated that this new protein structure will provide detailed structural information on specific active-site regions of the protein and insight into the mechanism of flavin reduction and transfer of reduced flavin.

#### *4.6 Summary*

There have been no detailed studies on the alkanesulfonate monooxygenase system since the initial identification of this system. Besides the importance of this system in the desulfonation of alkanesulfonates, it is an excellent model to study flavin transfer between the two enzyme components. The first step toward characterizing each protein is to express each protein in significant quantities for biophysical and kinetic characterization. Genes for the respective proteins were cloned into the T7 RNA polymerase-dependent expression vector pET21a. Proteins were purified by a combination of ammonium sulfate fractionation and column chromatography, a high yield was obtained for each protein. The molecular weight for each protein was determined by ESIMS, and SsuE was determined to be a dimer and SsuD a tetramer by analytical ultracentrifugation studies.

We were initially interested in determining the substrate specificity of the flavin reductase component. The kinetic results showed FMN as the preferred flavin substrate and there was no preference for pyridine nucleotides NADPH or NADH. Because SsuE does not contain flavin as a tightly bound prosthetic group, the binding affinity assays were necessary to identify the dissociation constant of SsuE for FMN. A  $K_d$  value of 0.015  $\mu\text{M}$  showed a tight binding of FMN to SsuE. Conversely, the binding of FMN to

SsuD with a  $K_d$  value of 10.2  $\mu\text{M}$  showed a loose binding of FMN to SsuD. The relative higher affinity of SsuE for oxidized FMN makes FMN an effective substrate.

Following the preliminary studies, a primary focus of this research was to delineate the kinetic mechanism of SsuE in the absence of SsuD. A sequential mechanism was established for the SsuE catalyzed Bi Bi reaction. The question arose on how to distinguish the ordered sequential from random sequential mechanism. A practical method to differentiate between the two mechanisms is product inhibition studies. Results from inhibition studies of SsuE support an ordered sequential mechanism with NADPH binding first to the enzyme and FMN second. After the reduction of FMN, the product FMNH<sub>2</sub> is released first with NADP<sup>+</sup> as the last product to dissociate.

SsuE provides reduced flavin for the desulfonation of alkanesulfonates by SsuD. Therefore, these two proteins may interact during flavin transfer to avoid flavin autooxidation. Kinetic studies were carried out to explore the effect of SsuD on the steady-state mechanism of SsuE. The kinetic mechanism of SsuE in the presence of SsuD and octanesulfonate was altered to a rapid equilibrium ordered mechanism with NADPH binding first to form a ternary complex, and the  $K_{m,\text{NADPH}}$  was appreciably lower than the dissociation constant. With the rapid equilibrium ordered mechanism, the reaction is driven in the forward direction even with a low concentration of NADPH present. The altered mechanism in the presence of SsuD and octanesulfonate ensures the effective utilization of substrate NADPH in the production of reduced flavin for the desulfonation reaction of SsuD. This is also an indication of protein-protein interactions during the flavin transfer reaction. There should be no change between the single enzyme and coupled assay if protein-protein interaction did not play a role in catalysis.

Flavin reductases containing flavin as a tightly bound cofactor typically catalyze the reduction of a flavin with the formation of a charge-transfer complex as the intermediate. Pre-steady-state kinetic studies of SsuE showed a fast formation of a CT-1 representing FMN associated with NADPH, and a slower conversion of CT-1 to CT-2 which is the reduced flavin FMNH<sub>2</sub> associated with NADP<sup>+</sup>. The result confirmed that SsuE utilized a similar mechanism to standard flavoproteins in flavin reduction reaction even though SsuE does not contain flavin as a cofactor, and uses flavin as a substrate.

Future studies will focus on putative active site residues involved in catalysis. SsuE has lost the ability to possess a tightly bound cofactor, but the sequence alignment with standard flavoproteins revealed a flavin binding motif R<sub>51</sub>XXS<sub>54</sub> in SsuE. The three dimensional crystallographic structure of ferredoxin-NADP<sup>+</sup> reductase FNR demonstrated serine 96 interacting with the N5 position of the isoalloxazine ring (Figure 4.4) [109]. Serine 96 is in hydrogen bonding distance with the N5 of the isoalloxazine ring of FAD. Mutational studies of serine to valine resulted in the significant loss of enzyme activity compared to the wild type [63]. The role of serine 96 in FNR may be similar with that of serine 54 in SsuE. Site-directed mutagenesis of serine 54 to alanine has been performed. The *K<sub>d</sub>* value of S54A was 8-fold higher than the value of wild type SsuE. This result is consistent with previous reports that serine in the conserved motif is involved in flavin binding [63]. Further studies of the S54A variant through the pre-steady-state kinetic analysis will be performed to examine the effect of mutations on the charge-transfer complex during flavin reduction.

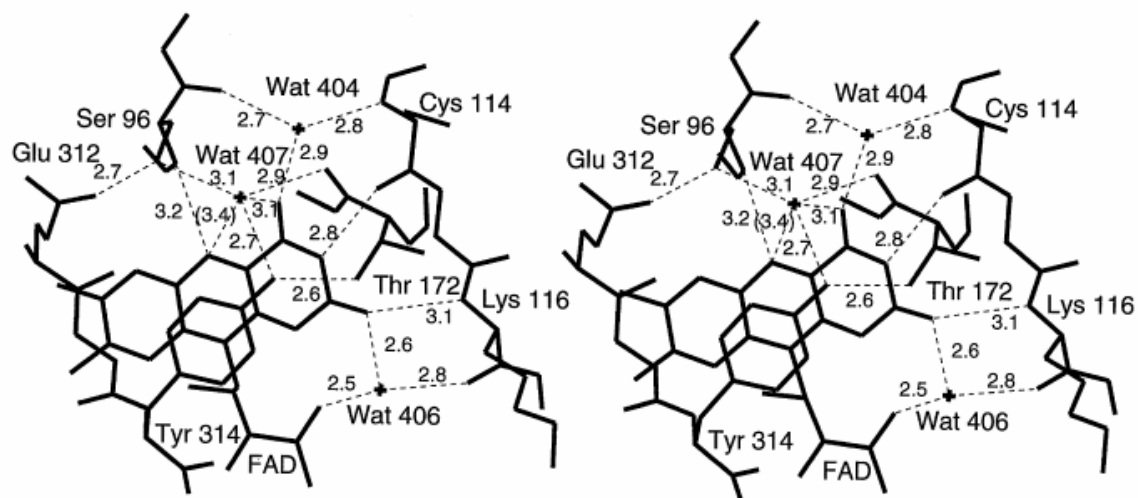


Figure 4.4. Hydrogen-bonding of the active site in FNR [109].



Crystallization of SsuE is an important part of this project due to the role of SsuE in the assimilation of sulfur from alternate sulfur sources. The lack of sulfur-containing amino acids limited the use of standard protocols to obtain selenomethionyl protein for MAD phasing. A conservative strategy is to replace leucine with methionine that has the same spacial volume with leucine. L114, 165M mutants were successfully achieved, and subsequently applied in the selenomethionyl SsuE expression under conditions of methionine pathway inhibition. Circular dichroism spectroscopy revealed no gross secondary structural changes. Crystals of selenomethioyl SsuE and wild type SsuE were formed with and without flavin bound. The preliminary X-ray diffraction analysis has been informative for space group of SsuE crystal, and further crystallographic studies are underway to solve the three-dimensional structure by MAD phasing. With the three-dimensional structure of SsuE, an in depth investigation of active site will provide solid information in the understanding of SsuE flavin reductase.

## REFERENCES

- [1] J.R. Van der Ploeg, M.A. Weiss, E. Saller, H. Nashimoto, N. Saito, M.A. Kertesz, T. Leisinger, Identification of sulfate starvation-regulated genes in *Escherichia coli*: a gene cluster involved in the utilization of taurine as a sulfur source, *J. Bacteriol.* 178 (1996) 5438-5446.
- [2] J.R. Van der Ploeg, E. Eichhorn, T. Leisinger, Sulfonate-sulfur metabolism and its regulation in *Escherichia coli*, *Arch Microbiol.* 176 (2001) 1-8.
- [3] A. Kahnert, P. Vermeij, C. Wietek, P. James, T. Leisinger, M.A. Kertesz, The *ssu* locus plays a key role in organosulfur metabolism in *Pseudomonas putida* S-313, *J. Bacteriol.* 182 (2000) 2869-2878.
- [4] M. Quadroni, W. Staudenmann, M. Kertesz, P. James, Analysis of global responses by protein and peptide fingerprinting of proteins isolated by two-dimensional gel electrophoresis. Application to the sulfate-starvation response of *Escherichia coli*, *Eur. J. Biochem.* 239 (1996) 773-781.
- [5] M.R. Uria-Nickelsen, E.R. Leadbetter, IIIW. Godchaux, Sulphonate utilization by enteric bacteria, *J. Gen. Microbiol.* 139 (1993) 203-208.
- [6] J.R. van der Ploeg, R. Iwanicka-Nowicka, T. Bykowski, M.M. Hryniewicz, T. Leisinger, The *Escherichia coli ssuEADCB* gene cluster is required for the utilization of

sulfur from aliphatic sulfonates and is regulated by the transcriptional activator Cbl, J. Biol. Chem. 274 (1999) 29358-29365.

[7] R. Hell, G. Schuster, W. Gruissem, An O-acetylserine (thiol) lyase cDNA from spinach, Plant Physiol. 102 (1993) 1057-1058.

[8] H.R. Ellis, L.B. Poole, Novel application of 7-chloro-4-nitrobenzo-2-oxa-1,3-diazole to identify cysteine sulfenic acid in the AhpC component of alkyl hydroperoxide reductase, Biochemistry 36 (1997) 15013-15018.

[9] H.R. Ellis, L.B. Poole, Roles for the two cysteine residues of AhpC in catalysis of peroxide reduction by alkyl hydroperoxide reductase from *Salmonella typhimurium*, Biochemistry 36 (1997) 13349-13356.

[10] L.B. Poole, H.R. Ellis, Flavin-dependent alkyl hydroperoxide reductase from *Salmonella typhimurium*. 1. Purification and enzymatic activities of overexpressed AhpF and AhpC proteins, Biochemistry 35 (1996) 56-64.

[11] E. Papinutto, H.J. Windle, L. Cendron, R. Battistutta, D. Kelleher, G. Zanotti, Crystal structure of alkyl hydroperoxide-reductase (AhpC) from *Helicobacter pylori*, Biochim Biophys Acta. 1753(2) (2005) 240-246.

[12] E. Eichhorn, J.R. Van der Ploeg, T. Leisinger, Deletion analysis of the *Escherichia coli* taurine and alkanesulfonate transport systems, J. Bacteriol. 182 (2000) 2687-2795.

[13] J.R. van der Ploeg, N.J. Cummings, T. Leisinger, I.F. Connerton, *Bacillus subtilis* genes for the utilization of sulfur from aliphatic sulfonates, Microbiology 144 (1998) 2555-2561.

[14] W.E. Gledhill, Linear alkylbenzene sulfonate: biodegradation and aquatic interactions, Adv. Appl. Microbiol. 17 (1974) 265-293.

- [15] M.J. Grossman, M.K. Lee, R.C. Prince, K.K. Garrett, G.N. George, I.J. Pickering, Microbial desulfurization of a crude oil middle-distillate fraction: Analysis of the extent of sulfur removal and the effect of removal on remaining sulfur, *Appl. Environ. Microbiol.* 65 (1999) 181-189.
- [16] B. Lei, S.-C. Tu, Gene expression, purification, and identification of a desulfurization enzyme from *Rhodococcus* sp. strain IGTS8 as a sulfide/sulfoxide monooxygenase, *J. Bacteriol.* 178 (1996) 5699-5705.
- [17] C. E. Jeffers, S.C. Tu, Differential transfers of reduced flavin cofactor and product by bacterial flavin reductase to luciferase. *Biochemistry* 40 (2001) 1749-1754.
- [18] E. Eichhorn, J.R. van der Ploeg, T. Leisinger, Characterization of a two-component alkanesulfonate monooxygenase from *Escherichia coli*. *J. Biol. Chem.* 274 (1999) 26639-26646.
- [19] M. Witschel, S. Nagel, T. Egli, Identification and characterization of the two-enzyme system catalyzing oxidation of EDTA in the EDTA-degrading bacterial strain DSM 9103, *J. Bacteriol.* 179 (1997) 6937-6943.
- [20] D. Thibaut, N. Ratet, D. Bisch, D. Faucher, L. Debussche, F. Blanche, Purification of the two-enzyme system catalyzing the oxidation of the D-proline residue of pristinamycin IIB during the last step of pristinamycin IIA biosynthesis, *J. Bacteriol.* 177 (1995) 5199-5205.
- [21] E. Jablonski, M. DeLuca, Studies of the control of luminescence in *Beneckeia harveyi*: properties of the NADH and NADPH:FMN oxidoreductases, *Biochemistry* 17 (1978) 672-678.
- [22] E. Gerlo, J. Charlier, Identification of NADH-specific and NADPH-specific FMN

- reductases in *Beneckeia harveyi*, Eur. J. Biochem. 57 (1975) 461-467.
- [23] W. Duane, J.W. Hastings, Flavin mononucleotide reductase of luminous bacteria, Mol. Cell. Biochem. 6 (1975) 53-64.
- [24] Y. Xu, M.W. Mortimer, T.S. Fisher, M.L. Kahn, F.J. Brockman, L. Xun, Cloning, sequencing, and analysis of a gene cluster from *Chelatobacter heintzii* ATCC 29600 encoding nitrilotriacetate monooxygenase and NADH:flavin mononucleotide oxidoreductase, J. Bacteriol. 179 (1997) 1112-1116.
- [25] R.J. Parry, W. Li, An NADPH:FAD oxidoreductase from the valanimycin producer, *Streptomyces viridifaciens*. Cloning, analysis, and overexpression, J. Biol. Chem. 272 (1997) 23303-23311.
- [26] B. Galan, E. Diaz, M.A. Prieto, J.L.Garcia, Functional analysis of the small component of the 4-hydroxyphenylacetate 3-monooxygenase of *Escherichia coli* W: a prototype of a new Flavin:NAD(P)H reductase subfamily, J. Bacteriol. 182 (2000) 627-636.
- [27] K. Otto, K. Hofstetter, M. Rothlisberger, B. Witholt, A. Schmid, Biochemical characterization of StyAB from *Pseudomonas sp.* strain VLB120 as a two-component flavin-diffusible monooxygenase, J. Bacteriol. 186 (2004) 5292-5302.
- [28] M.R. Gisi, L. Xun, Characterization of chlorophenol 4-monooxygenase (TftD) and NADH:flavin adenine dinucleotide oxidoreductase (TftC) of *Burkholderia cepacia* AC1100, J. Bacteriol. 185 (2003) 2786-2792.
- [29] P. Macheroux, S. Ghisla, J.W. Hastings, Spectral detection of an intermediate preceding the excited state in the bacterial luciferase reaction, Biochemistry 32 (1993) 14183-14186.

- [30] D. Sheng, D.P. Ballou, V. Massey, Mechanistic studies of cyclohexanone monooxygenase: chemical properties of intermediates involved in catalysis, *Biochemistry* 40 (2001) 11156-11167.
- [31] F. Müller, Flavin radicals: chemistry and biochemistry, *Free Radical Biology & Medicine* 3 (1987) 215-230.
- [32] D.B. McCormick, Metabolism of riboflavin, In: Rivlin, R.S., ed. *Riboflavin*, New York: Plenum Press; 1975. pp.153-198.
- [33] V. Massey, The chemical and biological versatility of riboflavin, *Biochemical Society Transactions* 28 (2000) 283-296.
- [34] D. Voet, J.G. Voet, *Biochemistry*, second edition, 1995, John Wiley & Sons, INC.
- [35] P. Hemmerich, F. Müller, Flavin-O<sub>2</sub> interaction mechanisms and the function of flavin in hydroxylation reactions, *Annals New York Academy of Sciences* 212 (1973) 13-26.
- [36] V. Job, G. L. Marcone, M.S. Pilone, L. Pollegioni, Glycine oxidase from *Bacillus subtilis*. Characterization of a new flavoprotein, *J. Biol. Chem.* 277 (2002) 6985-6993.
- [37] J.C.G. Woo, R.B. Silverman, Observation of two different chromophores in the resting state of monoamine oxidase B by fluorescence spectroscopy, *Biochem. Biophys. Res. Comm.* 202 (1994) 1574-1578.
- [38] S. Ghisla, V. Massey, J.-M. Lhoste, S.G. Mayhew, Fluorescence and optical characteristics of reduced flavins and flavoproteins, *Biochemistry* 13 (1974) 589-597.
- [39] M. Mewies, W.S. McIntire, N.S. Scrutton, Covalent attachment of flavin adenine dinucleotide (FAD) and flavin mononucleotide (FMN) to enzymes: The current state of affairs, *Protein Sci.* 7 (1998) 7-20.

- [40] U.V. Venkataram, T.C. Bruice, On the mechanism of flavin-catalyzed dehydrogenation  $\alpha,\beta$  to an Acyl function. The mechanism of 1,5-dihydroflavin reduction of maleimides, *J. Am. Chem. Soc.* 106 (1984) 5703-5709.
- [41] F. Müller, *Chemistry and Biochemistry of Flavoenzymes*, Vol I pp 402. 1991 by CRC Press.
- [42] V. Massey, Activation of molecular oxygen by flavin and flavoproteins, *J. Biol. Chem.* 269 (1994) 22459-22464.
- [43] M. Ortiz-Maldonado, B. Entsch, D.P. Ballou, Conformational changes combined with charge-transfer interactions are essential for reduction in catalysis by *p*-hydroxybenzoate hydroxylase, *Biochemistry* 42 (2003) 11234-11242.
- [44] B. Entsch, D.P. Ballou, V. Massey, Flavin-oxygen derivatives involved in hydroxylation by *p*-hydroxybenzoate hydroxylase, *J. Biol. Chem.* 251 (1976) 2550-2563.
- [45] D.R. Fravel, D.P. Roberts, *In situ* evidence for the role of glucose oxidase in the biocontrol of verticillium wilt by *T. flavus*, *Biocontrol Sci. Technol.* 1 (1991) 91-99.
- [46] K.K. Kim, D.R. Fravel, G.C. Papavizas, Identification of a metabolite produced by *Talaromyces flavus* as glucose oxidase and its role in the biocontrol of *Verticillium dahliae*, *Phytopathology* 78 (1988) 488-492.
- [47] K.K. Kim, D.R. Fravel, and G.C. Papavizas, Production, purification, and properties of glucose oxidase from the biocontrol fungus *Talaromyces flavus*, *Can. J. Microbiol.* 36 (1990)199-205.
- [48] K.K. Kim, D.R. Fravel, and G.C. Papavizas, Glucose oxidase as the antifungal principle of talaron from *Talaromyces flavus*, *Can. J. Microbiol.* 36 (1990)760-764.
- [49] S.K. Stosz, D.R. Fravel, D.P. Roberts, In vitro analysis of the role of glucose oxidase

from *Talaromyces flavus* in biocontrol of the plant pathogen *Verticillium Dahliae*, Appl Environ Microbiol 62 (1996) 3181-3186.

[50] H. Eichenseer, M.C. Mathews, J.L. Bi, J.B. Murphy, G.W. Felton, Salivary glucose oxidase: Multifunctional roles for *Helicoverpa zea*? Arch Insect Biochem Physiol 42 (1999) 99-109.

[51] Y. Nishiya, T. Imanaka, Purification and characterization of a novel glycine oxidase from *Bacillus subtilis*, FEBS Lett. 438 (1998) 263-266.

[52] C. Binda, A. Mattevi, D.E. Edmondson, Structure-function relationship in flavoenzyme-dependent amine oxidations: A comparison of polyamine oxidase and monoamine oxidase, J. Biol. Chem. 277 (2002) 23973-23976.

[53] E. Jablonski, M. DeLuca, Purification and properties of the NADH and NADPH specific FMN oxidoreductase from *Beneckeia harveyi*, Biochemistry 16 (1977) 2932-2936.

[54] B. Lei, M. Liu, S. Huang, S-C. Tu, *Vibrio harveyi* NADPH-flavin oxidoreductase: cloning, sequencing, and overexpression of the gene and purification of the cloned enzyme, J. Bacteriol. 176 (1994) 3552-3558.

[55] G.A. Michalyszyn, S.S. Wing, E.A. Meighen, Purification and properties of a NAD(P)H: flavin oxidoreductase from the luminous bacterium, *Beneckeia harveyi*, J. Biol. Chem. 252 (1977) 7495-7499.

[56] H. Watanabe, J.W. Hastings, Specificity and properties of three pyridine nucleotide-flavin mononucleotide reductases coupling to bacterial luciferase, Mol. Cell. Biochem. 44 (1982) 181-187.

[57] B. Gao, H.R. Ellis, Altered mechanism of the alkanesulfonate FMN reductase with



- the monooxygenase enzyme, *Biochem. Biophys. Res. Comm.* 331 (2005) 1137-1145.
- [58] B. Lei, S.C. Tu, Mechanism of reduced flavin transfer from *Vibrio harveyi* NADPH-FMN oxidoreductase to luciferase, *Biochemistry* 37 (1998) 14623-14629.
- [59] E. Jablonski, M. DeLuca, Studies of the control of luminescence in *Beneckea harveyi*; Properties of the NADH and NADPH:FMN oxidoreductases, *Biochemistry* 17 (1978) 672-678.
- [60] S.-C. Tu, J.E. Becvar, J.W. Hastings, Kinetic studies on the mechanism of bacterial NAD(P)H:flavin oxidoreductase, *Arch. Biochem. Biophys.* 193 (1979) 110-116.
- [61] F. Fieschi, V. Nivie` re, C. Frier, J.-L. De`cout, M. Fontecave, The mechanism and substrate specificity of the NADPH:Flavin oxidoreductase from *Escherichia coli*, *J. Biol. Chem.* 270 (1995) 30392-30400.
- [62] A. Fersht, Structure and mechanism in protein science, A guide to enzyme catalysis and protein folding, 1999, W. H. Freeman and Company, New York.
- [63] A. Aliverti, C. M. Bruns, V. E. Pandini, P. A. Karplus, M. A. Vanoni, B. Curti, G. Zanetti, Involvement of serine 96 in the catalytic mechanism of ferredoxin-NADP<sup>+</sup> reductase: Structure-function relationship as studied by site-directed mutagenesis and X-ray crystallography, *Biochemistry* 34 (1995) 8371-8379.
- [64] G. Gassner, L. Wang, C. Batie, D. P. Ballou, Reaction of phthalate dioxygenase reductase with NADH and NAD: Kinetic and spectral characterization of intermediates, *Biochemistry* 33 (1994) 12184-12193.
- [65] G. T. Gassner, D. P. Ballou, Preparation and characterization of a truncated form of phthalate dioxygenase reductase that lacks an iron-sulfur domain, *Biochemistry* 34 (1995) 13460-13471.

- [66] C. J. Batie, H. Kamin, Electron transfer by ferredoxin:NADP<sup>+</sup> reductase. Rapid-reaction evidence for participation of a ternary complex, *J. Biol. Chem.* 259 (1984) 11976-11985.
- [67] C. J. Batie, H. Kamin, Association of ferredoxin-NADP<sup>+</sup> reductase with NADP(H) specificity and oxidation-reduction properties, *J. Biol. Chem.* 261 (1986) 11214-11223.
- [68] V. Nivière, M. A. Vanoni, G. Zanetti, M. Fontecave, Reaction of the NAD(P)H:Flavin oxidoreductase from *Escherichia coli* with NADPH and riboflavin: Identification of intermediates, *Biochemistry* 37 (1998) 11879-11887.
- [69] L. Filisetti, M. Fontecave, V. Nivière, Mechanism and substrate specificity of the flavin reductase ActVB from *Streptomyces coelicolor*, *J. Biol. Chem.* 278 (2003) 296-303.
- [70] Q.H. Gibson, J.W. Hastings, The oxidation of reduced flavin mononucleotide by molecular oxygen, *Biochem. J.* 83 (1962) 368-377.
- [71] V. Massey, G. Palmer, D.P. Ballou, in *Oxidases and Related systems*, T.E. King, H.S. Mason, M. Morrison, eds, 1973, pp.25-43. University Park Press, Baltimore.
- [72] G. Eberlein, T.C. Bruice, The chemistry of a 1,5-diblocked flavin. 2. Proton and electron transfer steps in the reaction of dihydroflavins with oxygen, *J. Am. Chem. Soc.* 105 (1983) 6685-6697.
- [73] S.-C. Tu, Reduced flavin: donor and acceptor enzymes and mechanisms of channeling, *Antioxidants & Redox Signaling* (Mary Ann Liebert, Inc.),3 (2001) 881-897.
- [74] C.E. Jeffers, J.C. Nichols, S.C. Tu, Complex formation between *Vibrio harveyi* luciferase and monomeric NADPH:FMN oxidoreductase, *Biochemistry* 42 (2003) 529-534.

- [75] K. Abdurachim, H.R. Ellis, Detection of protein:protein interactions in the alkanesulfonate monooxygenase system from *Escherichia coli*, *J. Bacteriol.* 188 (2006) 8153-8159.
- [76] T.M. Louie, X.S. Xie, L. Xun, Coordinated production and utilization of FADH<sub>2</sub> by NAD(P)H-flavin oxidoreductase and 4-hydroxyphenylacetate 3-monooxygenase, *Biochemistry* 42 (2003) 7509-7517.
- [77] J. Valton, L. Filisetti, M. Fontecave, V. Nivière, A two-component flavin-dependent monooxygenase involved in actinorhodin biosynthesis in *Streptomyces coelicolor*, *J. Biol. Chem.* 279 (2004) 44362-44369.
- [78] U. Kirchner, A.H. Westphal, R. Müller, M.J.H. van Berkel, Phenol hydroxylase from *Bacillus thermoglucosidasius* A7, a two-protein component monooxygenase with a dual role for FAD, *J. Biol. Chem.* 278 (2003) 47545-47553.
- [79] L. Xun, E.R. Sandvik, Characterization of 4-hydroxyphenylacetate 3-hydroxylase (HpaB) of *Escherichia coli* as a reduced flavin adenine dinucleotide-utilizing monooxygenase, *Appl. Environ. Microbiol.* 66 (2000) 481-486.
- [80] P. Chaiyen, C. Suadee, P. Wilairat, A novel two-protein component flavoprotein hydroxylase, *Eur. J. Biochem.* 268 (2001) 5550-5561.
- [81] B. Gálan, E. Díaz, M.A. Prieto, J.L. García, Functional analysis of the small component of the 4-hydroxyphenylacetate 3-monooxygenase of *Escherichia coli* W: a prototype of a new Flavin:NAD(P)H reductase subfamily, *J. Bacteriol.* 182 (2000) 627-636.
- [82] F. Hollmann, P.C. Lin, B. Witholt, A. Schmid, Stereospecific biocatalytic epoxidation: the first example of direct regeneration of a FAD-dependent

monooxygenase for catalysis, *J. Am. Chem. Soc.* 125 (2003) 8209-8217.

[83] A. Kantz, F. Chin, N. Nallamotheu, T. Nguyen, G.T. Gassner, Mechanism of flavin transfer and oxygen activation by the two-component flavoenzyme styrene monooxygenase, *Arch. Biochem. Biophys.* 442 (2005) 102-116.

[84] W.F. III Scafford, Boundary analysis in sedimentation transport experiments: a procedure for obtaining sedimentation coefficient distributions using the time derivative of the concentration profile, *Anal. Biochem.* 203 (1992) 295-301.

[85] S.-S. Jeong, J. E. Gready, A method of preparation and purification of (4R)-deuterated-reduced nicotinamide adenine dinucleotide phosphate, *Anal. Biochem.* 221 (1994) 273-277.

[86] V. V. Pollock, M. J. Barber, Kinetic and mechanistic properties of biotin sulfoxide reductase, *Biochemistry* 40 (2001) 1430-1440.

[87] J. Jancarik, S.-H. Kim, Sparse matrix sampling: a screening method for crystallization of proteins, *J. Appl. Cryst.* 24 (1991) 409-411.

[88] J.W. Pflugrath, The finer things in X-ray diffraction data collection, *Acta Cryst. D55* (1999) 1718-1725.

[89] M. Eschenbrenner, J. Coves, M. Fontecave, The flavin reductase activity of the flavoprotein component of sulfite reductase from *Escherichia coli*. A new model for the protein structure, *J. Biol. Chem.* 270 (1995) 20550-20555.

[90] S. Inouye, H. Nakamura, Stereospecificity of hydride transfer and substrate specificity for FMN-containing NAD(P)H-flavin oxidoreductase from the luminescent bacterium, *Vibrio ischeri* ATCC 7744, *Biochem. Biophys. Res. Comm.* 205 (1994) 275-281.

- [91] P. Skae, R. J. Parry, Determination of the stereochemistry of hydride transfer from NADPH to FAD catalyzed by VlmR, a flavin reductase from the valanimycin biosynthetic pathway, *Org. Letters* 3 (2001) 1117-1119.
- [92] N.C. Gassner, B.W. Matthews, Use of differentially substituted selenomethionine protein in X-ray structure determination, *Acta Cryst. D* 55 (1999) 1967-1970.
- [93] M. Eschenbrenner, J. Coves, M. Fontecave, The flavin reductase activity of the flavoprotein component of sulfite reductase from *Escherichia coli*. A new model for the protein structure, *J. Biol. Chem.* 270 (1995) 20550-20555.
- [94] A. Gutierrez, L.-Y. Lian, C. R. Wolf, N. S. Scrutton, G. C. K. Roberts, Stopped-flow kinetic studies of flavin reductase in human cytochrome P450 reductase and its component domains, *Biochemistry* 40 (2001) 1964-1975
- [95] K. Knight, N. S. Scrutton, Stopped-flow kinetic studies of electron transfer in the reductase domain of neuronal nitric oxide synthase: re-evaluation of the kinetic mechanism reveals new enzyme intermediates and variation with cytochrome P450 reductase, *Biochem. J.* 367 (2002) 19-30.
- [96] K. R. Wolthers, N. S. Scrutton, Electron transfer in human methionine synthase reductase studied by stopped-flow spectrophotometry, *Biochemistry* 43 (2004) 490-500.
- [97] W. H. Campbell, Nitrate reductase structure, function and regulation: Bridging the gap between biochemistry and physiology, *Annu. Rev. Plant Physiol. Plant Mol. Biol.* 50 (1999) 277-303.
- [98] L. P., Solomonson, M. J. Barber, Assimilatory nitrate reductase: Functional properties and regulation, *Annu. Rev. Plant Physiol. Plant Mol. Biol.* 41(1990) 225-253.
- [99] K. Ratnam, N. Shiraishi, W. H. Campbell, R. Hille, Spectroscopic and kinetic

- characterization of the recombinant cytochrome c reductase fragment of nitrate reductase. Identification of the rate-limiting catalytic step, *J. Biol. Chem.* 272 (1997) 2122-2128.
- [100] C. J. Kay, M. J. Barber, Assimilatory nitrate reductase from *Chlorella*. Effect of ionic strength and pH on catalytic activity, *J. Biol. Chem.* 261 (1986) 14125-14129.
- [101] C. J. Kay, L. P. Solomonson, M. J. Barber, Electrochemical and kinetic analysis of electron-transfer reactions of *Chlorella* nitrate reductase, *Biochemistry* 30 (1991) 11445-11450.
- [102] T. M. Louie, H. Yang, P. Karnchanaphanurach, X. S. Xie, L. Xun, FAD is a preferred substrate and an inhibitor of *Escherichia coli* general NAD(P)H:flavin oxidoreductase, *J. Biol. Chem.* 277 (2002) 39450-39455.
- [103] G. T. Gassner, M. L. Ludwig, D. L. Gatti, C. C. Correll, D. P. Ballou, Structure and mechanism of the iron-sulfur flavoprotein phthalate dioxygenase reductase, *FASEB J.* 9 (1995) 1411-1418.
- [104] M.J.I. Paine, S. Avivor, A. Munro, P. Tsan, L.-Y. Lian, G.C.K. Roberts, C.R. Wolf, Role of the conserved phenylalanine 181 of NADPH-cytochrome P450 oxidoreductase in FMN binding and catalytic activity, *Biochemistry* 40 (2001) 13439-13447.
- [105] P. A. Karplus, M. J. Daniels, J. R. Herriott, Atomic structure of ferredoxin-NADP<sup>+</sup> reductase: prototype for a structurally novel flavoenzyme family, *Science* 251 (1991) 60-66.
- [106] A. Gutierrez, M. Paine, C. R. Wolf, N. S. Scrutton, G. C. Roberts, Relaxation kinetics of cytochrome P450 reductase: internal electron transfer is limited by conformational change and regulated by coenzyme binding, *Biochemistry* 41 (2002) 4626-4637.

[107] V. Nivière, F. Fieschi, J.-L. Décout, M. Fontecave, Is the NAD(P)H:flavin oxidoreductase from *Escherichia coli* a member of the ferredoxin-NADP<sup>+</sup> reductase family?, *J. Biol. Chem.* 271 (1996) 16656-16661.

[108] M. Ingelman, S. Ramaswamy, V. Niviere, M. Fontecave, H. Eklund, Crystal structure of NAD(P)H:flavin oxidoreductase from *Escherichia coli*, *Biochemistry* 38 (1999) 7040-9.

[109] C.M. Bruns, P.A. Karplus, Refined crystal structure of spinach ferredoxin reductase at 1.7 Å resolution: Oxidized, reduced and 2'-Phospho-5'-AMP bound states, *J. Mol. Biol.* 247 (1995) 125-145.